Three mutations in *SASH1* cause the pathogenesy of dyschromatosis universalis hereditaria (DUH)

Zhou ding'an[1], Wei zhiyun[2], Wang teng[1], Sang qing[1] , Zhang junyu[1] ,Guo Luo[1], Wang Honglian[1], Lin Sheyu[1], Xu Jiawei, Li Qiaoli[1], He lin[1,2,3] and Xing qinghe[1]

[1]Institutes of Biomedical Sciences， Fudan University,138Yixueyuan Road,Shanghai 200032,China.

[2]Bio-X Center, Key Laboratory for the Genetics of Developmental and Neuropsychiatric Disorders (Ministry of Education), Shanghai Jiao Tong University, 1954 Huashan Road, Shanghai 200030, China

[3]Institute for Nutritional Sciences, Shanghai Institutes of Biological Sciences, Chinese Academy of Sciences, Shanghai 200031, China.

Authors for correspondence

Dr Lin He and Dr Qinghe Xing, Institutes of Biomedical Sciences, Fudan University, Shanghai, China or

Bio-X Center, Shanghai Jiao Tong University, 1954 Hua Shan Road, Shanghai 200030, China. E-mail:

helinhelin@gmail.com and xingqinghef@gmail.com, Tel & fax: 86-21-62822491

ABSTRACT

Dyschromatosis universalis hereditaria (DUH) is a rare genodermatosis characterized by hyper- and hypopigmented macules which form a reticulate or mottled pattern. The causal gene and the precise pathogenesis of DUH have been unclear since the disease was initially reported in 1933. However, we found three heterozygous mutations encoding amino acid substitutions in *SASH1* in each of three nonconsanguineous DUH families. Immunohistochemisty and melanin staining showed distribution heterogenicity of melanocytes, predominantly melanized melanocytes in the epidernal tissues of a DUH patient. Specifically, we identified that mutations of *SASH1* can up-regulate resident melanogenic proteins, transport protein of melanosome and induce increased mobility of melanocytes *in vitro* and *in vivo* to enhance incressed biosynthesis of melanin . Furthermore, SASH1 was shown to interact with several proteins associated with melanogenesis in the MAPK signaling pathway and the endothelin signaling pathway, indicating an additional melanogenesis signaling pathway in the regulation of melanin biosynthesis. Collectively, these observations suggest that DUH is a heterogeneous disorder of increased production and transport of melanosomes caused by *SASH1* mutations together with melanocytes maldistribution.

Dyschromatosis universalis hereditaria (DUH) is a clinically heterogeneous disorder characterized by generalized mottled pigmentation. It was initially described by Ichikawa and Hiraga in two generations of two families in 1933[1] . We discovered similar Chinese predigrees in 2003[2], and identified them as having autosomal dominant DUH[3]. Although the precise etiology of this disorder is not yet known, a recent study by Yusuf indicates that clinicopathological findings implicate an inherent abnormality of melanosomes or melanin processing[4]. Other studies have supported the Yusuf findings, pointing to the existence of significantly melanized melanocytes and keratinocytes with increased melanin content in the epidermiss of DUH patients[5-8]. Taken together, this evidence indicates that DUH, both genetically and ultrastructurally, is a heterogeneous disorder different from dyschromatosis symmetrica hereditaria (DSH).

Stuhrmann identified a new locus for DUH on chromosome 12q21-q23 in an Arab family[9], but found no mutation in a region spanning a distance of 18.9 cM and a region of 20.9 Mb and containing 125 known or predicted genes. By contrast, we found three heterozygous mutations encoding amino acid substitutions in the SAM and SH3 domain containing I (*SASH1*) .

Biosynthesis of melanins, the major pigments synthesized by mammals, is sequestered within melanosomes containing unique membrane enclosed structures of melanocytes. Melanosomes and their precursors can be classified into four stages of development based on morphology. Consistent with their singular structure and function, melanosomes contain specific resident proteins expressed only in melanocytes and retinal epithelium cells. Most of those characterized are integral membrane proteins, such as tyrosinase, tyrosine-related protein1 (TYRP1; gp75, Brown locus protein), and Pmel17 (gp100,SILV, Silver locus protein). Pmel17 is a matrix protein of premelanosomes whereas TYRP1 is a component of mature melanosomes[10]. Pmel17 localizes to intralumenal striations of stage II premelanosomes and its localization to intralumenal membranes of MVBs (multivesicular bodies) appears to precede striation formation. The striations appear to recruit Pmel17 from the intralumenal vesicles. These results suggest that Pmel17 is a major biogenetic component of the striations[11]. Pmel17 is first enriched in stage I-like structures, and accumulates to a higher extent in stage II premelanosomes. In contrast, TYRP1 is almost undetectable in stage I structures, and only a small percentage of labeling is observed in stage II. Although stage III and particularly stage IV melanosomes are densely labeled for TYRP1, the levels of detectable Pmel17 strongly decrease in these structures. Studies on Rab27a (a small Ras-like GTPase belonging to the Rab family, encoded by ashen (Rab27a ash)) have provided strong evidence that Rab27a regulates the transport of organelles (melanosomes) in melanocytes[12].

Our findings indicate that stable expressions of mutated *SASH1* genes enhance expression of premelanosome and mature melanosome resident proteins (TYRP1 and Pmel17), and melanosome transport protein (Rab 27a) to increase the biosynthesis and transport of melanin in melanocytes. And we had observed these changes in the epidermis of the Chinese DUH patient in our study .

RESULTS

Mutations of *SASH1* in patients with DUH

We had previously mapped the locus for autosomal dominant DUH to a 10.2 Mb region on

chromosome 6q24.2-q25.2 flanked by markers D6S1703 and D6S1708, which contained more than 50 candidate genes. We screened selected genes in this region and found heterozygous mutations encoding amino acid substitutions in the 21st gene, SAM and SH3 domain containing I (*SASH1*), in the probands in each of the three nonconsanguineous DUH families. These were: T→G substitution at nucleotide 2126 in exon 14 in family I; T→C substitution at nucleotide 2019 in exon 13 in family II; and G→A substitution at position 2000 in exon 13 in family III (Fig.1a). The three nucleotide changes cause nonconservative, missense mutations in *SASH1*, resulting in amino acid substitutions of Tyr to Asp at codon 551 (TAC→GAC), designated Y551D (Mutation 3); Leu to Pro at codon 515 (CTC→CCC), designated L515P (Mutation 2); and Glu to Lys at codon 509 (GAA→AAA), designated E509K (Mutation 1) (Fig.1a). These sequence changes were also confirmed in all the affected family members tested, but were not observed in unaffected family members illustrating concordant segregation with the phenotype. None of the three mutations were observed in 500 normal individual controls or in any of the current databases including the HapMap database. The mutations are therefore unlikely to be general SNPs.

Increased quantity of melanin and hyperdispersion of melanin exist in basal layers and the upper layers above basal layers in a DUH patient's epidermal tissues.

Melanin maldistribution and increased melanin were clearly evident in melanocytes of basal layers and stratum spinosum, stratum granulosum and even stratum lucidum of the epidermal tissue of a DUH patient with *SASH1* Mutant 3. The pathological characteristics can be described in detail as follows.

(1) Massive and darker melanin not only localized in the tops of melanocytes but also in the bottoms of melanocytes in basal layers (Fig. 1b, e, f and h). Meanwhile , in the tops and bottoms of melanocytes in those layers above basal layers (stratum spinosum, stratum granulosum and stratum lucidum), melanin was also clearly observed (Fig. 1b,e and h). In hypopigmention regions, low or zero levels of synthetic melanin were observed in basal layers and in those layers above basal layers of the DUH patient's epidermal tissue (Fig. 1 d and i).

(2) The cells transferred from stratum basale to the layers above basal layers were identified as melanocytes by the application of HMB45 antibody using a specific marker of melanocyte, Pmel17 [12] (Supplementary Fig. 1). Transferred melanocytes can be observed in the upper layers above basal layers in the DUH patient's epidermis (Supplementary Fig.1a, b and d).

(3) The thickening of layers above the basal layers and the deformation of melanocyte morphology in different epithelium layers were also observed in the DUH patient's tissues compared with those of normal controls (Supplementary Fig.1 a, b and d).

(4) The amount of melanin quantified by the Image Pro plus 5.1 software analysis indicated higher and more skewed melanin values (integrated optical density, IOD) in the epidermal tissue of the DUH patient compared to that of normal controls (Supplementary Fig.6). Furthermore, most of the melanin quantitative values of the DUH patient were higher than those of normal controls.

(5)Although there were increased melanocytes levels in several regions and lower levels in other several regions in the basal layers of the DUH patient, there was no total variance in the quantity of melanocytes in the epidermis of the DUH patient relative to normal controls (Supplementary Fig. 2 i and j).

Mutations of SASH1 increase mobility of melanocytes *in vitro*.

Mutation of SASH1 can encourage increased mobility of melanocytes from stratum basale to stratum spinosum, stratum granulosum and even stratum lucidun in the DUH patient's epithelium (Supplementary Fig1. a, b and d). Given the important indications that mutant *SASH1* enhances the mobility of melanocytes, we mimicked the mobility of melanocytes in vitro using migration assay and invasion assay. As shown in Supplementary Fig. 2 A to F and Supplementary Fig S2 m, the number of migrating cells of BM1-, BM2- and BM3-A375 all exceeded significantly that of the A375 cells, BF- and BM0-A375. Analogously, the numbers of invasive cells of BM2- and BM3-A375 were also more than those of BM0-A375 (Supplementary Fig.2 G to L and n). Interestingly, overexpression of wild type *SASH1* in A375 cells can promote the invasion of A375 as shown by the comparison of the number of invasive cells between A375, BF- and BM0-A375(Supplementary Fig. S2 G,H and I), indicating that SASH1 can stimulate the invasion of melanoma cells. The increased mobility of melanocytes caused by *SASH1* mutation probably suggests augmented movements of melanocytes *in intro* and *in vivo*.

Wild type *SASH1* and mutated *SASH1* localize in the edge of cytoplasm in A375 cells and ectogenesis *SASH1* mutation introduced in A375 cells results in elevated expression of *SASH1*

The functional domains of SAM and SH3 of SASH1 suggest its role in signaling molecules, adapters and scaffold protein in signaling pathways[13]. We further characterized the expression and subcellular localization of SASH1 in A375 cells. The colocalization of ectogenous wild type SASH1 and Flag could be clearly observed at the edge of cellular membrane (BM0-A375 D and H in Fig. 2a). The colocalization site of SASH1 and Flag in cytoplasm would appeared to be localized in the site of the ongoing cell fusion of two cells (indicated by red arrows in BM0-A375H of Fig. 2a) , which indicates that SASH1 was probably involved in the migration or invasion and metastasis of A375 melanoma cells. Actually, the wound-healing assay and the increase of matrix metalloproteinase1 (MMP1), MMP2 and MMP8 in melanoma cells in our test supports this hypothesis (data not shown). The phenomenon of locally increasing expression of SASH1 in cell plasma gradually disappeared when two-cell fusion had taken place (indicated by blue arrows in BM0-A375 H in Fig.2a). Mutant *SASH1* and Flag fusion also localized in cytoplasm. Nevertheless, unlike the colocalization of wild type of SASH1-Flag fusion protein which showed obvious local expression at the edge of cytoplasm, the colocalization of mutated SASH1-Flag fusion protein presented a more disperse distribution in the cytoplasm. The relationship of the colocalization sites of mutated SASH1 and Flag to the site and direction of two cell fusion is less obvious than those of wild type of SASH1 and Flag (Fig. 2b,c,d).

When mutant *SASH1* gene is stably expressed in A375 cells, mutations of *SASH1* can induce significant up-regulation of SASH1 (Fig. 3a , b and c and Supplementary Fig.3) . Immunohistochemistry (IHC) analysis shows that SASH1 has a similar or identical hyperdispersion and high expression with melanin (Fig. 3d,f and g). Obviously, high levels of SASH1 not only express in melanocytes of basal layers but also in those of the layers above basal layers (Fig. 3d and g). Surprisingly, low or zero levels of SASH1 were also observed in the hypopigmentary regions (Fig. 3e

and h). In conclusion, elevated SASH1 expression in melanocytes of the DUH patient epidermis and in A375 stably expressed mutant *SASH1* showed that *SASH1* mutation produced activation of SASH1 *in vivo* and *in vitro*. This leaves the question of the effect of SASH1 mutation on melanin synthesis.

Activation of SASH1 results in up-regulation of the matrix protein of pre-melanosomes and mature melanosomes, Pmel17 and TYRP1 in a DUH patients' tissues and in A375 cells

The first problem we addressed was whether elevated expression of SASH1 leads to increase expression of the matrix protein of premelanosomes and mature melanosomes, leading to increased melanin synthesis in melanocytes. Mutation of *SASH1* can induce up-regulation of *Pmel17* and *TYRP1* (Fig. 4a, b and c, Supplementary Fig. 4a, b, c, d and e). In addition, immunofluorescence analysis shows that mutation of *SASH1* can induce increased expression of Pmel17 and TYRP1 and differential expression of Pmel17 and TYRP1 as between A375 stably expressing wild type *SASH1* and mutant *SASH1* (Fig. 4d, d and f, Supplementary Fig. 4f, g and h).

Similarly, IHC analysis (Fig. 4g, i and j; Fig.4m, o and p) shows hyperdispersion and overexpression of Pmel17 and TYRP1 to be mainly concentrated in melanocytes of basal layers in the DUH patient tissue apart from some minor expressions of Pmel17 and TYRP1 in melanocytes in the upper layers above the basal layers. Compared with the regions with high levels of Pmel17 expression in some regions, relatively lower levels of Pmel17 and TYRP1 were observed in melanocytes in hypopigmentary regions (Fig.4h; and Fig.4n and q). Western blotting (Fig. 4c) shows that mutation of *SASH1* can significantly increase TYRP1 expression in BM2- and BM3-A375 cells at 75KDa molecular weight. As well as the prominent band of TYRP1 which was visible at 75KDa from A375 cells to BM3-A375 cells, another more prominent band of TYRP1 about 120KDa was detectable in BM0-, BM1-, BM2- and BM3-A375 cells. There was a noticeable difference in 120KDa molecular weight of TYRP1 in BM0-, BM1-, BM2-and BM3-A375 cells.

Elevated expression of SASH1 results in up-regulation of the transport protein of melanosomes, Rab 27a in a DUH patient's tissues and in A375 cells

The second problem to be clarified was whether SASH1 activation can enhance the movement of melanosome along microtubules towards the cell periphery in melanoncytes. In fact, elevated expression of SASH1 enhanced expression of Rab 27a (Fig. 5a and b, Supplementary Fig. 5a, b and c). In addition, immunofluorescence analysis (Fig.5c and d) showed that elevated expression of SASH1 can induce increased expression of Rab 27a . Rab 27a in BM0-, BM1-, especially in BM2- and BM3-A375 cells showed significantly increased expression and flash point-like distribution in the cell periphery. Similarly, immunohistochemistry analysis revealed much more expression and hyperdispersion of Rab 27a in epidermal melanocytes of the DUH patient's epidermal tissues (Fig.5e, g and h). However, in the hypopigmentary regions, low or zero levels of Rab 27a expression were observed in epidermal melanocytes and epidermal keratinocytes (Fig.5f and i).

Results of pull down assay and Nano-flow LC-MS/MS indicate that SASH1 is involved in melanin metabolism.

Since *SASH1* mutation can induce the abnormal expression of melanosome associated proteins, the

third problem we wanted to investigate was how SASH1 regulates the melanin metabolism. We used pull down assay and Nano-flow LC-MS/MS in duplicate experiments to investigate the interaction of proteins with SASH1 in BM0-A375 cells. The results of pull down assay and LC-MS/MS of BM0-A375 cells showed that SASH1 interacted with MAP4K4, MAPKK2 and CALM, all of which are important proteins related to melanogenesis (Supplementary Fig.7, Supplementary Table 1), in regulating melanin metabolism. Mass spectrum analysis of BM0-A375 cells and the breast cancer cell line, MDA-MB-231 stably transfected with wild type of *SASH1,* has shown that SASH1 interacts with IQGAP1 (Supplementary Fig.7b), the protein responsible for cell motility and invasion[14].The information on "melanogenesis" presented in http://www. genome.jp/dbget -bin/show_pathway? hsa04916 +5605 suggests that MAPKK2 (MEK2) is located in the MAPK signal pathway and regulates melanogenesis in melanocytes. In addition, the information on MAP4K4 presented in http://www.genome. jp/dbget-bin/show_pathway? hsa04010+9448 indicates that MAP4K4 indirectly activates MAPKK2 through MEKK1. Importantly, SASH1 can interact with CALM to directly regulate melanin synthesis (Fig.6, Supplementary Fig.7e). The PANTHER function classification indicates that the identified proteins are involved in cell adhesion, metabolic process and enzyme regulator activity (Supplementary Fig.7c, Supplementary Table 2). Importantly, according to PANTHER function pathway classification, several identified proteins are members of the Ras pathway and the endothelin signaling pathway, two pathways associated with melanogenesis (Supplementary Table 1 and 2). Overall, we can come to the preliminary conclusion that SASH1 is involved in melanogenesis and melanin synthesis through the MAPK signaling pathway and/or the endothelin signaling pathway (Fig. 6).

DISCUSSION

Dyschromatosis universalis hereditaria (DUH) is a clinically heterogeneous disorder that shows generalized mottled pigmentation and was first reported by Ichikawa and Hiraga in 1933. We had established that *SASH1* is the disease causing gene in autosomal dominant DUH and that mutation of *SASH1* can effect the activation of SASH1. Activation of SASH1 promotes increased biosynthesis of melanosome matrix protein and melanosome transport protein to augment melanin production and melanin transport in melanocytes. In addition, we established that DUH is a disorder of increased production of melanosomes caused by *SASH1* mutation together with distribution heterogenicity of melanocytes. Most importantly, we identified that SASH1 could interact with several proteins involved in melanogenesis, and this provides important evidence for the investigation of the molecular mechanism associated with increased melanogenesis caused by *SASH1* mutation. The present study had made an comprehesive interpretation on pathogenesis of dyschromatosis universalis hereditaria.

Stuhrmann revealed the first locus for autosomal recessive DUH and which is in line with recent evidence that DSH and DUH are genetically distinct disorders[3]. Zhang et al [15]mapped the gene for DSH to 1q11-1q21 and found that a novel mutation of a heterozygous nucleotide A→G transition at position 2879 in exon 10 of the *DSRAD* gene is involved in DSH. Subsequent research on dyspigmentation has demonstrated that the pathogenicity gene for DSH is localized in the *DSRAD* gene on chromosome 1q[16-23]**.** Mutations in the *ADAR* (*DSRAD*) gene have been identified in Japanese, Chinese and Taiwanese families with autosomal dominant DSH[8]. Following on from Stuhrmann's

findings, our own earlier study presented photographic evidence of dyschromatosis over large areas of the bodies of DUH patients[6], revealed the first locus for autosomal dominant DUH and identified *SASH1* as the disease causing gene for DUH.

There is considerable ultrastructural skin and immunochemistry data to suggest that DUH may be a disorder of melanosome production and distribution in melanocytes and keratinocytes rather than a disorder of melanocyte numbers in hyperchromic macules[5-8] and our own observations are consistent with this. *SASH1* mutation can encourage the mobility of melanocytes *in vitro* and *in vivo*, which, to a degree, illustrates increased movement in melanocytes from basal layer to the layers above basal layers. In addition, SASH1 may participate melanogenesis in melanocytes through the SASH1/MAP4K4/MEKK1/MEK2/ERK1/2/MITF/TYRP1 signal pathway and/or the SASH1/CALM signal pathway. Taken together, our observations indicate that SASH1 is a new and important molecule responsible for melanin biosynthesis and that SASH1 activation and activation of downstream molecules caused by *SASH1* activation in the two putative signal pathways are likely to be important etiological factors in DUH.

Normally, skin pigment melanin is synthesized by melanosome in melanocytes, which are located in the basal layer of the epidermis. Melanosomes begin to mature with the transformation of vacuolar endosome intermediates (stage I) into nonpigmented stage II premelanosomes bearing intralumenal fibrillar sheets upon which melanin ultimately deposits. Pmel17 localizes to stage II premelanosomes only after passing through the coated endosome. Melanin synthesis in late-stage (III and IV) melanosomes requires the selective targeting of integral membrane melanogenic enzymes, such as tyrosinase and TYRP1 and other components that regulate enzyme activity[11,24]. The present study suggests that activation of SASH1 can results in up-regulation of Pmel17, the protein responsible for melanin and melanin polymerization and TYRP1, the protein responsible for melanin biosynthesis and tyrosinase stabilization in the tissue of DUH patients and in A375 cells. The increased expression of TYRP and Pmel17 indicates intensive activity of melanogenic enzymes in melanosomes or increased melanosome synthesis. Although melanosome-like structures were not observed by our electronicmicroscope examinations (data not shown), our findings suggest that many more matrix proteins of melanosomes are involved in melanosome synthesis or that more melanosomes were synthesized to produce more matrix proteins of melanosomes.

Myosin VIIa and Rab27a, whose function is transporting and constraining melanosomes within a region of filamentous actin, are particularly important for melanosome motility and localization in the retinal pigmented epithelium (RPE) cells[25]. Our data suggest that *SASH1* mutations in A375 melanoma cell and the epidermal tissues of DUH patients permit up-regulation of Rab 27a. This implies that mutation of *SASH1* not only arouses increased biogenesis of melanosomal compartments but also enhances the transport of melanosomes in melanoncytes. There exists increased transport of melanosomes and no imbalance of melanin transport between melanocytes and keratinocytes .

SASH1 had originally been identified as a candidate tumour suppressor gene in breast cancer[13]. Expression levels of *SASH1* are strongly and significantly reduced in the advanced stages of colon cancer as well as in liver metastases. Downregulation of *SASH1* expression is correlated with the formation of metachronous distant metastasis and is an independent negative prognostic parameter for

patient survival[26]. Novel candidates including signaling adapter SASH1 have been shown to bind to 14-3-3s in response to IGF1/PI 3-kinase signaling[27]. Our pull down and LC- MS/MS analysis demonstrated that SASH1 interacts with three 14-3-3s (Supplementary Table 1). Our study also provides additional significant data on SASH1 with regard to melanogenesis and tumor metastasis, which should assist further investigation of this new gene.

The occurrence of hyper and hypopigmented macules over the entire body is the principal feature of DUH[28]. We can summarise our findings *in vivo* and *in vitro* by highlighting the four stages in the pathogenesis of dyschromatosis universalis hereditaria . The first stage is the activation of *SASH1* induced mutation of *SASH1*; the second is the activation of the downstream molecules by SASH1 in the SASH1/MAP4K4/MEKK1/MEK2/ERK1/2 /MITF/ TYRP1 signal pathway and/or the SASH1/CALM signal pathway followed by increased activity of melanogenic enzymes to elevate the biosynthesis of melanosomes and the transport of melanosome in melanoncytes; the third is increased biosynthesis and transport of melanosomes produces increased biosynthesis of melanin and increased transfer of stage IV melanosome from melanocytes to neighbour keratinocytes; the fourth is an increase in melanin in keratinocytes eventually results in the formation of hyperpigmented macules. Functional analysis of SASH1 provides convincing evidence that *SASH1* is the pathogenic gene for DUH and that *SASH1* mutation Leu to Pro at codon 515 (CTC→CCC) and especially the Tyr to Asp at codon 551 (TAC→GAC) are responsible for the pathogenesis of DUH. These findings on the disease causing gene and on the pathogenesy of DUH should assist in the prevention and therapeutics of DUH, and, in addition ,the analysis of the pathogenesy of DUH will provide important references in explaining the pathogenesis of other dermatoses.

METHODS

Patients and cells

This research was approved by the ethical review committees of the appropriate institutions. In total, 50 family members participated in the study after giving informed consent. Samples of peripheral- blood DNA were taken from all available family members. A375 cells (a malignant melanoma cells or a melaocytes) was obtained from the Shanghai Institute for Biological Sciences, Chinese Academy of Sciences, and cultured in Dulbecco's modified Eaglemedium (DMEM) with 10% FRONT^{TM} fetal brovine serum (FRONT BIOMEDICALS,USA) at 37℃ in a 5% CO_2 incubator (Thermo scientific).

PCR, sequencing and mutational analysis

Genomic DNA was extracted from peripheral blood leucocytes using standard procedures. We carried out mutational screening by bi-directional sequencing using an ABI BigDye terminator Sequencing Kit 3.1 (Perkin Elmer) and an ABI 3100 Genetic Analyzer (Perkin Elmer). We imported the sequence information into Vector NTI version 7.0 and aligned the sequences of the affected and normal individuals to identify variations .

Synthesis of full cDNA sequence of wild type *SASH1*, plasmid construction and site-directed mutagenesis of *SASH1* gene

For reference purposes we categorized the three SASH1 mutations we found as Mutation1(M1),

Mutation2(M2) and Mutation3 (M3) . Wild type SASH1 is named Mutation0 (M0). A full cDNA sequence (3744bp) of the CDS of wild type SASH1 was synthesized artificially and cloned into pEGFP (Biosciences Clontech) via the Hind III and Kpn restriction sites using SASH1 primers: SASH1F 5'-cccaagcttatggaggacgcgggagcagc-3', SASH1R 5'-cggggtaccctaca tggcctcagggcctgg We followed the protocol and used the mutagenesis primers as directed by the site t https://www. genomics. agilent.com/CollectionSubpage.aspx? PageType=Tool&Sub PageType= Tool QCPD&PageID=15. The three mutations were performed following the site-directed mutagenesis of QuikChange® II XL Site-Directed Mutagenesis Kit (Stratagene). The site directed mutagenesis primers are indicated in table S3.

Plasmid Construction and Transfection

We first had to synthnize a pair of complementary sequences containing XhoI and HpaI restriction enzyme sites for insertion into the multiple cloning site (MCS) of the retrovirus pBABE vector (Cell Biolabs, Inc,USA), with which MCS had been cloned with streptavidin binding protein (SBP), calmodulin binding protein (CBP) and Flag tag sequences. The forward primer of the complementary sequence was 5'AATTCCCGCTCGAGCG GGTT AACATGG3'; the reverse primer was 5'TCGAC CAT GTTAAC CCG CTCGAG CGG G3', enabling the wild type and mutated SASH1 cDNA sequence to be ligated into the MCS of the modified retrovirus pBABE vector from the SASH1-pEGFP recombined vectors. The modified retrovirus pBABE vectors were transfected into HEK 293T cells for virus packaging and A375 cell infection. The infected A375 cells were screened with 1.5μg/ml puromycin to construct A375 cells stably expressing both the wild type and the three mutant SASH1 (s). Different groups of A375 cells stably expressing ectogenic wild type and three mutant SASH1 genes were named BM0-A375, BM1-A375, BM2-A375, BM3-A375 cells, respectively. The A375 cells which were stably expressed and those not infected by the pBABE virus were named BF-A375 cells and A375 cell, respectively.

The subcellular location of SASH1 identified by immunofluorescence and confocal microscope

BM0-, BM1-, BM2- and BM3-A375 cells were plated in 6-well chamber slides and incubated at 37□ for at least 48h and were stained using the indirect immunofluorescence methods. When the slides were confluent monolayer cells, they were taken out of culture for immunofluorescence analysis. Immunofluorescence assay were performed according to the protocol of manufacturer (GENMED SCIENTIFICS INC, USA). This cells were incubated with mouse anti-SASH1 Antibody, (1:50 in PBS,Abnova) and rabbit anti-DYKDDDDK Flag polyclonal antibody (1:50 in PBS, SAB,USA)for overnight at 4 □. After three times wash in phosphate buffered saline, Cy3-conjugated affinipure goat anti-mouse IgG(H+L)(1:100 in PBS) was reacted with mouse anti-SASH1 Antibody; DyLight488 goat anti-rabbit IgG(H+L)(1:100 in PBS,MULTI SCIENCES,USA) was reacted with rabbit anti-DYKDDDDK Flag antibody. The reactivities of DyLight488 (488nm) , Cy3(552 nm) and DAPI were visualized as green, red and blue signal, respectively. Fluorescenc signals were also obtained and analyzed by LSM 510 inverted Confocal Laser Scan Microscope (Zeiss, Germany) .

Melanin staining and immunohistochemistry of epithelial tissues from one DUH patient in family I with Mutation 3

1.Melanin staining The paraffin sections with 5 μm epithelial tissue were incubated in 80□-baking oven for 30min and kept at room temperature for 15min. These sections were incubated successively in GENMED dewaxing liquid for 45min, GENMED dehydration liquid for 3min, GENMED strengthening

liquid for 3min, GENMED supernatant for 3min and GENMED cleaning liquid for 3min(GENMED SCIENTIFICS INC. U.S.A) and cleaning liquid was removed finally. Samples on sections were fully covered with 200 μL GENMED staining working fluid and kept in a dark incubator at 45℃until liquid on the sections had appeared dark brown. Then GENMED working fluid on sections was removed and sections were carefully placed into 50mL cleaning liquid and incubated for 2min.Finally the cleaning liquid on sections was charily dislodged and covered with 200mL GENMED equilibrium liquid and incubated for 3min, finally, equilibrium liquid was discarded. Sections were placed into 50mL GENMED cleaning liquid for 2 min incubator at room temperature , followed by cleaning liquid removal. And samples on sections were wholly covered with GENMED stabilizing fluid and incubated for 2min. The stabilizing fluid was removed and samples were performed with transparent disposal and sealed with slides and then observed under a light microscope.

2.Immunohistochemical staining

Epithelial tissues from one patient in family I with mutation 3 were fixed in 10% formalin at 4 □ for 24 hr and then embedded in paraffin. Paraffin sections (5 μm) incubated in 56□ overnight were deparaffinized and rehydrated using xylene and gradient ethanol. The sections were incubated with blocking solution (5% BSA in phosphate-buffered saline) for 30 min at room temperature, followed by a 37□-1h incubation and a 4□ overnight incubation with SASH1 monoclonal antibody (1:50, Bethyl,USA),HMB45 monoclonal antibody (1:50, Santa Cruz Biotechnology Inc), TYRP1 monoclonal antibody(TA99,1:50,Abcam) and Rab 27a monoclonal antibody (3μg/ml, Abcam) in PBS. After 5min/time wash with TBS for 3 times, horseradish peroxidase-linked-anti-rabbit and anti-mouse universal secondary antibody was added to incubate for 30min at 37□. Subsequently, the immune complexes were visualized with diaminobenzidine (DAB) using the positive position microscope BX51 (Olympus,Japan) and DAB colouration was terminated by PBS timely when yellow staining appeared. Finally, sections were counterstained with hematoxylin, mounted and finally observed and photographed under the positive position microscope BX51 at magnifications of ×1000.

Melanocyte mobility assay

Capability of migration and invasion of melanocytes was assessed in a transwell system using polycarbonate filters with 8.0um pores (BD Biosciences and Millipore Corporation, Bedford, MA). Prior to invasion, the upper polycarbonate filters were coated with 20μg of Matrigel and the filter was dried at room temperature. Different A375 cells were washed three times with FBS-free DMEM and cell suspension (100μl,containing 6.75×10^4 cells) was placed in the upper compartment in three separate experiments performed in triplicate. 0.6 ml of DMEM containing 10% FBS was added in the lower compartment. After crystal violet staining, cells that migrated and invaded during the 24hr period were counted in at least five areas in a transwell plate and photographed by bright-field microscopy(50X magnification and 100X magnification for each groups of cells).

Design ,Preparation and Transfection of dsRNA

SiRNAs (19+2 format; 19 nucleotide duplex with two 3′uracyl nucleotide overhangs) were synthesized by Shanghai GenePharma Co.,Ltd (Shanghai, China) . The sense and antisense strands for each siRNA for

SASH1,*GAPDH* and negative control are shown in table S3. SiRNAs were dissolved in 150μL of diethyl pyrocarbonate (DEPC) treated water (20mM final concentration) and 15 μL of aliquots were removed for analysis. When the A375 cells stably expressed wild type and mutated *SASH1* gene and pBABE retrovirus vector grown to 80% cell confluency in 6-well dish and for transfection, cells were transfected (in triplicate) with 3.33μg of *SASH* specific siRNA ,negative control and GAPDH Positive control (113.6 nM final concentration), diluted in 37.5μL in optiMEM medium (Invitrogen). 27μL of EntransterTM-R transfection reagent (Engreen Biosystem Co.,Ltd,UK) were diluted in 23μL optiMEM medium and incubated at room temperature for 5 minutes. This EntransterTM-R transfection reagent mixture was added to the siRNA mixure and incubated for 20 minutes at room temperature . The transfection efficiency was observed by fluorescence microscope after 24hr.

Real-time RT-PCR for determination of *SASH1,TYRP1, Pmel17* and *Rab 27a* mRNA

Total RNAs from different groups of A375 cells were isolated in triplicate using TRIzol Reagent (Invitrogen). Reverse transcription was carried out according to the protocol of PrimeScript TM RT reagent Kit (TaKaRa, Japan). The sense and antisense primer sequence of *SASH1* ,*TYRP1* , *Pmel17*, *Rab 27a*,and *GAPDH* are presented in tableS3. The PCR products were confirmed by agarose gel electrophoresis. Real-time PCR was performed using Applied Biosystems 7500 with SYBR Premix Ex TaqTM (TaKaRa, Japan). The quantity of each mRNA was detected and normalized to that of *GAPDH* mRNA.

Immunofluorescence and confocal microscopy for melanosome matrix proteins and transport protein

When the confluence of cells reached 50%-70%,BF- and BM0-, BM1-, BM2-, BM3-A375 cells grown on coverslips in 12 well dishes were washed with PBS precooled at 4□. Then these cells were fixed in methyl alcohol /acetone mixed solution (volume ratio is1:1) precooled at -20℃ for 6min at 4□ and permeabilized with 0.1% Triton X-100 in PBS for 5 minutes. For immunofluorescence, cells were incubated with the following primary antibodies: HMB45 (anti Pmel17) mAb (1:50 in PBS; Santa Cruz Biotechnology Inc.) and TA99 (anti-TRP1) mAb (1:50 in PBS;abcam) and Rab 27a mAb (3μg/ml in PBS;abcam) . The primary antibodies were visualized after appropriate washing with PBS, using the DyLight TM 488 Conjugated Goat anti- mouse IgG-(H+L) (1:100 in PBS; MULTISCIENCES, USA). Nuclei were visualized using DAPI (1:10000 in PBS; Sigma Chemicals Co). In addition, BF-, BM0-, BM1-,BM2- and BM3-A375 cells on coverslips in 12-well dish were transfected with specific dsRNA of *SASH1* ,*GAPDH* Positive control and negative control when the confluence of cells reached 50%-70%. After the knockdown of *SASH1* gene for 72hr by its specific dsRNA, the same immunofluorescence procedure as described above were performed. Fluorescenc signals were analyzed both by recording stained images using inverted fluorescence microscope system (OLYMPUS, Japan) and DPC controller software (OLYMPUS, Japan). Fluorescence signals were also obtained and analyzed on an LSM 510 inverted Confocal Laser Scan Microscope (Zeiss, Germany) and a Nikon A1R inverted Confocal Laser Scan Microscope (Nikon,Japan). A total of 15 randomly microsopic fields of vision in different A375 cells expressed mutated or wild type SASH1 gene were analyzed and photographed to measure IOD (integrated optical density) using Image-Pro Plus 6.0 image analysis software.

Electrophoresis and Western Blotting of SASH1 ,TYRP1 and Rab 27a

Cell extracts were prepared using mammalian cell protein extraction reagent with a mixture of protease inhibitors and protein concentrations were measured using BCA protein assay kit. Cell extracts were mixed with 5×SDS-PAGE loading buffer supplemented with 0.1% beta- mercaptoethanol and were boiled for 10 min. Samples were then separated using 1× Tris- Glycine- Buffer (8%-10% Tris-glycine gels, Bio-Rad), and were transferred to PVDF transfer membranes (Millipore Corporation, USA). Blots were blocked in 5% (w/v) non-fat dry milk in TBS-T for 1 hr at room temperature and were then incubated with the appropriate SASH1 antibody (1:400, Bethyl, USA), anti-DYKDDDDK Flag monoclonal antibody (Shanghai Genomics, China), TYRP1 antibody (abcam) and Rab 27a antibody (abcam) diluted in 5% non-fat dry milk in TBS-T overnight at 4□. After 3 times wash with TBS-T, blots were also incubated in horseradish peroxidase-linked anti-rabbit or anti-mouse whole antibodies in 5% nonfat dry milk in TBS-T for 1hr at room temperature. After 3 times of further washes with TBS-T, the immunoreactivities of the antibodies were detected by LAS-3000 fluorescence and a chemiluminescence image formation system (Japan) using a Thermo SCIENTIFIC SuperSignal West Pico Chemiluminescent Substrate (Thermo Fisher Scientific Inc., USA).

Pull down assay and Nano-flow LC-MS/MS.

1.Pull down assay Ten 150 mm plates stable cells were splited with 10ml of NP40 buffer(50mM pH7.4 Tris-HCl,150mM NaCl, 0.5%NP40) on ice for 30 min and the cell lysis buffer was transformed into a centrifuge tube and centrifuged at 4□,13000rpm for 15min.The supernatant was collected into a eppendorf tube and added 60 μl of SBP beads for 3hr rotation at 4℃.Then the mixture of cell lytics and SBP beads was centrifuged at 4℃, 2000rpm for 1min and the supernatant was discarded. After 4℃ -2000rpm-1min centrifugation and washing with PBS for two times, the precipitates were added 1 ml of 50mM NH4HCO3 and digested with 2μg trypsin on the rotator at 37□ overnight.The digestion products were centrifuged at 4℃, 2000rpm for 1min and supernatants were collected and digested with 2μg trypsin on the rotator for 8hr at 37℃again.Finally, the two digestion products was treated with vacuum drying.

2.Nano-flow LC-MS/MS A Nano-LC MS/MS experiment was performed on an HPLC system composed by two LC-20AD nano-flow LC pumps, an SIL-20 AC auto-sampler and an LC-20AB micro-flow LC pump(Shimadzu, Tokyo, Japan) connected to an LTQ-Orbitrap mass spectrometer (ThermoFisher, San Jose, CA). Sample was loaded onto a CAPTRAP column (0.5 ×2 mm, MICHROM Bioresources, Auburn, CA) in 6 min at a flow rate of 25μL/min. The sample was subsequently separated by a C18 reverse-phase column (0.10 ×150 mm, packed with 3 μm Magic C18-AQ particles, MICHROM Bioresources, Auburn CA) at a flow rate of 500nL/min. The mobile phases were 5% acetonitrile with 0.1% formic acid (phase A and the loading phase) and 95% acenitrile with 0.1% formic acid (phase B). To achieve proper separation, a 90-min linear gradient from 5 to 45% phase B was employed. The separated sample was introduced into the mass spectrometer via an ADVANCE 30μm silica tip (MICHROM

Bioresources, Auburn CA). The spray voltage was set at 1.9 kV and the heated capillary at 180℃. The mass spectrometer was operated in data-dependent mode and each cycle of duty consisted of one full- MS survey scan at the mass range 385~2000 Da with resolution power of 100,000 using the Orbitrap section, followed by MS/MS experiments for 10 strongest peaks using the LTQ section. The AGC expectation during full-MS and MS/MS were 1,000,000 and 10,000, respectively. Peptides were fragmented in the LTQ section using collision-induced dissociation with helium and the normalized collision energy value set at 35%.Previously fragmented peptides were excluded for 60s.

3.Database Search Tandem mass spectra were analyzed using Sequest (ThermoFisher, San Jose, CA; version 28). Sequest was set up to search the human proteome database from UniProt release 2010_08 (downloaded from http://www.uniprot.org/uniprot/?query=organism:9606+keyword:181) . Peptide probability was specified by PeptideProphet and protein probabilities by ProteinProphet. Proteins that contained similar peptides were grouped together.

4.Bioinformatic analysis for function classification

We classified the function of proteins according to three criteria, the Molecular Function (MF) and Biological Process (BP) from Gene ontology (GO) database (http://www.geneontology.org/, 10/11/2010) and the PANTHER pathway from PANTHER (http://www.pantherdb.org/, 10/11/2010). The GO terms we used are the first level of GO topologies, that is, the direct child GO term to "GO: 0003674, molecular function" and "GO: 0008150, biological process". After downloading the GO annotation for homo sapiens, we add the parent GO annotations to each protein according to the Parent-child topology. Then, for each MF, BP or pathway, we found all matching proteins annotated from the list and calculated the percentage divided by the total number of proteins as shown in tables S1 and S2. The pie chart for function classification shows the proportion of each function within the functions analyzed.

Statistical analysis

Data are presented as mean value ± standard error. These data were firstly analyzed using a homogeneity of variance test and the data of heterogeneity of variance were analysed by change of variable. Statistical significance was made by one-factor analysis of variance using LSD on SPSS16.0 to generate the required p-values. The cartograms were made and plotted using GraphPad Prism 5.

References

1. Ichikawa, T., Hiraga,Y. A previously undescribed anomaly of pigmentation dyschromatosis universalis hereditaria. *Jpn J Dermatol* **34**, 360-4 (1933).
2. Xing, Q., et al. A Gene Locus Responsible for Dyschromatosis Symmetrica Hereditaria (DSH) Maps to Chromosome 6q24.2-q25.2. *Am. J. Hum. Genet* **73**, 377–82. (2003).
3. Stuhrmann, M., et al. Dyschromatosis universalis hereditaria: evidence for autosomal recessive inheritance and identification of a new locus on chromosome 12q21-q23. *Clin Genet* **73** 566-72. (2008).
4. Yusuf, S., et al. Dyschromatosis universalis hereditaria in a young Nigerian female. *Int J Dermatol*

48, 749-750 (2009).

5. Wang, G., et al. Dyschromatosis universalis hereditaria: two cases in a Chinese family. . *Clinical and Experimental Dermatology* **30**, 494-496 (2005).
6. Nuber , U., Tinschert,S., Mundlos,S., Hauber,I. Dyschromatosis universalis hereditaria: familial case and ultrastructural skin Investigation. *Am J MedGenet A* **125**, 261–266 (2004).
7. Hata, S., Yokomi,I. Density of dopa-positive melanocytes in dyschromatosis symmetrica hereditaria. *Dermatologica* **171**, 27-9. (1985).
8. Kim, N., et al. Dyschromatosis universalis hereditaria: an electron microscopic examination. *J Dermatol* **24**, 161-4 (1997).
9. Raposo, G.et al. Distinct Protein Sorting and Localization to Premelanosomes, Melanosomes, and Lysosomes in Pigmented Melanocytic Cells. *The Journal of Cell Biology* **152**, 809–823 (2001).
10. Raposo, G.a.M., MS. The Dark Side of Lysosome-Related Organelles:Specialization of the Endocytic Pathway for Melanosome Biogenesis. *Traffic* **3**, 237-248 (2002).
11. Marks, M.a.S., MC. THE MELANOSOME: MEMBRANE DYNAMICS IN BLACK AND WHITE. *Nat Rev Mol Cell Biol.* **2**, 738-748. (2001).
12. Clarkson, K.S., Sturdgess,I C.,Molyneux,A J. The usefulness of tyrosinase in the immuno-histochemical assessment of melanocytic lesions: a comparison of the novel T311 antibody (anti-tyrosinase) with S-100, HMB45, and A103 (anti-melan-A). *J Clin Pathol* **54:**, 196–200 (2001).
13. Zeller, C ，et al. SASH1: a candidate tumor suppressor gene on chromosome 6q24.3 is downregulated in breast cancer. *Oncogene* **22**, 2972–2983 (2003).
14. M., J. IQGAP1 Promotes Cell Motility and Invasion. *J Biol Chem.* **278**, 41237-45. (2003).
15. Zhang, X., et al. Identification of a locus for dyschromatosis symmetrica hereditaria at chromosome 1q11-1q21. *The Society for Investigative Dermatology* **120**, 776-80 (2003).
16. Miyamura Y, et al. Mutations of the RNA-Specific Adenosine Deaminase Gene (DSRAD) are involved in Dyschromatosis Symmetrica Hereditaria. . *Am. J. Hum. Genet* **73**, 693-99 (2003).
17. Liu Q, et al. Novel Mutations of the RNA-Specific Adenosine Deaminase Gene (DSRAD) in Chinese Families with Dyschromatosis Symmetrica Hereditaria. *J Invest Dermatol* **122**, 896 -99 (2004).
18. Xing Q, et al. Identification of a novel ADAR mutation in a Chinese family with dyschromatosis symmetrica hereditaria (DSH). *Arch Dermatol Res* **297**, 139-42 (2005).
19. Xing Q, et al. Novel deletion mutation of DSRAD in a Chinese family with Dyschromatosis Symmetrica Hereditaria (DSH). *EJD* **17**, 247-48 (2007).
20. Suzuki N, et al. Mutation Analysis of the ADAR1 Gene in Dyschromatosis Symmetrica Hereditaria and Genetic Differentiation from both Dyschromatosis Universalis Hereditaria and Acropigmentatio Reticularis. *The Society for Investigative Dermatology* **124**, 1186-92 (2005).
21. Li M, Y.L., Zhu XH.Identification of a novel DSRAD gene mutation in a Chinese family with dyschromatosis symmetrica hereditaria. *Clinical and Experimental Dermatology* **33**, 644-46 (2008).
22. Lu J, et al. Identification of two novel DSRAD mutations in two Chinese families with dyschromatosis symmetrica hereditaria. *Arch Dermatol Res* **298**, 357-60 (2006).

23. Suzuki N, et al. Ten Novel Mutations of the ADAR1 Gene in Japanese Patients with Dyschromatosis Symmetrica Hereditaria. *Journal of Investigative Dermatology* **127**, 309- 311 (2007).
24. Delevoye, C., et al. AP-1 and KIF13A coordinate endosomal sorting and positioning during melanosome biogenesis. *J Cell Biol* **19**, 247-64 (2009).
25. Gibbs, D., et al . Williams.Role of myosin VIIa and Rab27a in the motility and localization of RPE melanosomes. *Journal of Cell Science* **117**, 6473-83 (2004).
26. Rimkus, C., et al. Prognostic significance of downregulated expression of the candidate tumour suppressor gene SASH1 in colon cancer. *British Journal of Cancer* **95**, 1419-23 (2006).
27. Dubois, F., et al. Differential 14-3-3-affinity capture reveals new downstream targets of PI 3-kinase signaling. *Mol Cell Proteomics* **8**, 2487-99 (2009).
28. Kenani, N., et al. Dyschromatosis universalis hereditaria: Two cases. . *Dermatol Online J* **2008**, 16.

Figure legends

Figure 1 | Mutational sites of the *SASH1* gene in DUH patients and the epidermal tissues of a DUH patient of family I with SASH1 Mutant 3 exhibiting increased melanin in most basal layers together with heterogenicity of melanin distribution. a,Mutational sites of the SASH1 gene in three families with DUH. The three nucleotide changes cause nonconservative, missense mutations in SASH1, resulting in amino acid substitutions of Tyr to Asp at codon 551 (TAC→GAC) in pedigree A (family I), designated as Mutation3 (M3); Leu to Pro at codon 515 (CTC→CCC) in pedigree B (familyII), designated as Mutation2 (M2); and Glu to Lys at codon 509 (GAA→AAA) in pedigree C (family III), designated Mutation1 (M1). **b and f,** High levels of melanin and hyperdispension of melanin distribute mainly in basal layers and a few melanin distribute in stratum spinosum, stratum granulosum, even stratum lucidum of the DUH patient's epidermal tissues(40X magnification and 100X magnification). **c and g ,** Normal levels of melanin distribute in basal layers of some regions of the DUH patient's epidermal tissues(40X magnification and 100X magnification). **d and i** , Low or zero levels of melanin are observed in basal layers of some regions of the DUH patient's epidermis(40X magnification and 100X magnification). **e,** High (indicated by red arrows) and low levels of melanin (indicated by yellow arrows) display simultaneously existing patterns in the same sections of the DUH patient's epidermal tissues (40X magnification). **h,** High level of melanin is not only shown in basal layers but in upper layers above basal layers in the DUH patient's epidermal tissues (100X magnification). **j and k,** Normal levels of melanin and homogeneity of melanin distribution are displayed in the epidermal tissues of normal controls(40X magnification and 100X magnification).

Figure 2 | SASH1 localizes at the cytoplasm margin of A375 cells and wild type SASH1 may be involved in directional migration of A375 cells. a, The green fluorescent color indicates the subcellular expression of Flag. The red fluorescent color indicates the subcellular expression of SASH1; while the fluorescent blue color stained with DAPI indicates cell nucleus. The yellow fluorescent color indicates the merging of the green and red fluorescent colors (indicated by blue arrowheads in BM0-A375 D, BM1-A375 D, BM2-A375 D and BM3-A375 D). The red arrowheads shown in BM0-A375 H point to the sites and directions of two-cells ongoing fusion. The blue arrowheads shown in BM0-A375 H point to the sites of two cells already having fused. **b,c and d,** The colocalization of mutated SASH1-Flag fusion protein (yellow fluorescent indicated in BM1-A375 D, BM2-A375 D and BM3-A375 D) presented more dispersed distribution in the cytoplam. The relationship of the colocalization sites and directions of mutated SASH1-Flag fusion protein to the site and direction of two cell fusion is less conspicuous than that of wild type of SASH1-Flag fusion protein (indicated in BM1-A375 H, BM2-A375 H and BM3-A375H).

Figure 3 | Mutations of SASH1 induce enhanced expression of SASH1 in A375 cells and in a DUH patient of family I with SASH1 Mutant 3. a, Real time RT-PCR shows differential expression of SASH1 between BM1-, BM2-, BM3- and BM0-A375 cells, respectively. There is significant difference in expression of SASH1 between BM1-, BM2-, BM3-A375 cells and BM0-A375 cells (n=4). **b,** Western blotting shows differential expression of SASH1 protein in different A375 cells. Immunoblotting, using the SASH1 monoclonal antibody, demonstrates that SASH1 expression in BM1-, BM2- and BM3-A375 cells is higher than that of A375, BF- and BM0-A375 cells (n=4). A particularly prominent band with 180KDa molecular weight was visible at 180 KDa, somewhat exceeding the predicted molecular weight of 136 KDa. **c,** Immunoblotting exhibits enhanced expression of SASH1 protein between BM0- and BM1-, BM2-, BM3-A375 cells with the Flag monoclonal antibody using 8% Tris-glycine gel (n=4). Also, a prominent band of SASH1-Flag fusion protein with 190KDa molecular weight was observed at 190KDa. A second prominent band about 136 KDa was detected and the differential expression of SASH1 between BM3-A375 cells and BM0-A375 cells is much more obvious than that of BM1- and BM2-A375 cells. **d,** High levels of SASH1 expression and SASH1 maldistribution were shown in the whole cytoplasm of melanocytes in basal layers and the upper strata above the basal layer of epidermal tissues of the DUH patient (red arrows indicate higher expression of SASH1, yellow arrows indicate lower or no SASH1 expression,40X magnification). **e,** Low levels of SASH1 expression and SASH1 maldistribution in melanocytes were displayed in basal layers of the DUH patient (red arrows indicate higher expression of SASH1, yellow arrows indicate little or no SASH1 expression,40X magnification). **f and g,** demonstrates higher expression of SASH1 in basal layers and the layers above basal layers of the DUH patient's epidermis (100X magnification). **h,** Low and no SASH1 expression was demonstrated in melanocytes of the DUH patient's epidermis (100X magnification). **i and j,** Normal and homogeneous expression and distribution of SASH1 were shown in the basal layers of epidermis of normal controls (40X magnification and 100X magnification).

Figure 4 | Mutations of *SASH1* increase expression of Pmel17 and TYRP1 in A375 cells and in a DUH patient of family I with *SASH1* Mutant 3. a, Differential expression of *Pmel17* between BM2-, BM3-A375 cells and BM0-A375 cells, respectively (n=4). **b,** Differential expression of *TYRP1* in BM1-,BM2-, BM3-A375 cells and BM0-A375 cells, respectively (n=4). **c,**Western blotting shows differential expression of TYRP1 protein in different A375 cells (n=4). A prominent band of TYRP1 was visible at 75KDa from A375 cells to BM3-A375 cells and another more prominent band of TYRP1 about 120KDa can be detected in BM0-, BM1-, BM2- and BM3-A375 cells. Obvious expression difference of 75KDa molecular weight of TYRP1 exists between BM2-, BM3-A375 cells and A375, BF-, BM0-A375 cells. Noticeable difference of 120KDa molecular weight of TYRP1 exists between BM0-, BM1, BM2- and BM3-A375 cells and A375 and BF-A375 cells. **d and e,**Increase of immunofluorescence signal of Pmel17and TYRP1 can be in turn observed from BF-A375 to BM3-A375 cells. **f,** Statistical difference of integrated optical density (IOD) of Pmel17 and TYRP1 in different A375 cells (n=15). **g,** High levels of Pmel17 expression and Pmel17 maldistribution were shown in the whole cytoplasm of melanocytes in basal layers and the transferred melanocytes in stratum spinosum, stratum granulosum, and even stratum lucidun in epidermal tissues of the DUH patients (40X magnification, red arrows indicate higher expression of Pmel17, yellow arrows indicate lower or no Pmel17 expression). **h,** Low levels of Pmel17 expression and Pmel17 maldistribution were displayed in basal layers of the DUH patient (red arrows indicate higher expression of Pmel17, yellow arrows indicate little or no Pmel17 expression,40X magnification). **i and j,** Higher expression of Pmel17 demonstrates in melanocytes of the DUH patient's epidermis(100X magnification). **k and l,** Normal and homogeneous expression and distribution of Pmel17 were shown in basal layers of epidermis of normal controls (40X magnification and 100X magnification). **m,** High levels of TYRP1 expression and TYRP1 maldistribution were shown in the whole cytoplasm of melanocytes in basal layers and in transferred melanocytes in the upper layers above basal layer of the DUH patients's epidermis (red arrows indicate higher expression of TYRP1, yellow arrows indicate lower or no TYRP1 expression,40X magnification). **n,** Low levels of TYRP1 expression and TYRP1 maldistribution displayed in most melanocytes in basal layers of the DUH patient (red arrows indicate higher expression of TYRP1, yellow arrows indicate little or no TYRP1 expression,40X magnification). **o and p,** Higher expression of TYRP1 was demonstrated in melanocytes and transferred melanocytes in the DUH patient's epidermis(100X magnification). **q,** No TYRP1 expression demonstrates in the DUH patient's epidermis(100X magnification). **r and s ,**Normal and homogeneous expression and distribution of TYRP1 were shown in basal layers of epidermis of normal controls (40X magnification and 100X magnification).

Figure 5 | Mutations of *SASH1* encourage up-regulation of Rab27a in A375 cells and in a DUH patient of family I with *SASH1* Mutant 3. a, Real time RT-PCR shows that differential expression of Rab 27a exists between BM2-, BM3-A375 and BM0-A375 cells (n=4). **b,** Difference of Rab27a expression between BM2-, BM3-A375 cells and A375, BF- and BM0-A375 cells . There is no difference of Rab 27a expression between BM1-A375 cells and A375, BF- and BM0-A375 cells. **c and d,** Immunofluorescence analysis shows that mutations of *SASH1* induce the increased expression of Rab 27a. The red arrowheads indicate flash point-like distribution of Rab 27a in cytoplasm. Much

more Rab27a green immunofluorescence can be observed in BM2- and BM3-A375 cells, compared with BF-A375, BM0- A375, BM1-A375 cells(n=10). **e,** High levels of Rab27a expression and Rab27a maldistribution were shown in the whole cytoplasm of melanocytes in basal layers and transferred melanocytes in the upper layers above basal layer of epidermal tissues of the DUH patients (red arrows indicate higher expression of Rab27a, yellow arrows indicate lower or no SASH1 expression,40X magnification). **f,** Low levels of Rab27a expression and Rab27a maldistribution were displayed in most melanocytes in basal layersof the DUH patient (red arrows indicate higher expression of Rab27a , yellow arrows indicate little or no Rab27a expression, 40X magnification). **g and h,** Higher expression of Rab27a was demonstrated in melanocytes and transferred melanocytes of the DUH patient's epidermis (100X magnification). **i,** demonstrates slight Rab27a expression in melanocytes of the DUH patient's epidermis(100X magnification). **j and k,** Normal and homogeneous expression and distribution of Rab27a were shown in basal layers of epidermis of normal controls (40X magnification,100X magnification).

Figure 6 | SASH1 related biological pathway in KEGG database (map04916). After elimination of the interacting proteins with empty pBABE vector in BF-A375 cells, the pull down assay and LC-MS/MS analysis demonstrates that SASH1 can interact with MAP4K4, MAPKK2 (MEK2) to participate in the MAPK signaling pathway and regulate melanogenesis. Meanwhile, SASH1 can interact with CALM in the endothelin signaling pathway to directly participate in melanin synthesis.

Supplementary Figure 1 The epidermal tissues of a DUH patient of family I with *SASH1* Mutant 3 exhibit identical quantities of melanocytes to normal controls with maldistribution of melanocyte numbers. a, Hyperplastic melancytes not only present in the basal layers but in the upper layers above basal layers of epithelial tissues in the same sections (magnification,×40). **b,** Increased melanocytes (indicated by red arrows) and decreased melanocytes (indicated by yellow arrows) i.e. maldistribution of melanocytes in the same section (magnification ×40). **c and f,** There are almost no melanocytes present in the basal layers in hypopigmentation regions (magnification ×40 and ×100), respectively. **d,** Transferred melanocytes could be observed form basal layer to the layers above basal layers in the DUH epdermis(magnification ×100). **e,** Increasing expression of Pmel17 in melanocytes exists in basal layers without increased quantity of melanocytes, (magnification ×100). **g and h,** Normal level expression of Pmel17 and normal quantity of melanocytes in palisade layers of normal control, (magnification ×40 and ×100), respectively. **i and j,** The statistical analysis of melanocytes quantities as between the DUH patient and normal controls(p=0.161,number of DUH patient =34,number of normal controls=25). The epidermal tissues of a DUH patient of family I with *SASH1* Mutant 3 show exactly the same numbers of melanocytes as those of normal controls using HE staining(M: melanocytes).

Supplementary Figure 2 Mutations of SASH1 can strengthen the mobility of melanocytes. A to F, A transwell migration assay using different A375 cells was performed on polycarbonate filters no pre-coated with 20μg of matrigel. Images are representative of the different groups of migrated A375 cells in three separate experiments performed in triplicate. The magnifications for each group of A375

cells were ×50 and ×100, respectively. **G to L**, A transwell invasion assay using different groups of A375 cells was also performed on polycarbonate filters pre-coated with 20 μg of matrigel. Images are representative of the different groups of invasive A375 cells in three separate experiments performed in triplicate. The magnifications for each group of A375 cells were ×50 and ×100, respectively. **m,** Data collected in (A to F) represent the statistical difference of numbers of different groups of A375 cells that migrated during 24hr period (n=15). A two- to four fold increase in migration of mutant SASH1-overexpressing cells compared with wild type SASH1-overexpression in cells was routinely observed and was dependent upon the passage number of migrated cells. **n,** Data collected in (**G to L**) represent the statistical difference of numbers of different A375 cells that invaded during 24hr period (n=12). A significant three- to four fold increase in invasion of wild type SASH1-overexpressing cells compared with A375 and BF-A375 cells was observed, and a two fold increase in invasion of mutant SASH1-overexpressing cells compared with wild type SASH1-overexpressing cells was also observed and was dependent upon the passage number of invasive cells.

Supplementary Figure 3 *SASH1* knockdown by its specific dsRNA removes up-regulation of SASH1 induced by SASH1 mutations. **a,** SASH1 expression in different A375 cells after knockdown of SASH1. Knoc-BM0, Knoc-BM1, Knoc-BM2, Knoc-BM3 means BM0-, BM1-, BM2-, BM3-A375 cells after SASH1 knockdown by specific SASH1 dsRNA, respectively. The only differential expression of SASH1 is between Knoc-BM0-A375 cells and Knoc-BM2-A375 cells (n=4). **b,** The comparison of SASH1 expression between different A375 cells and those of different A375 cells after knockdown by specific dsRNA of SASH1 (n=4). **c,** Immunoblotting shows that the differential expression of SASH1 protein between A375 cells, BF-, BM0-A375 cells and BM1-, BM2- and BM3-A375 cells was removed after *SASH1* knockdown by specific *SASH1* dsRNA. **d,** Immunoblotting illustrates the removal of differential expression of SASH1 protein between BM0- and BM1-, BM2- and BM3-A375 cells by specific dsRNA of *SASH1* using Flag monoclonal antibody(n=4).

Supplementary Figure 4 ***SASH1* knockdown by its specific dsRNA removes increased expression of Pmel17 and TYRP1 induced by *SASH1* mutations. a,**Pmel17 expression in BM0-,BM1-, BM2- and BM3-A375 cells after SASH1 knockdown. The only differential expression of Pmel17 is between BM0-A375 cells and BM2-A375 cells (n=4). **b,**The comparison of Pmel17 expression between different A375 cells and that of different A375 cells after SASH1 knockdown (n=4). **c,***TYRP1* expression in different A375 cells after *SASH1* knockdown . The only differential expression of *TYRP1* is between Knoc-BM0-A375 cells and Knoc-BM2-A375 cells (n=4). **d,**The comparison of *TYRP1* expression in different A375 cells and that of A375 cells after knockdown of *SASH1* (n=4). **e,**Western blotting shows expression of TYRP1 protein in different A375 cells after *SASH1* knockdown. There is almost no expression difference of TYRP1 in different A375 cells. **f and g,** Immunofluorescence analysis shows expression of Pmel17 and TYRP1 in BF-,BM0- , BM1-, BM2- and BM3-A375 cells after knock down of *SASH1*. **h,** There is no expression difference of Pmel17 and TYRP1 between BM0-A375 cells and BM1-,BM2-,BM3-A375 cells (n=15).

Supplementary Figure 5 ***SASH1*** **knockdown deletes enhanced expression of Rab27a induced by** ***SASH1*** **mutations in A375 cells and** ***SASH1*** **Mutant 3 increase expression of Rab 27a in the tissues of a DUH patient of family I. a,** Rab 27a expression in different A375 cells after knockdown of *SASH1*. The only differential expression of Rab27a is between Knoc-BM0-A375 cells and Knoc-BM2-A375 cells (n=4). **b,** The comparison of Rab 27a expression in A375 cells before and after knockdown of specific dsRNA of *SASH1* (n=4). **c,**Rab 27a expression in different A375 cells after knockdown of SASH1. There is almost no difference between different A375 cells (n=3).

Supplementary Figure 6 Statistical analysis of the immunohistochemistry (IHC) of SASH1, Pmel17, TYRP1 and Rab 27a and melanin staining results. a, The cartogram demonstrates the degree of divergence of SASH1, Pmel17(SILV), TYRP1 and Rab 27a and melanin as between a DUH patient with Mutation 3 and normal controls (n=15). **b,**The variance homogeneity of IOD value of SASH1 and TYRP1 was transformed by change of variable using the square root of 1/IOD. There is obvious differential expression of SASH1 and TYRP1 between the DUH patient's tissues and those of normal controls (n=15).

Supplementary Figure 7 Identification of SASH1 and several important proteins interacting with SASH1 using automated nano-flow LC-MS/MS analysis. Several important proteins are involved in melanogenesis and adhernce junction of tumor cells. The graphs represent the repetitive data collected in BM0-A375 cells during the LC-MS/MS analysis from duplicate experiments after elimination the interacting proteins with empty pBABE vector in BF-A375 cells. **a,** The LC-MS/MS spectrum confirmed the amino acid sequnce "PGAGTSEAFSR" to be the SASH1 peptide sequence. **b,** The LC-MS/MS spectrum identified the amino acid sequnce "FDVPGDENA EMDAR" to be the peptide sequence of IQGAP1. **c,** The LC-MS/MS spectrum confirmed the amino acid sequnce" RPHPQHSQQPPPPQQER" as the M4K4 peptide sequence. **d,**The LC-MS/MS spectrum confirmed the amino acid sequence "DYFLFNPVTDIEEIIR" as the SCMC1 peptide sequence. **e,**The LC-MS/MS spectrum confirmed the amino acid sequence "EADIDGDGQVNYEEFVQMMTAK" as the CALM peptide sequence. **f,** The LC-MS/MS spectrum confirmed the amino acid sequnce "PAMAIFELLDYIVNEPPPK" as the MAPKK2 (MEK2) peptide sequence.

Supplementary Figure 8 Bioinformation analysis of identified protein in BM0-A375 cells after elimination of the interacting proteins with empty pBABE vector in BF-A375 cells . a,Categorizations were based on information provided by the online resource PANTHER function classification and Gene ontology system. Pie chart representations of the distribution of identified proteins in the nano-flow LC-MS/MS analysis according to their biologica process (BP in Gene Ontology). **b,** Pie chart representations of the distribution of identified proteins according to their molecular function (MF in Gene Ontology). **c,** Pie chart representations of the distribution of identified proteins according to their PANTHER pathway.

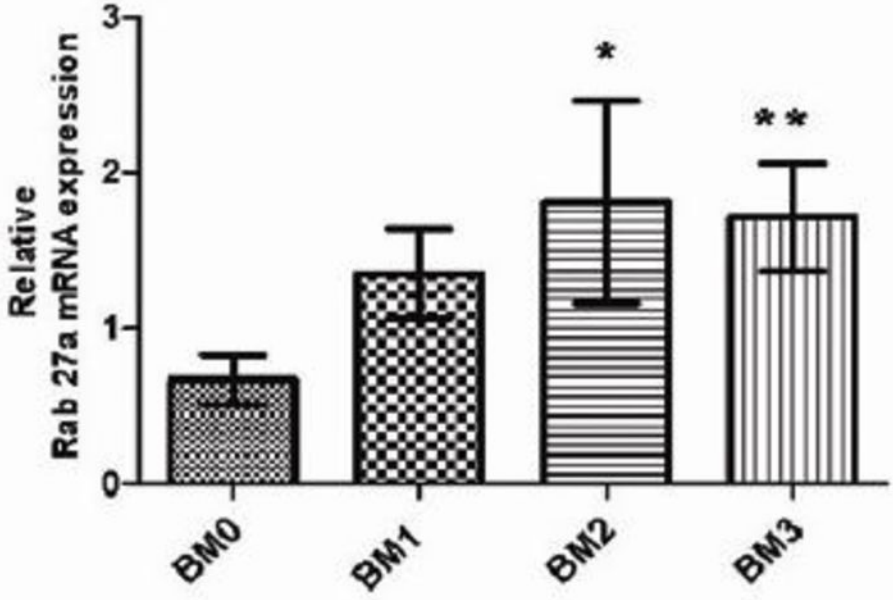

*indicates BM2 vsBM0,p=0.008;

**indicates BM2 vsBM0,p=0.013.

a

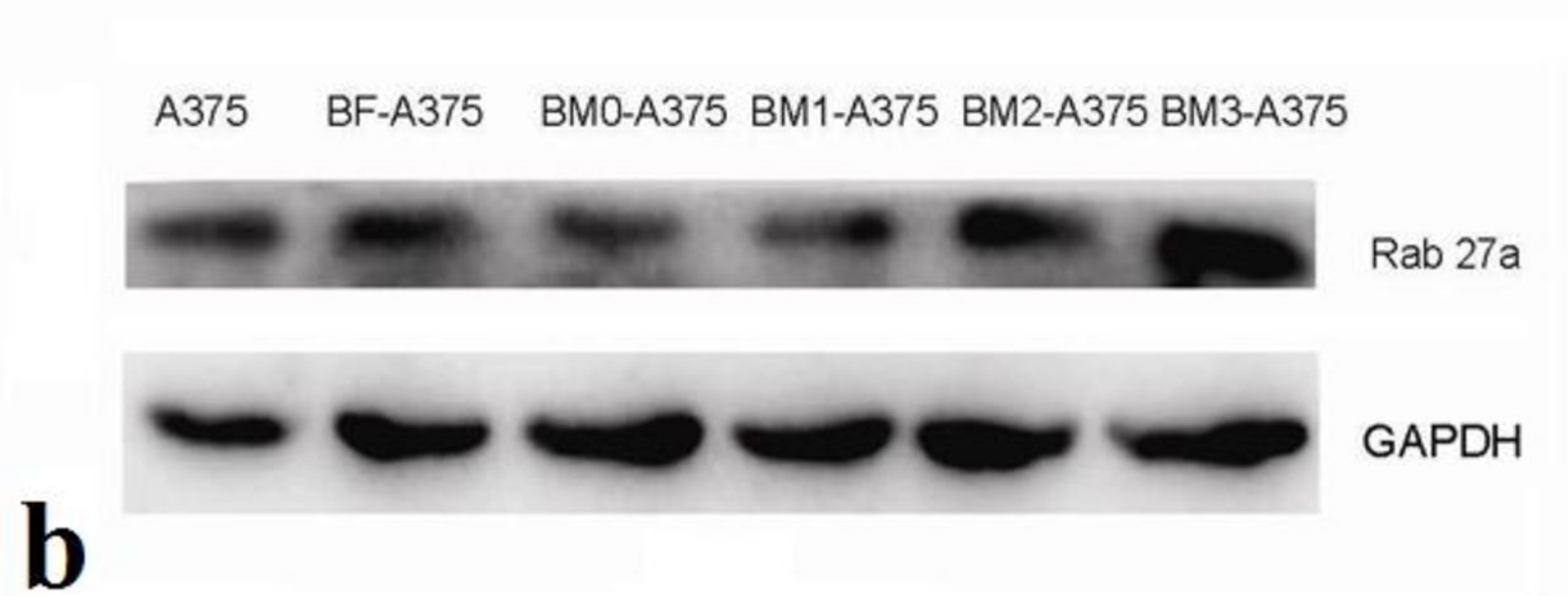
A375
BF-A375
BM0-A375
BM1-A375
BM2-A375
BM3-A375
Rab 27a
GAPDH
b

BF-A375-Rab27a

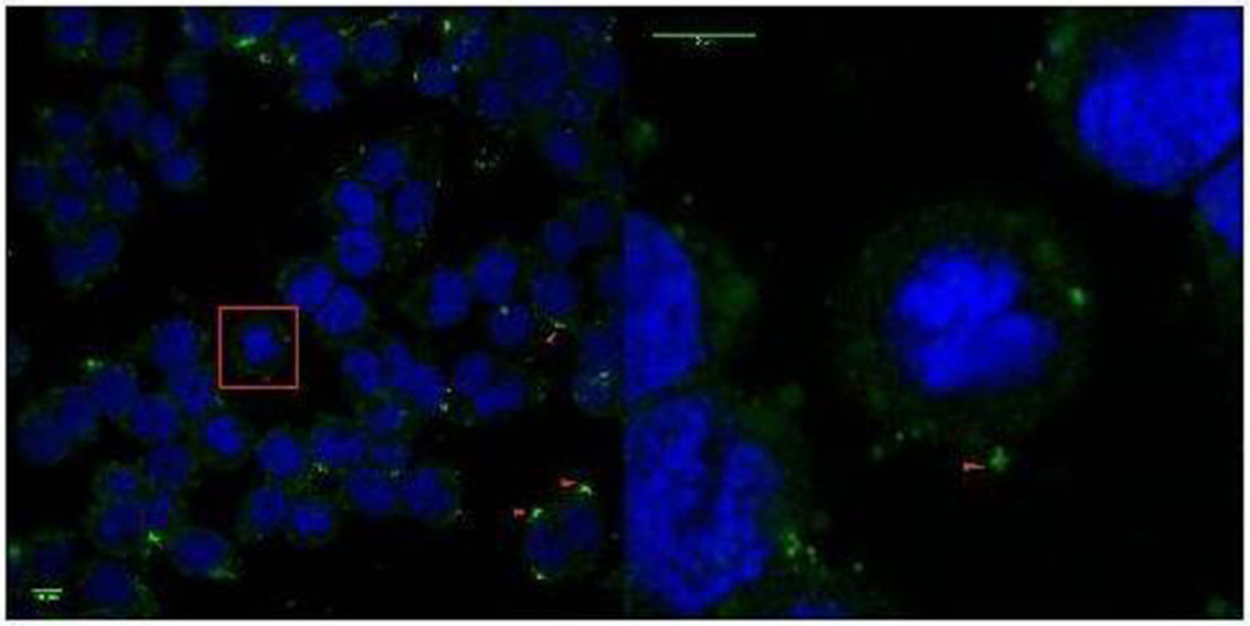

BM0-A375-Rab27a

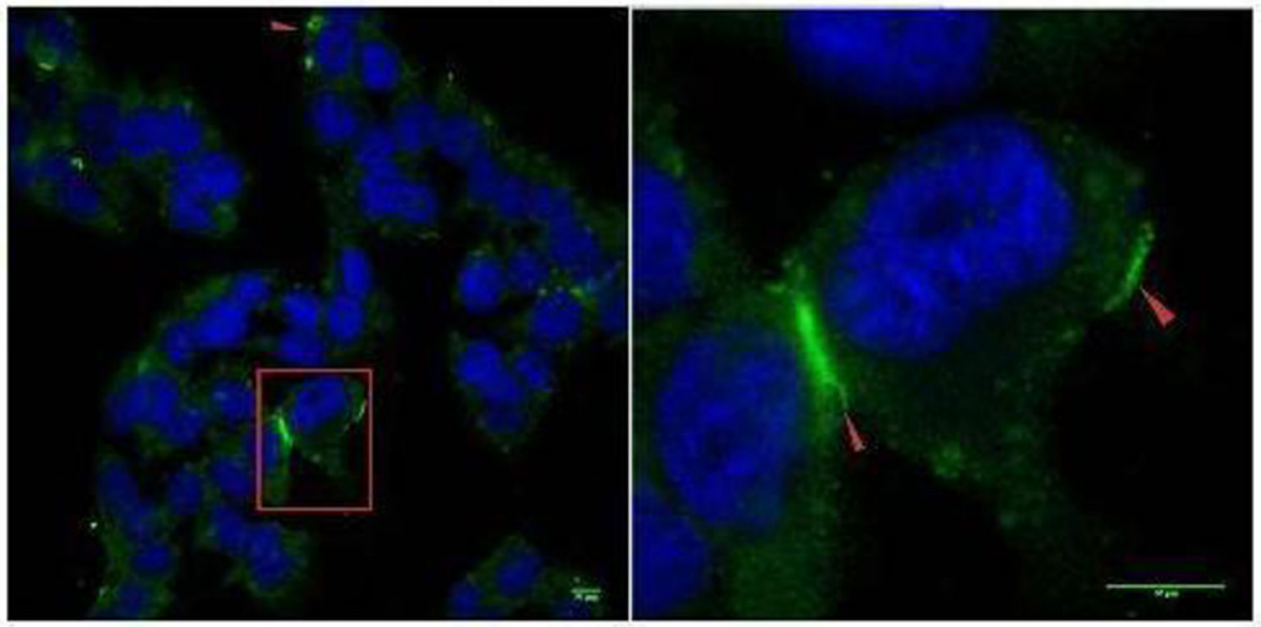

BM1-A375-Rab27a

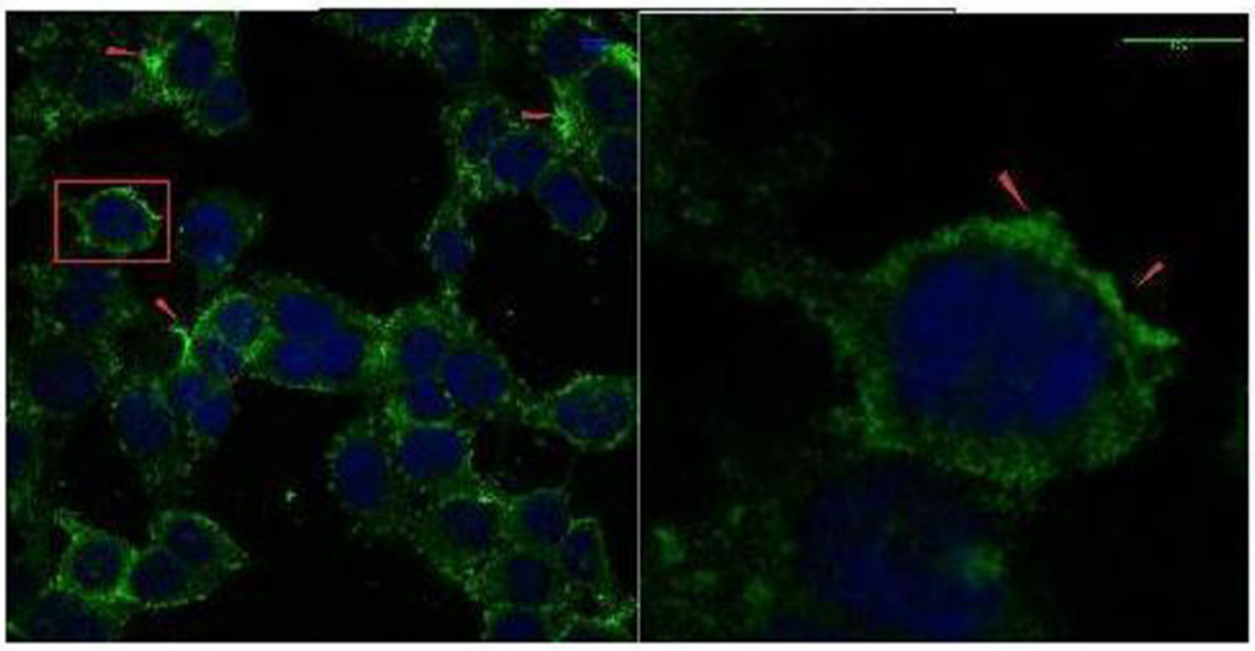

BM2-A375-Rab 27a

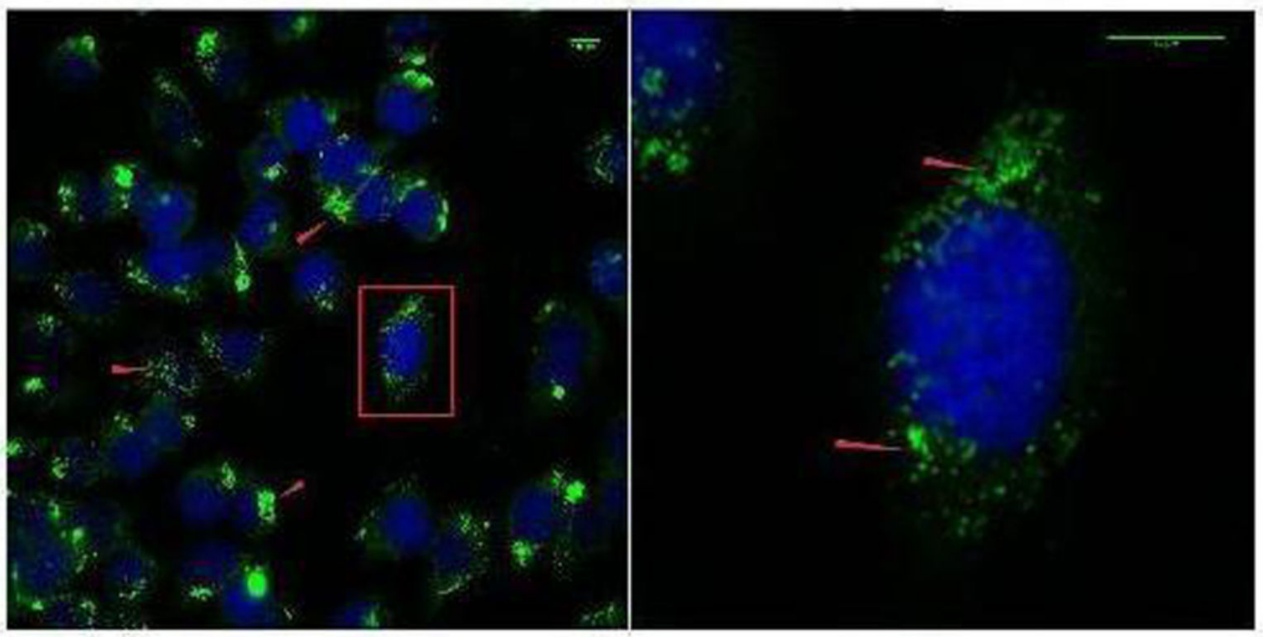

BM3-A375-Rab 27a

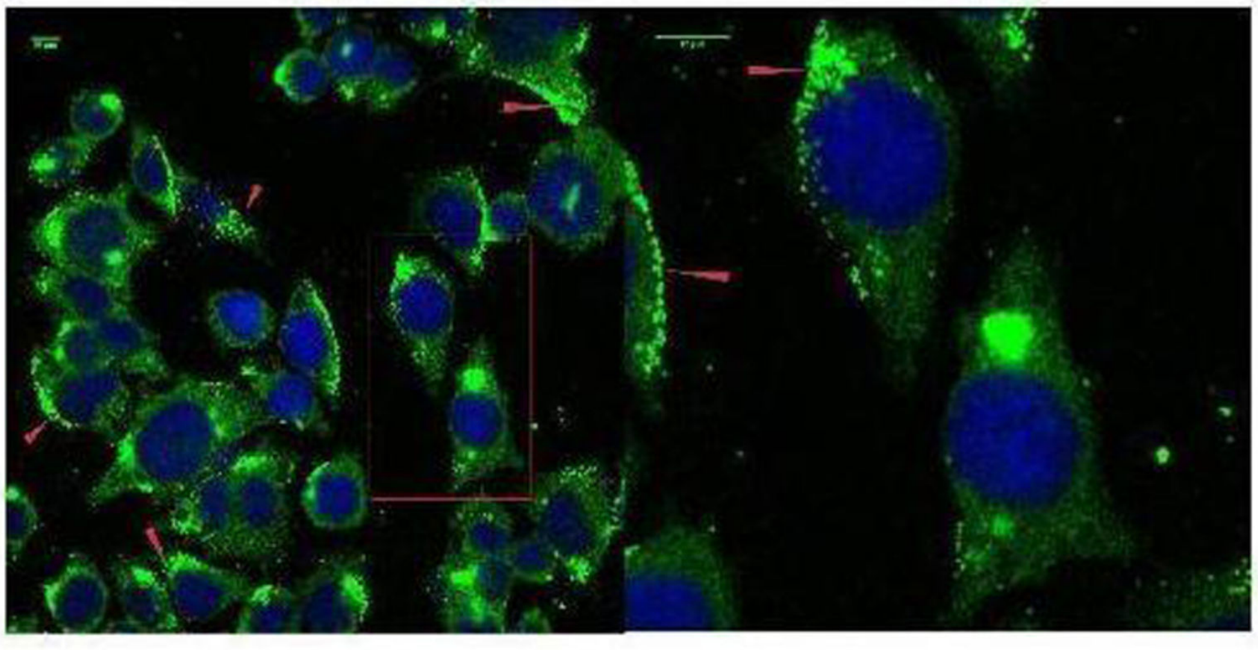

C

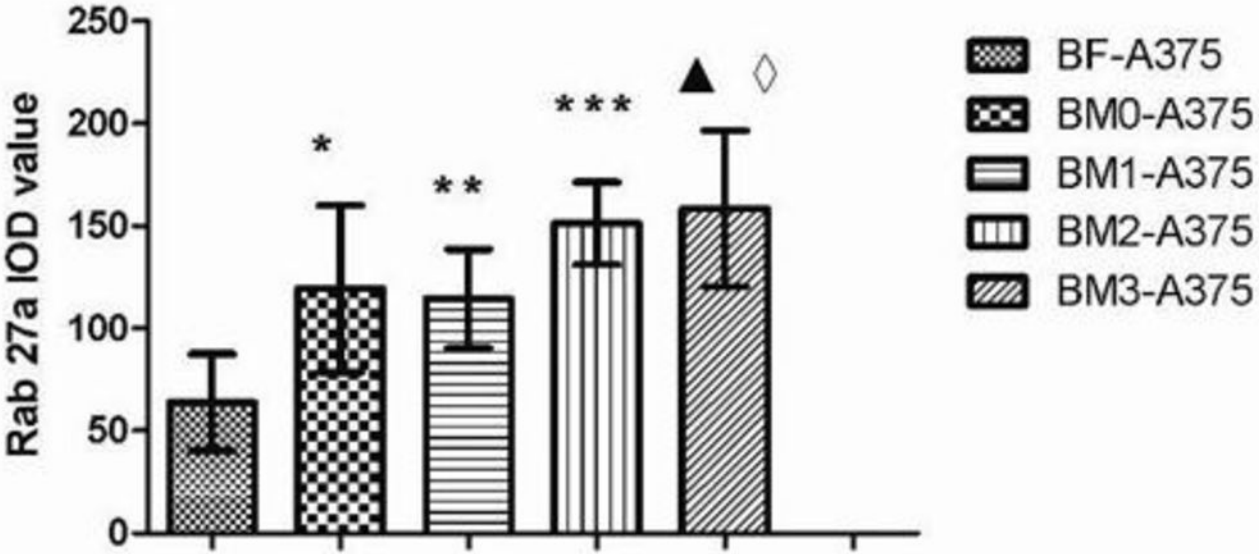

* indicates BM0-A375 vs BF-A375,p= 0.007;** indicates BM1-A375 vs BF-A375,p=0.013;***indicates BM2-A375 vs BF-A375,p=0.013; ▲ indicates BM3-A375 vs BF-A375,p=0.000; ◊ indicates BM3-A375 vs BM0-A375,p=0.000.

d

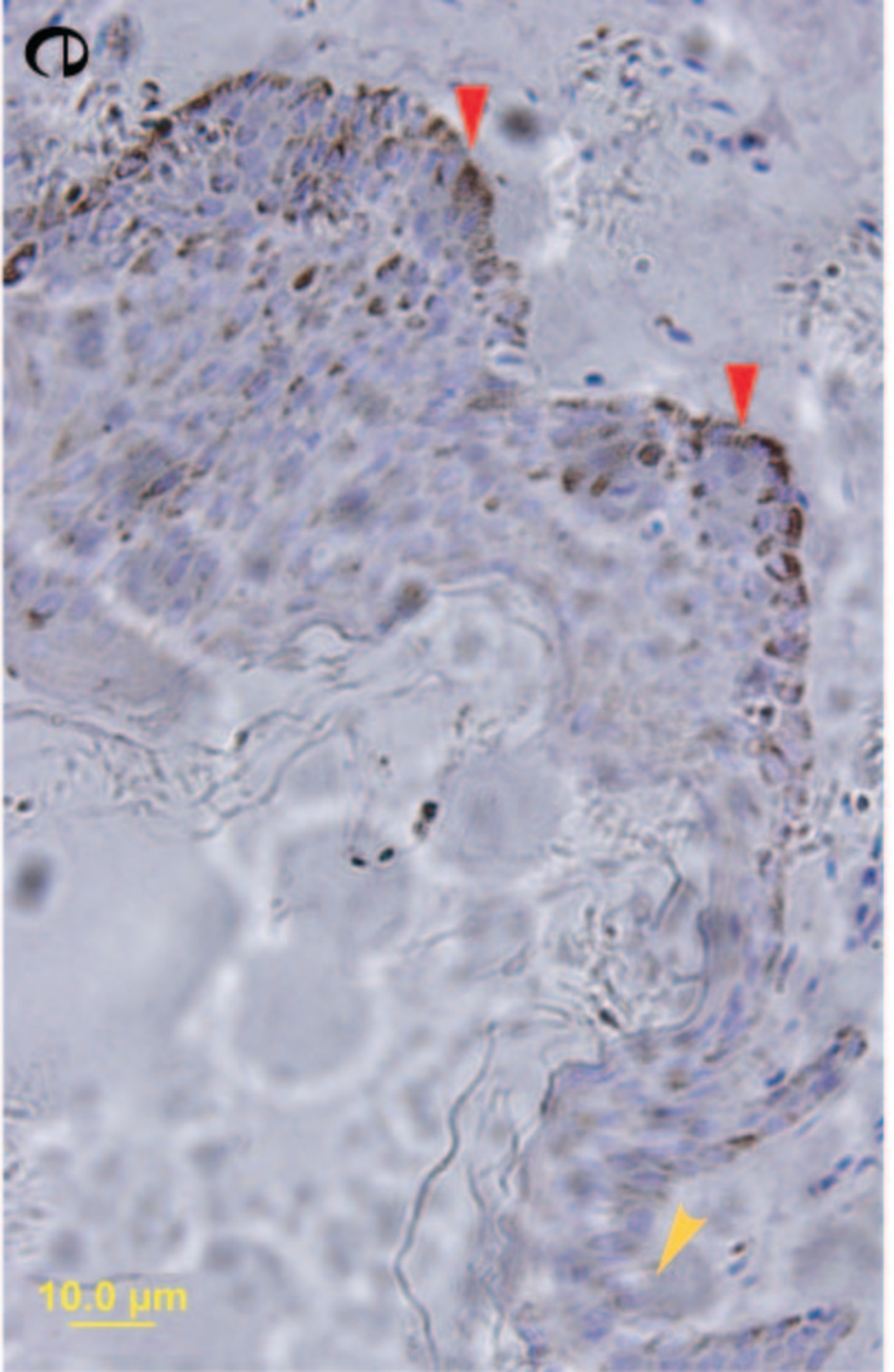
10.0 µm

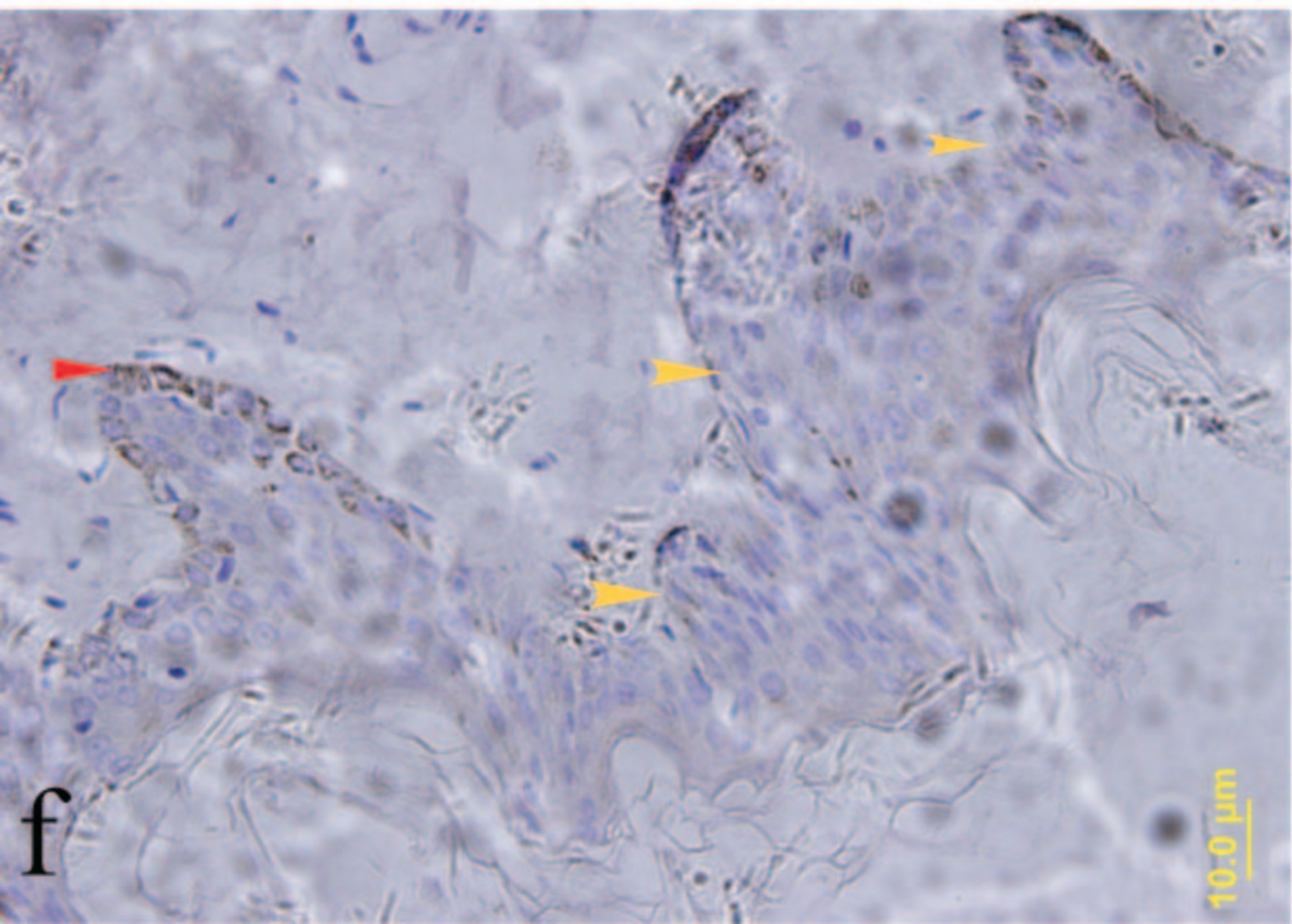
f
10.0 µm

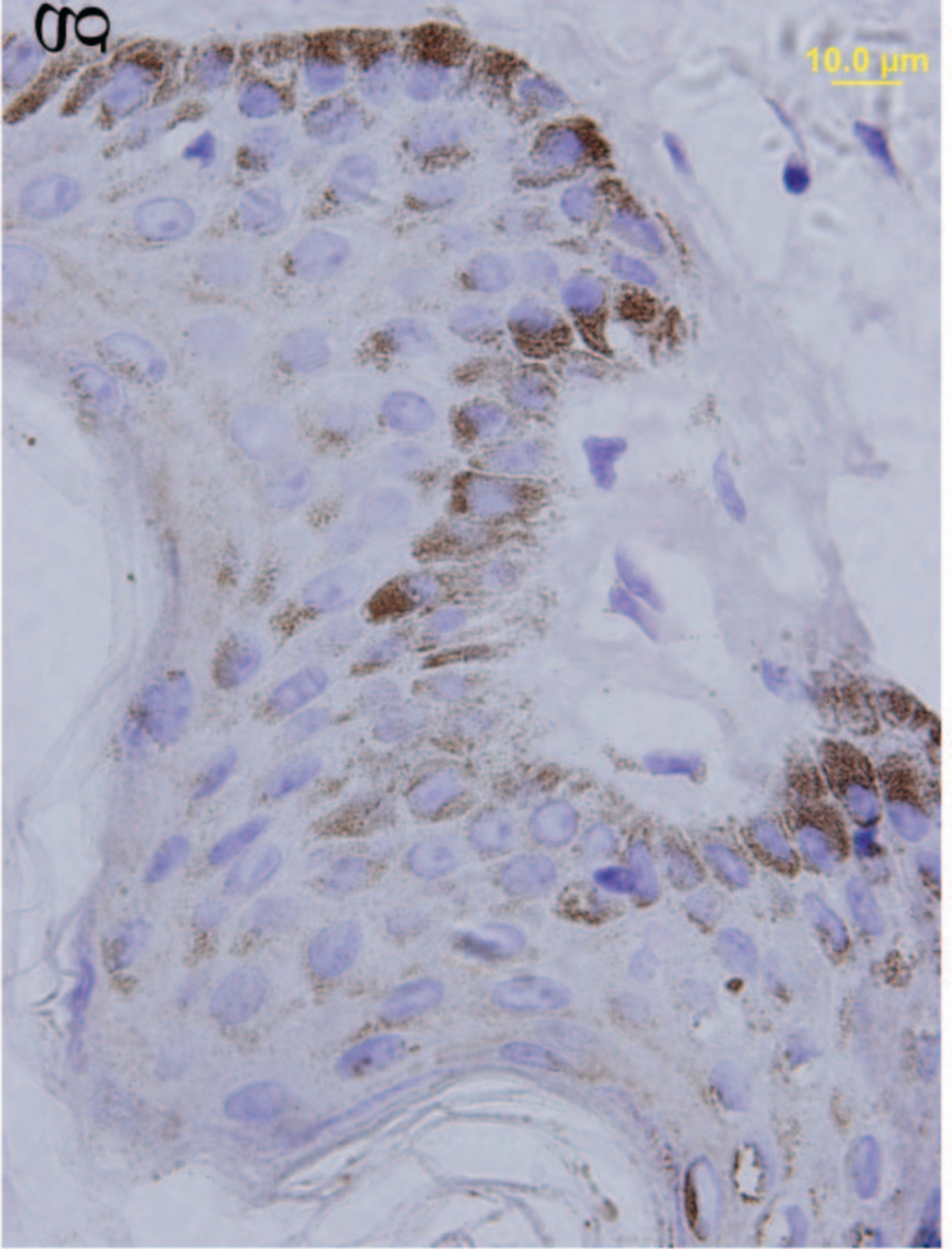
09
10.0 µm

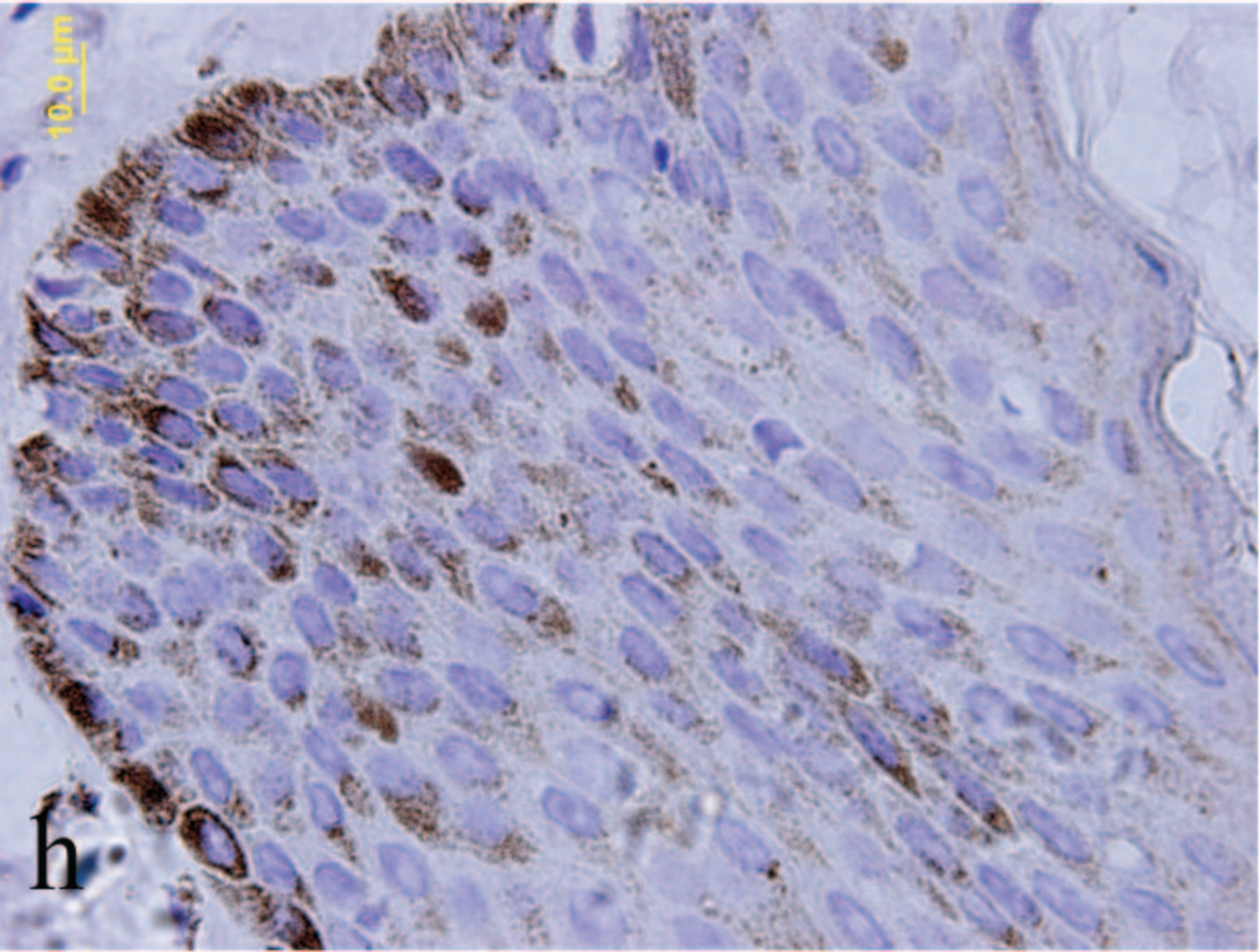
10.0 µm
h

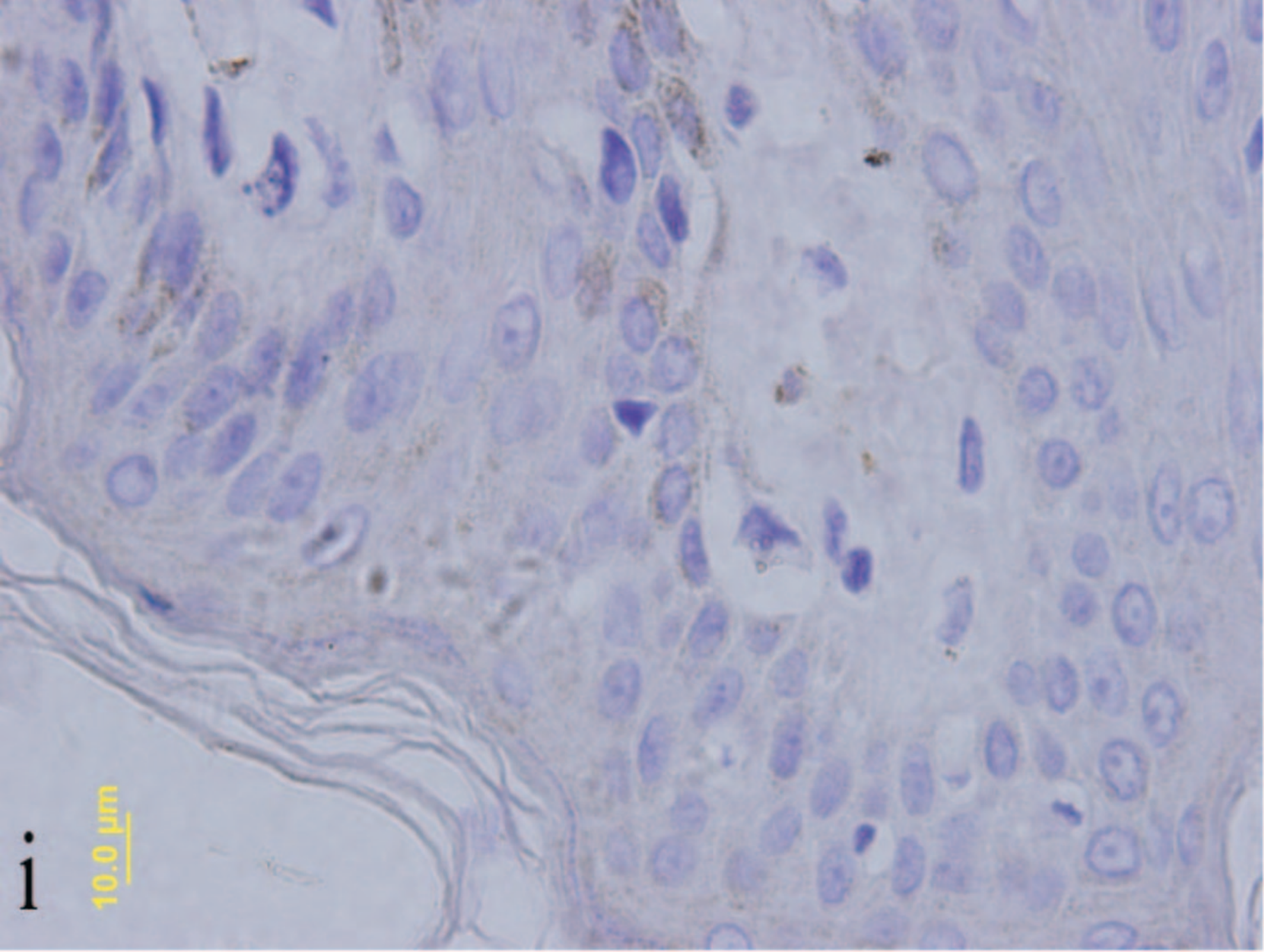
i
10.0 µm

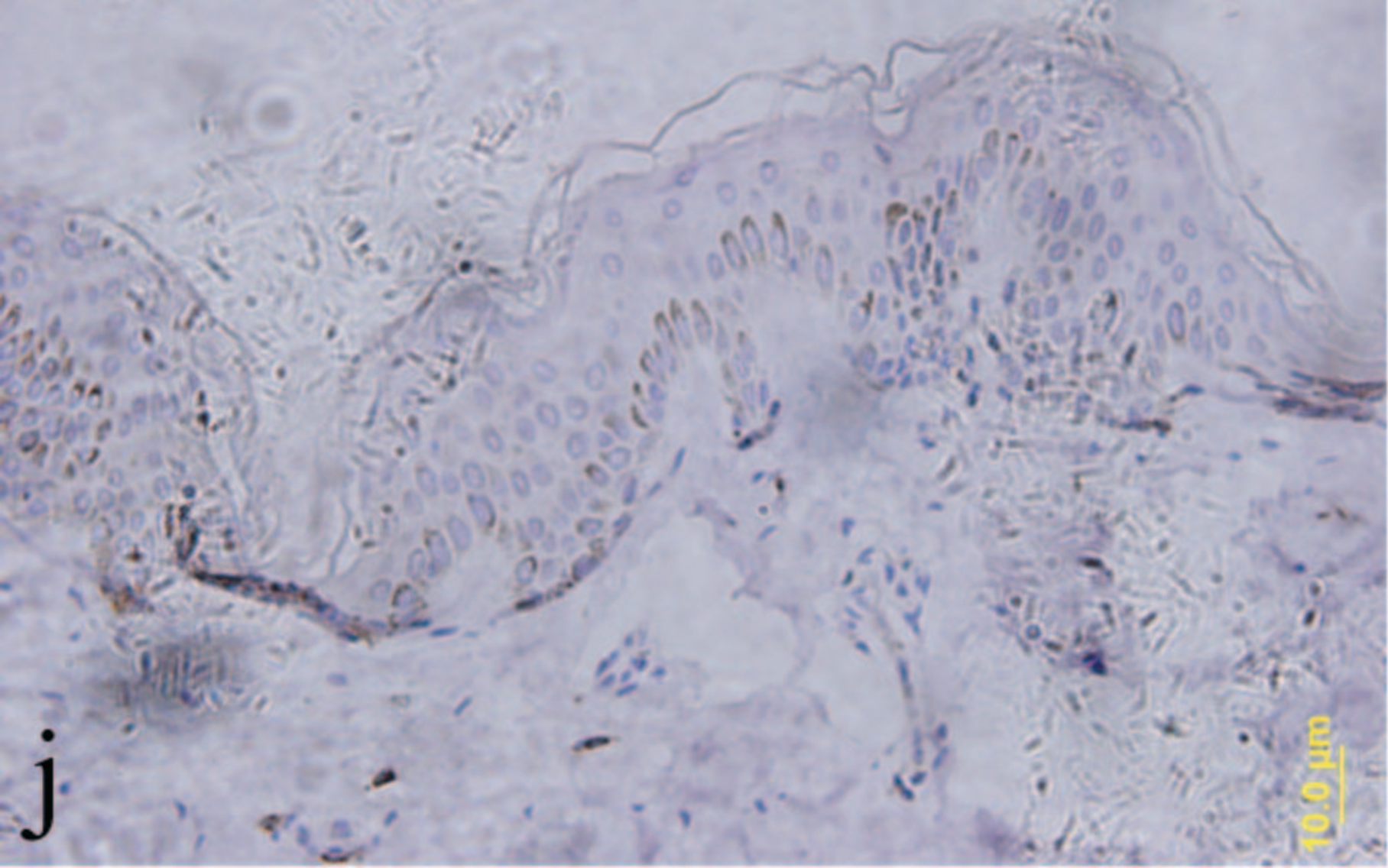
j
10.0 µm

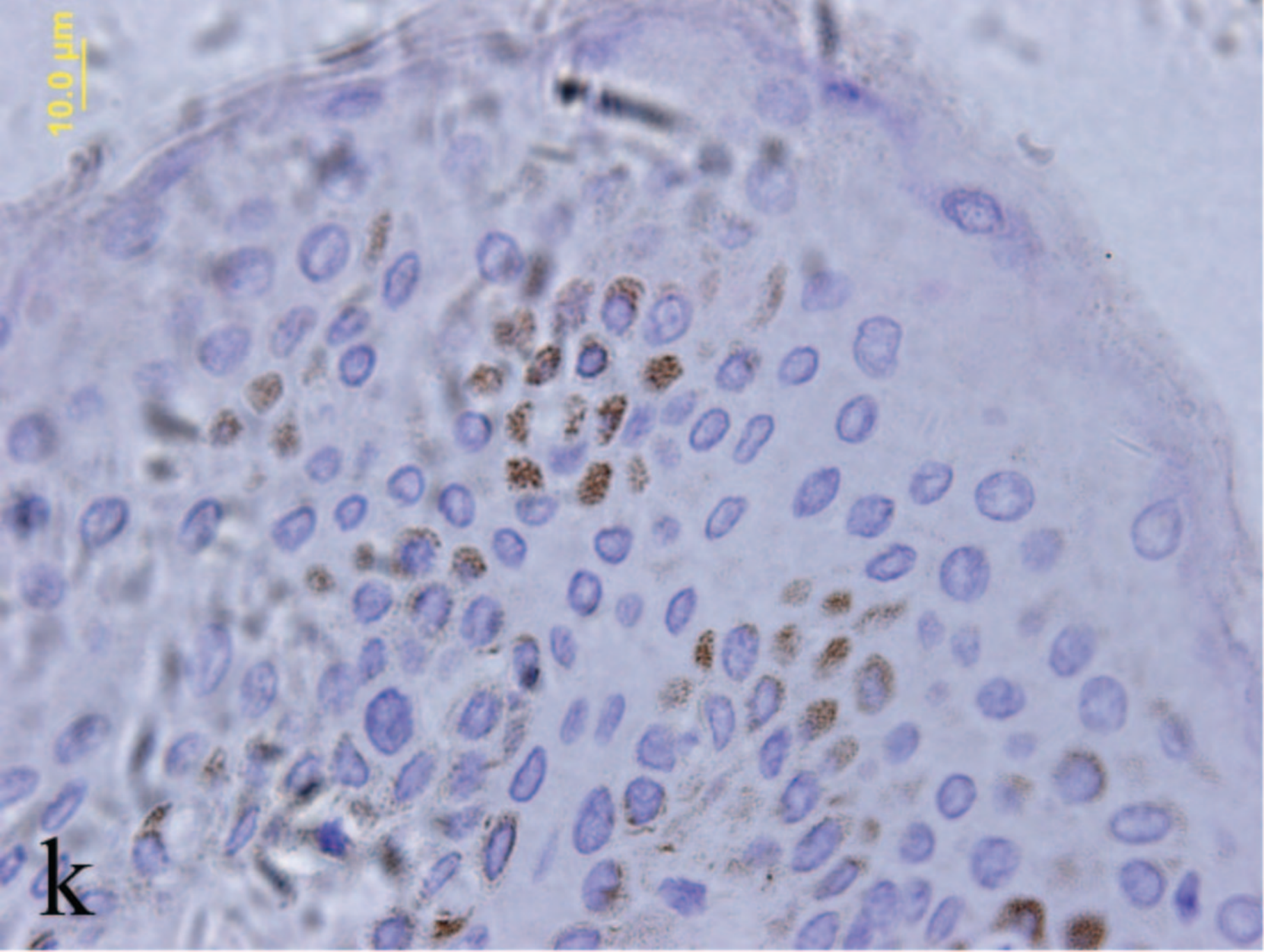
10.0 µm
k

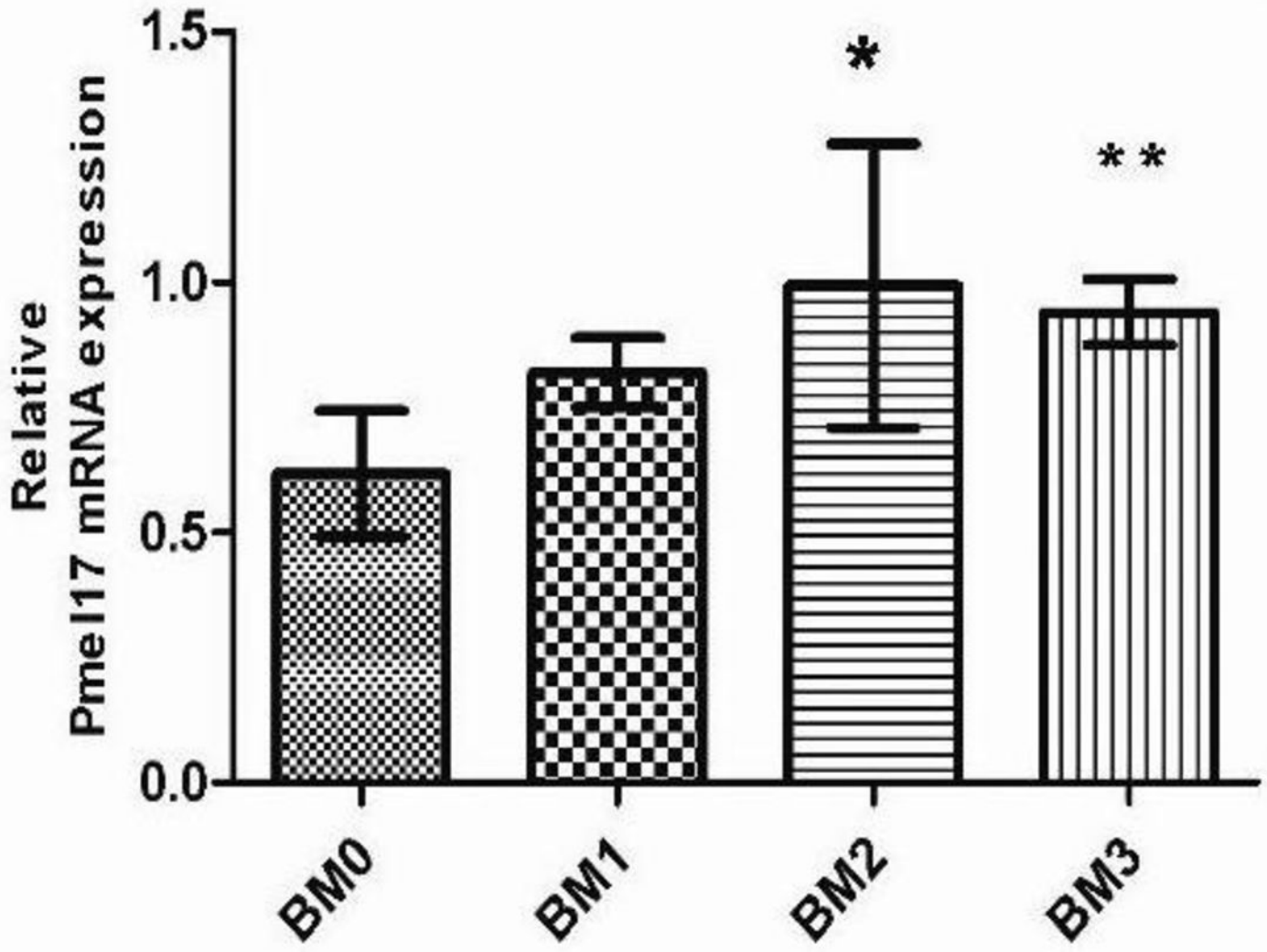

* indicates BM2 vs BM0 p=0.022,

** indicates BM3 vs BM0 p=0.041.

a

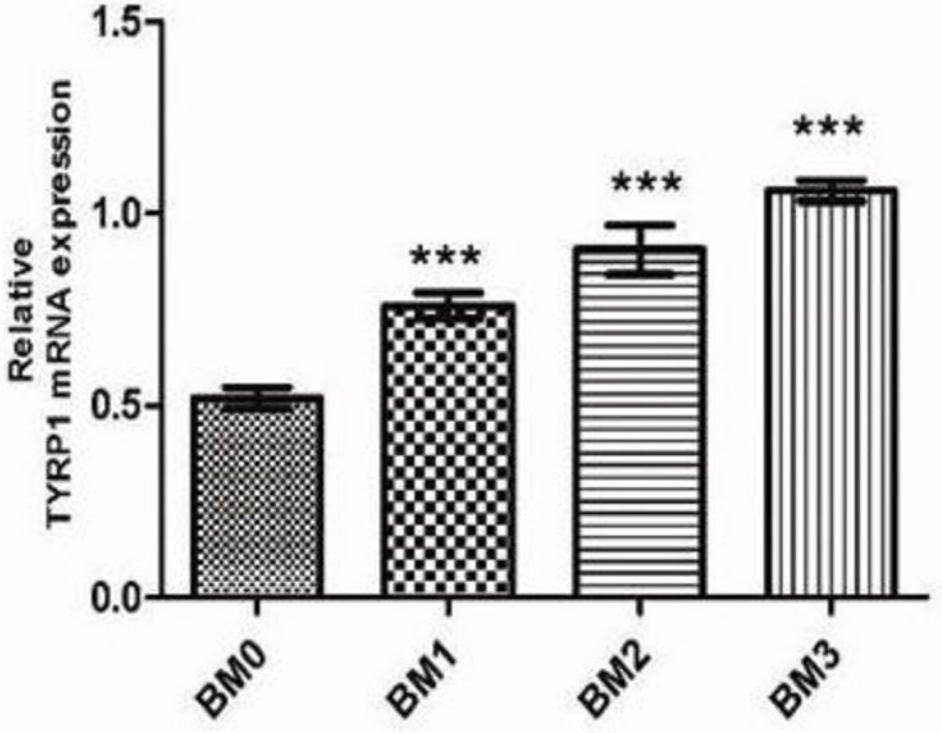

*** indicates BM1, BM2 and BM3 vs BM0 ,respectively,p=0.000.

b

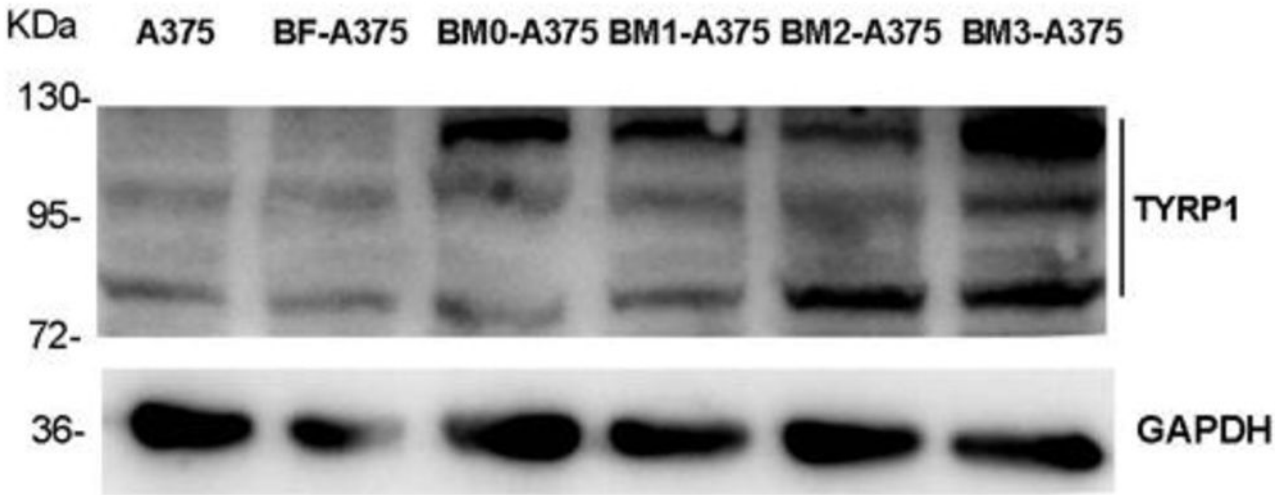
KDa
A375
BF-A375
BM0-A375
BM1-A375
BM2-A375
BM3-A375
130-
95-
72-
36-
TYRP1
GAPDH

c

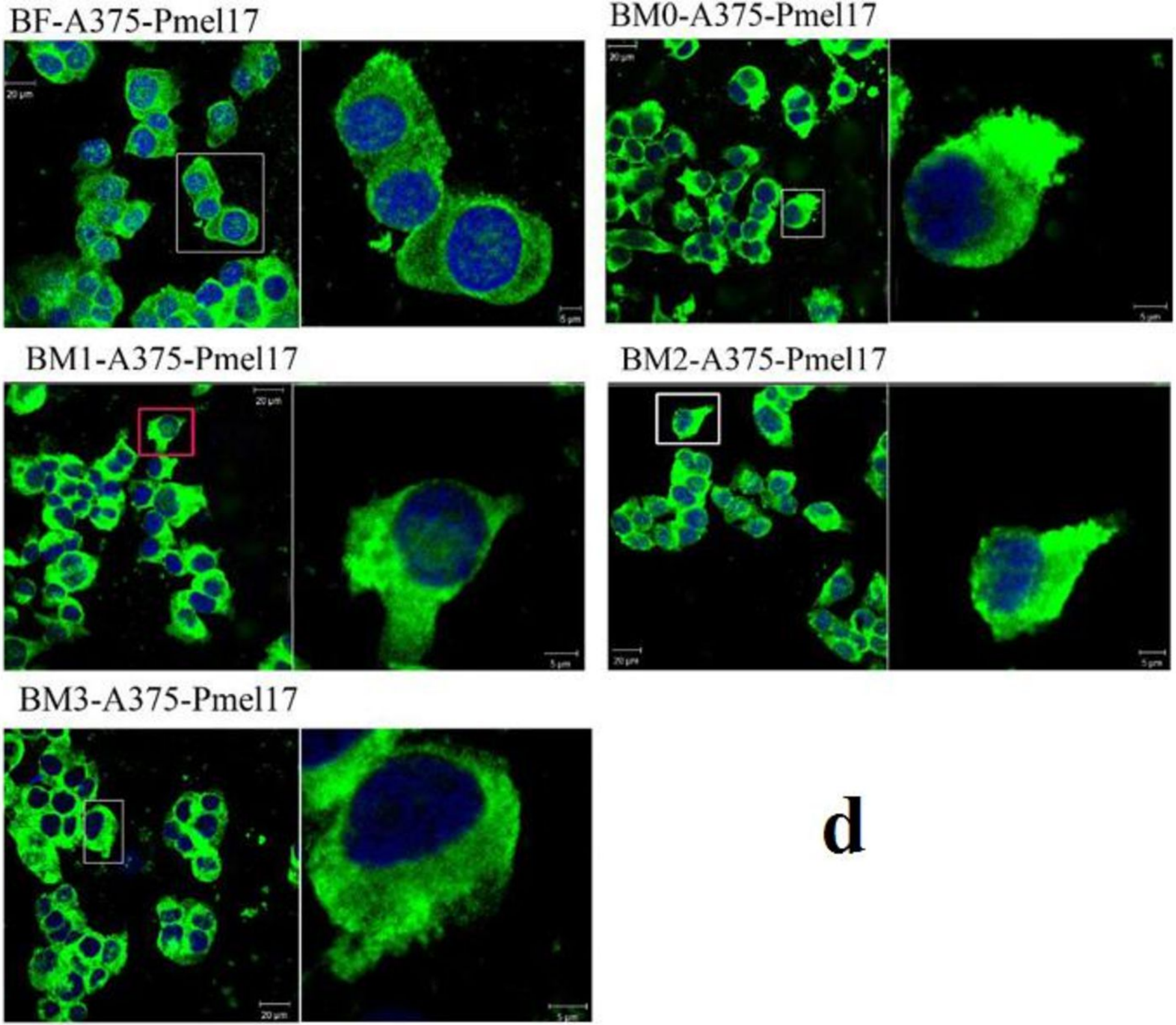
BF-A375-Pmel17
BM0-A375-Pmel17
BM1-A375-Pmel17
BM2-A375-Pmel17
BM3-A375-Pmel17
d

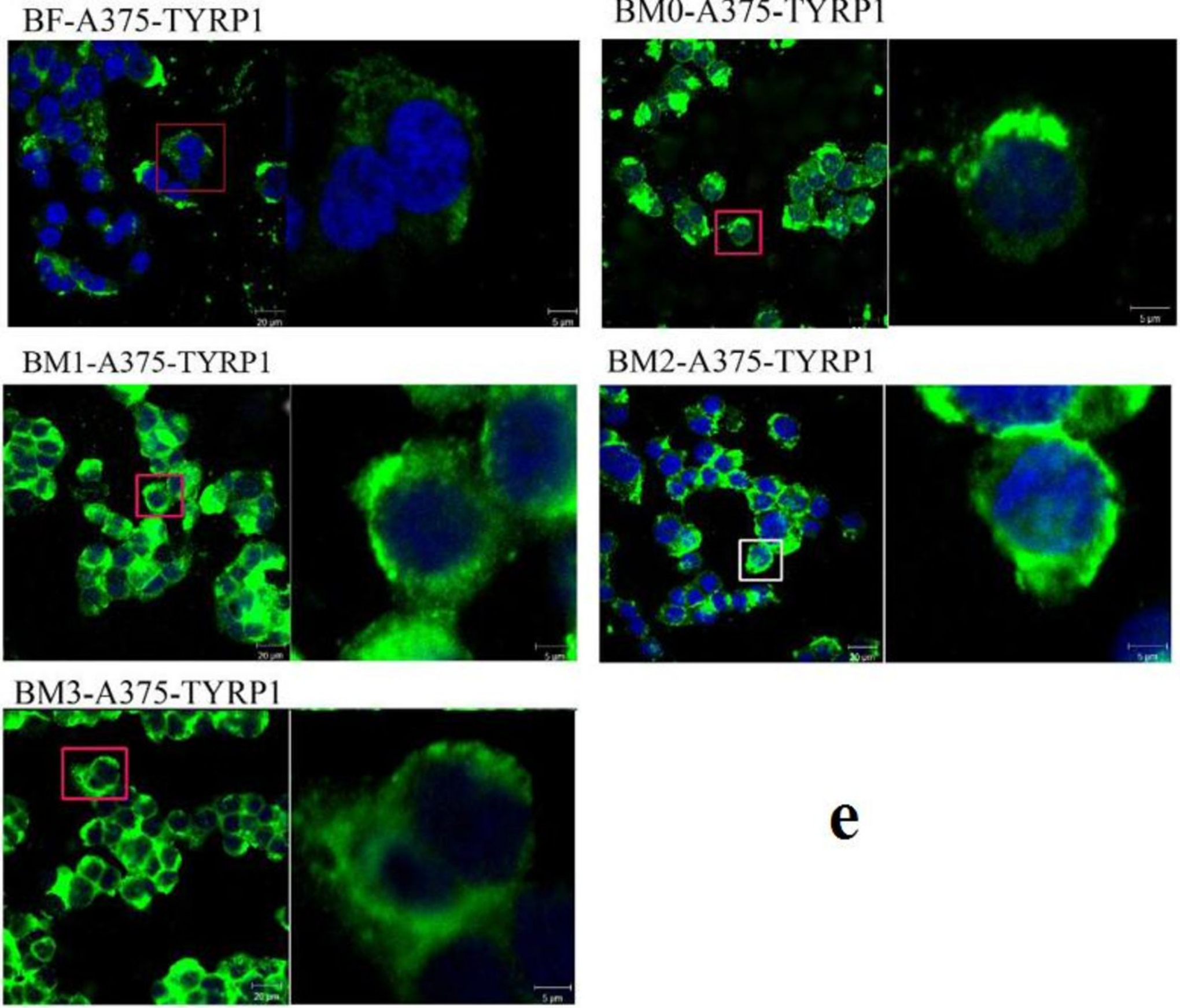
BF-A375-TYRP1
BM0-A375-TYRP1
BM1-A375-TYRP1
BM2-A375-TYRP1
BM3-A375-TYRP1
e

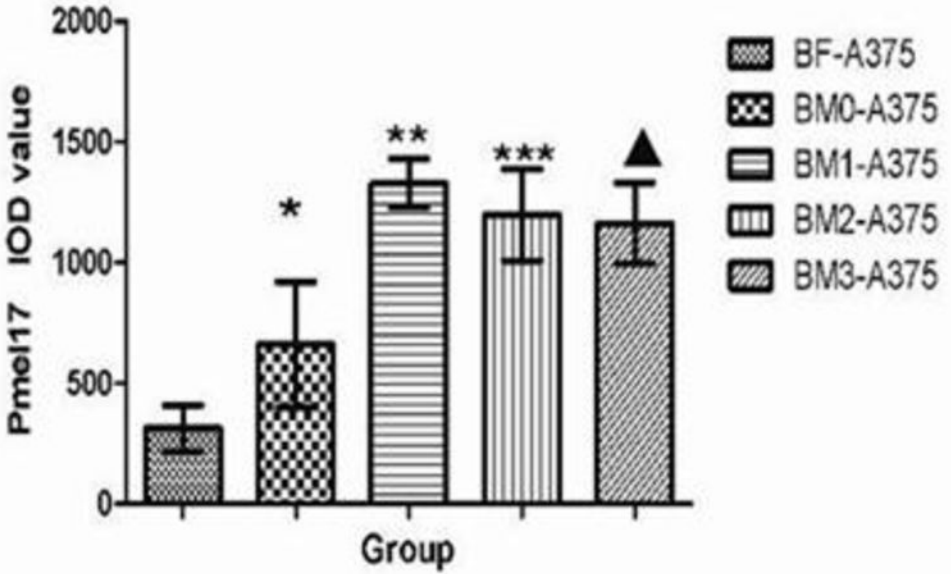

*** indicates BM0-A375 vs BF-A375,p=0.028;** indicates BM1-A375 vs BM0-A375,p=0.000; ***indicates BM2-A375 vs BM0-A375,p=0.002;▲indicates BM2-A375 vs BM0-A375,p=0.002.**

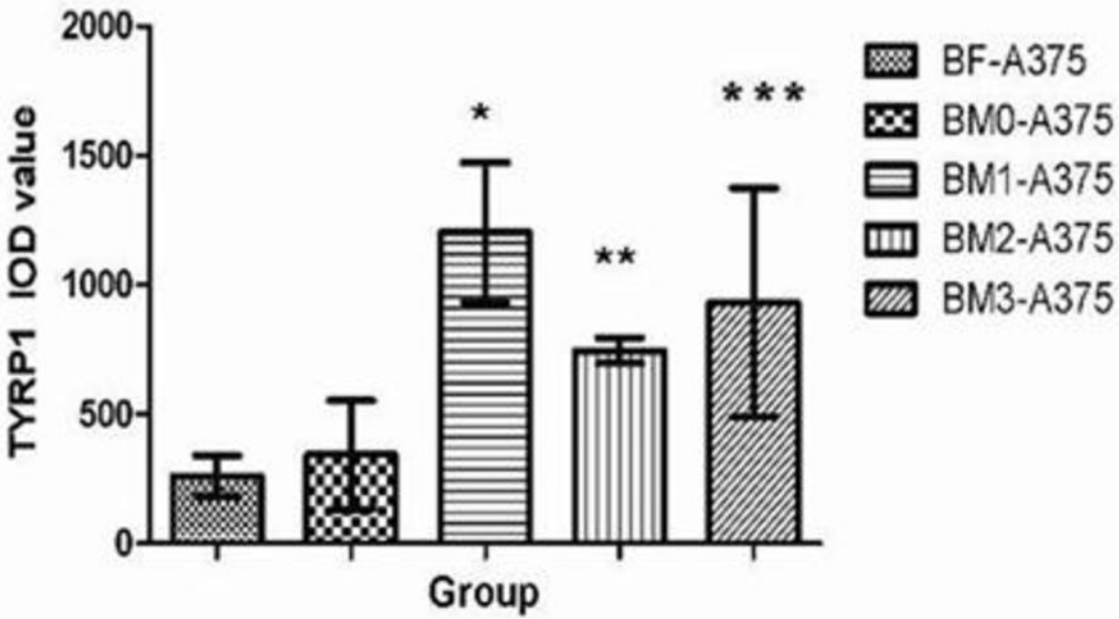

*** indicates BM1-A375 vs BM0-A375,p=0.000; ** indicates BM2-A375 vs BM0-A375,p=0.002; ***indicates BM3-A375 vs BM0 -A375 ,p=0.000.**

f

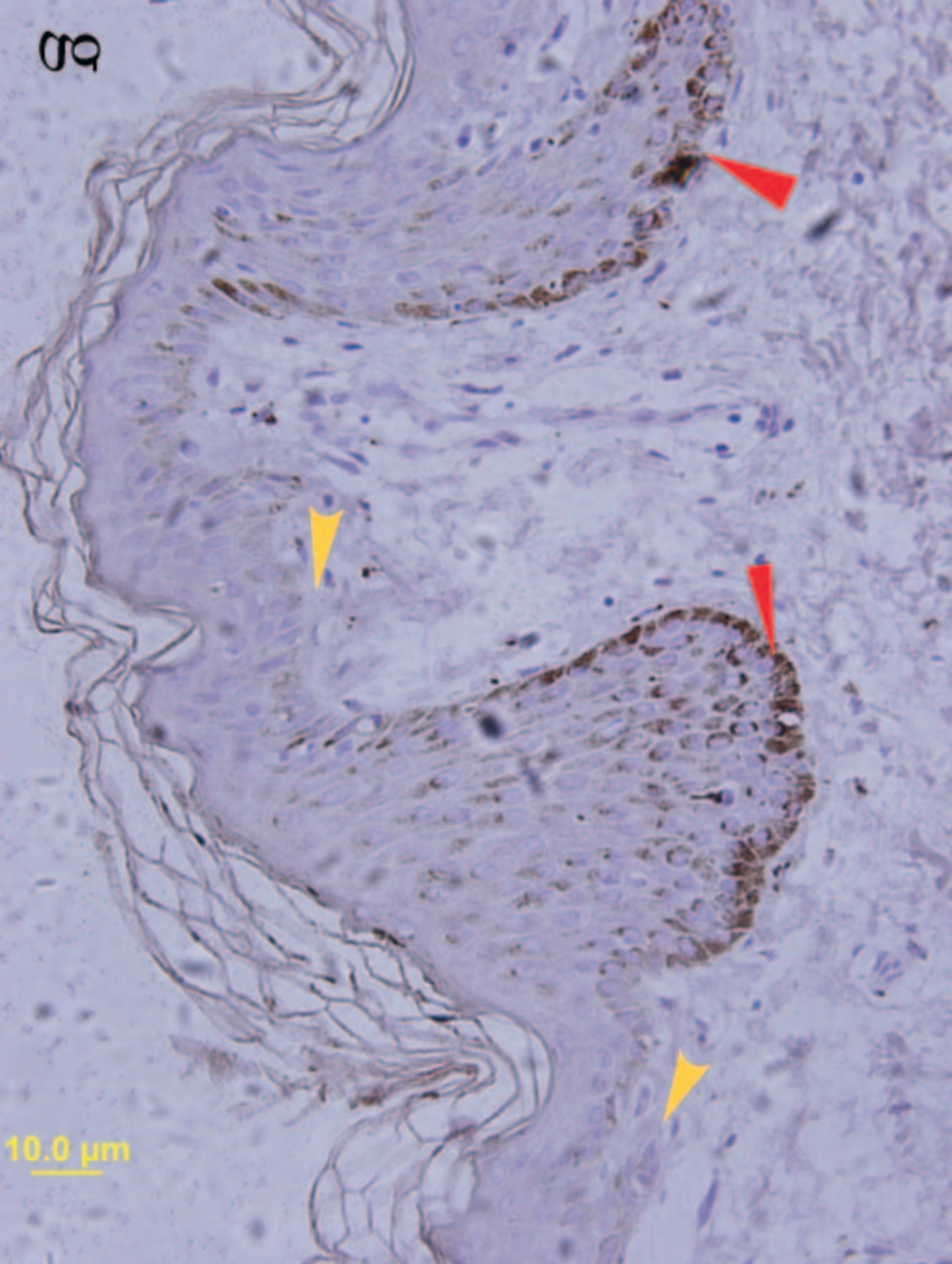
09
10.0 µm

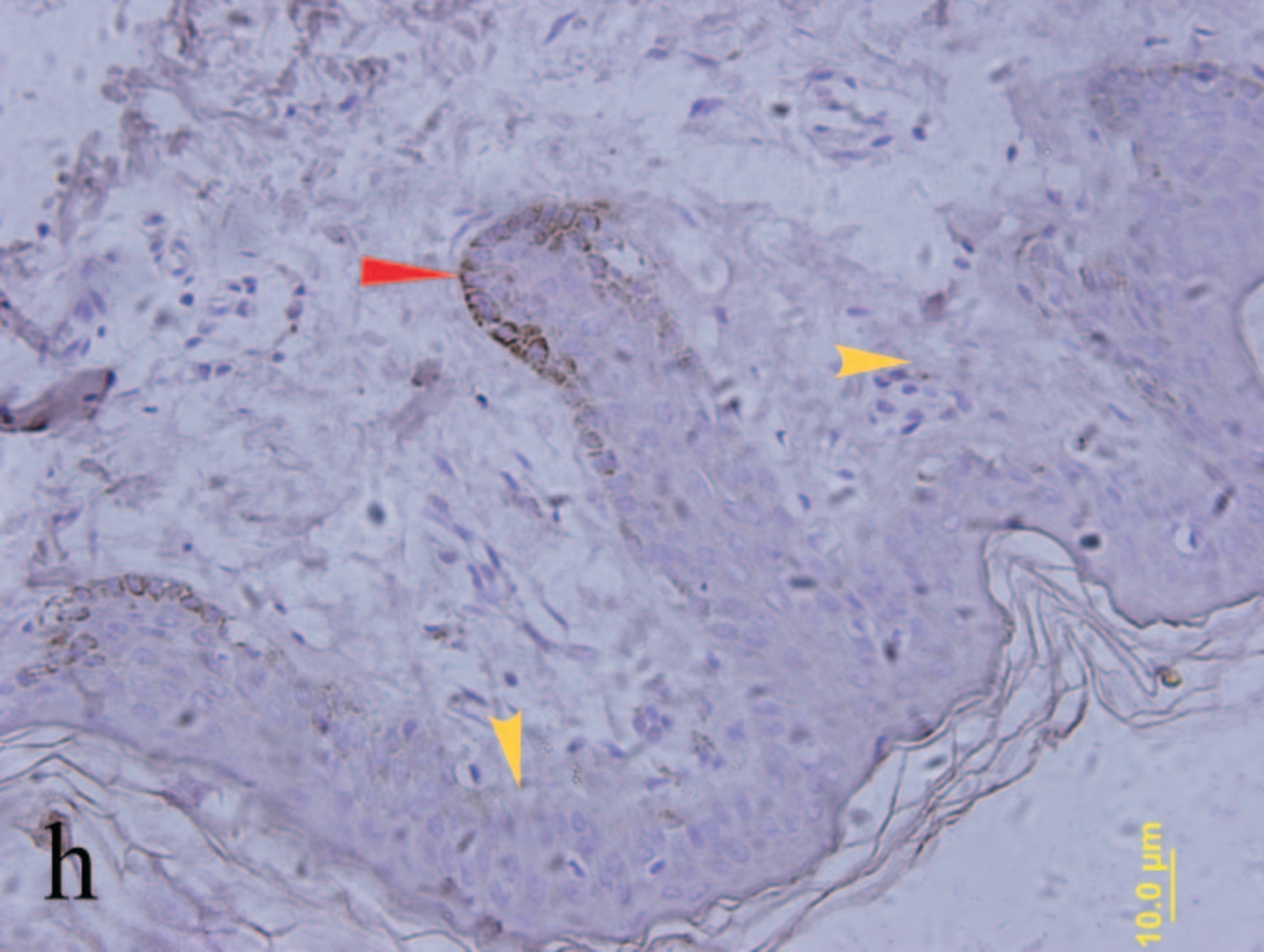
h
10.0 µm

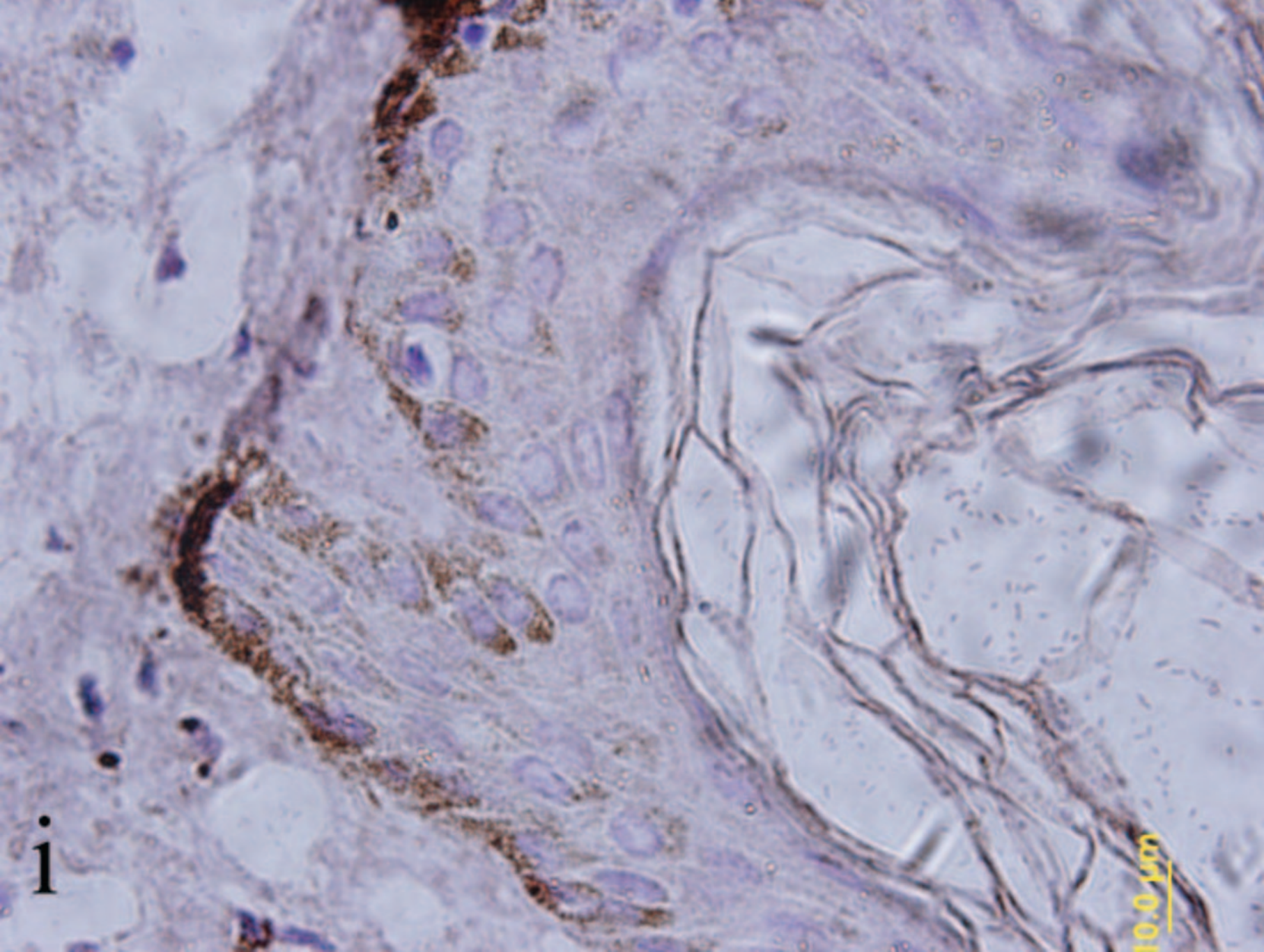
i
100.0 µm

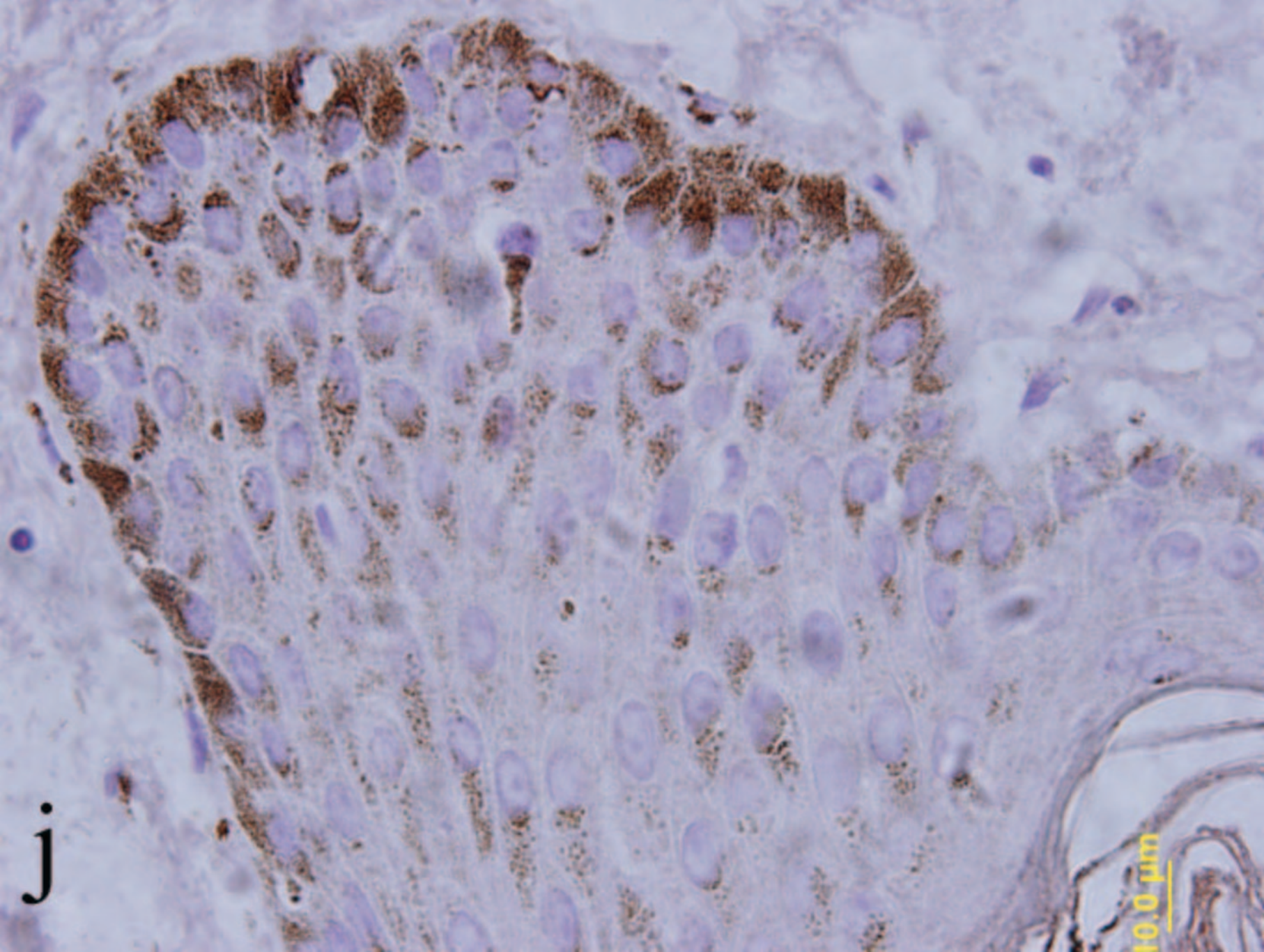
j

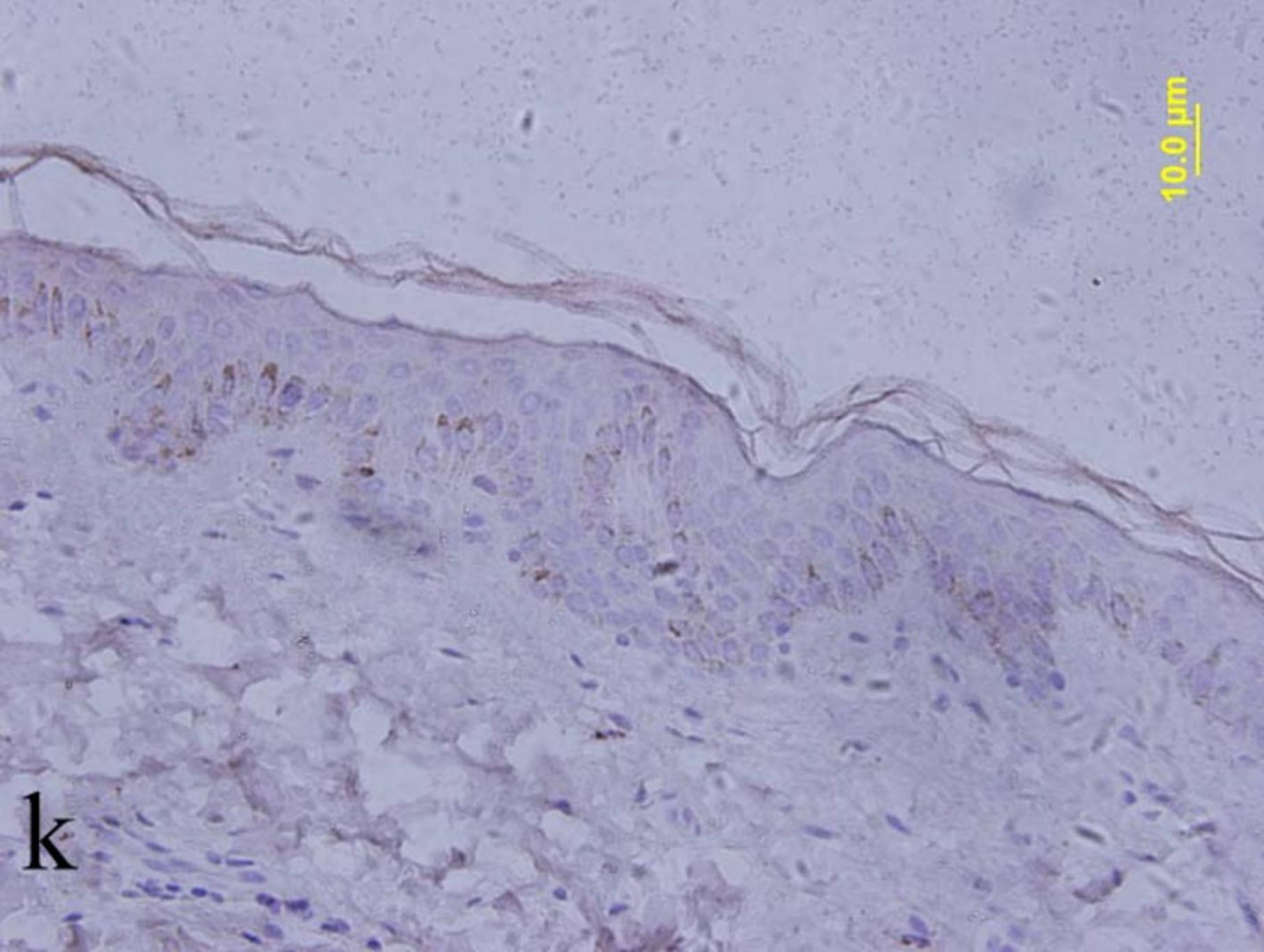
10.0 µm
k

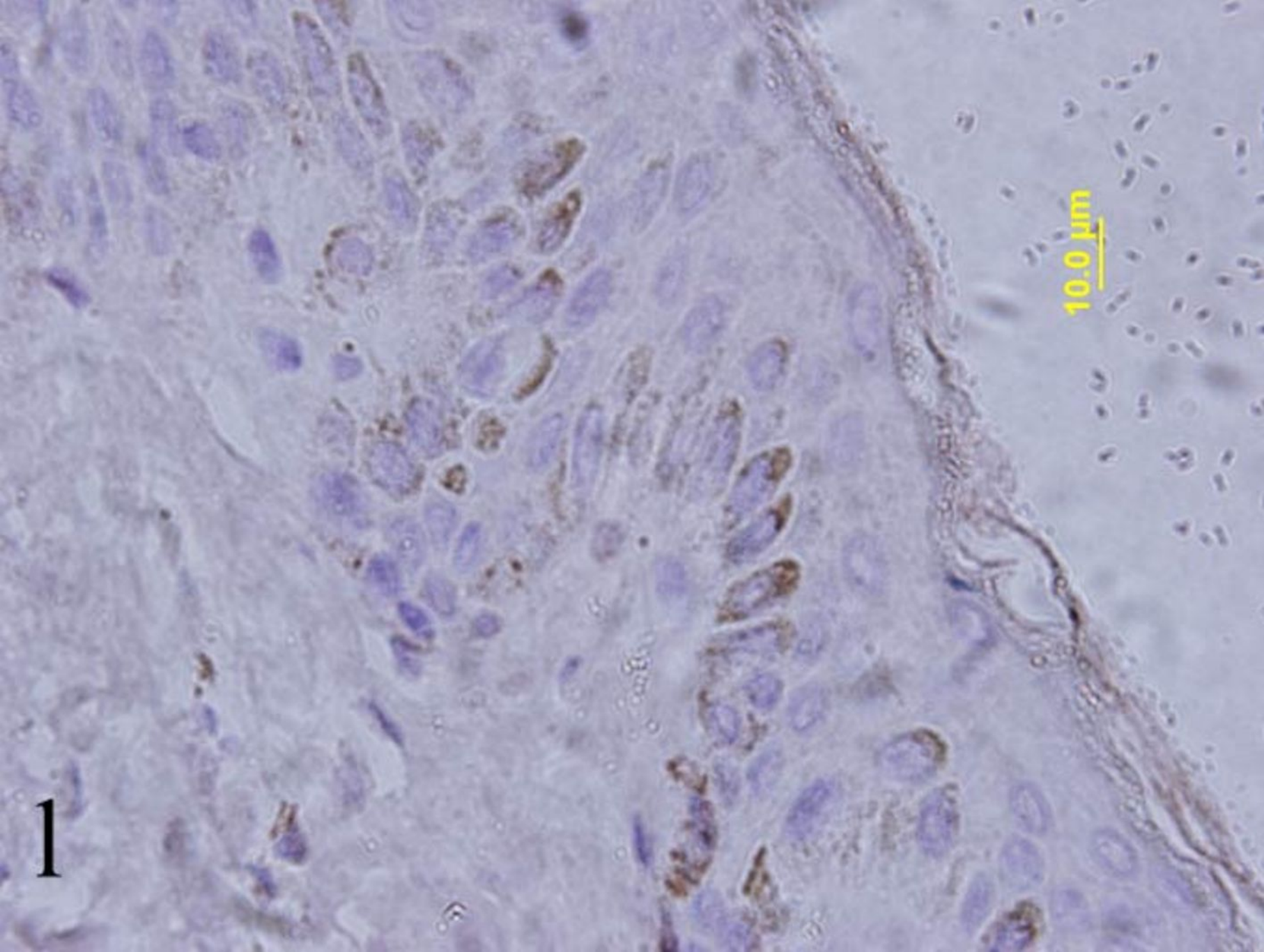

1

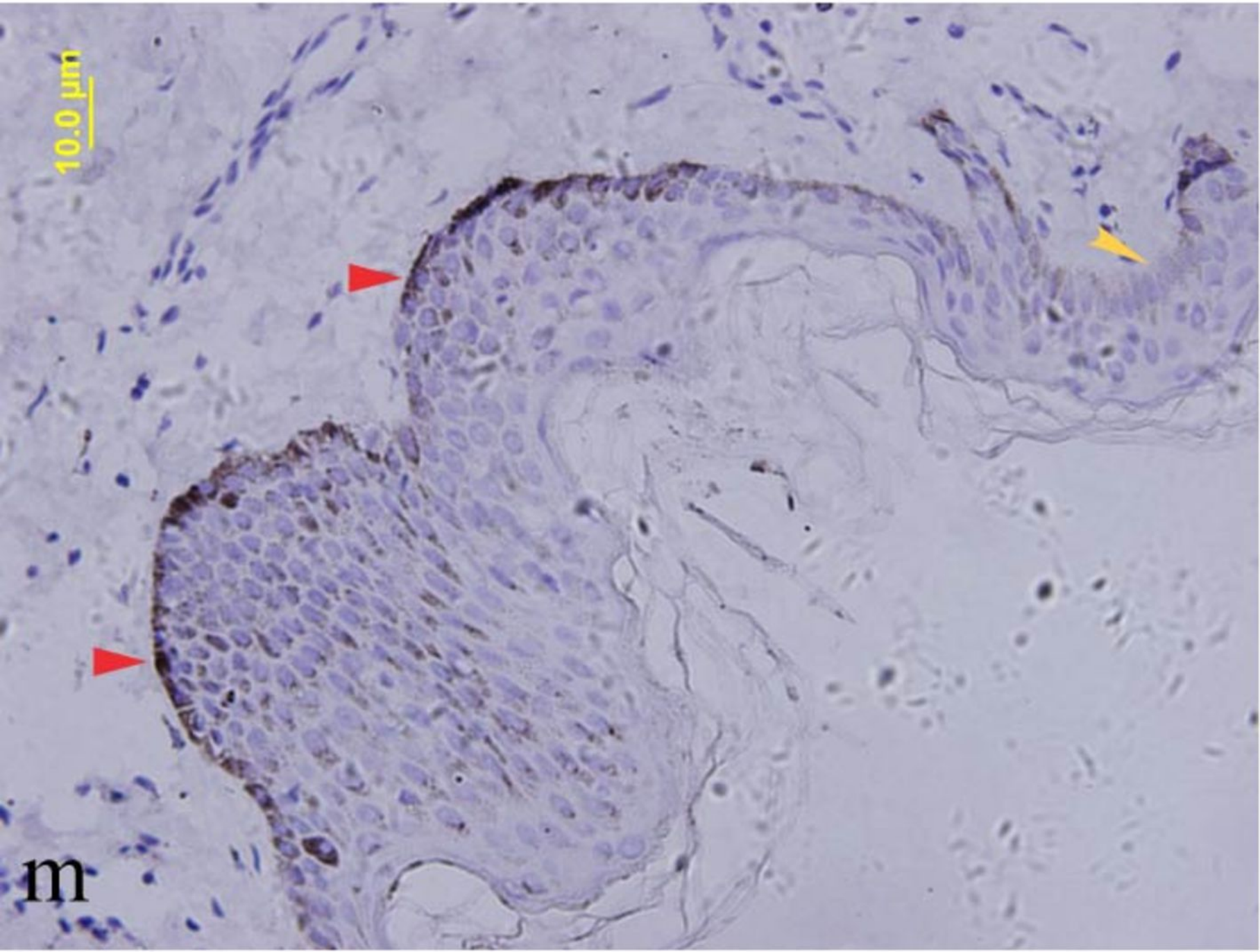
10.0 µm
m

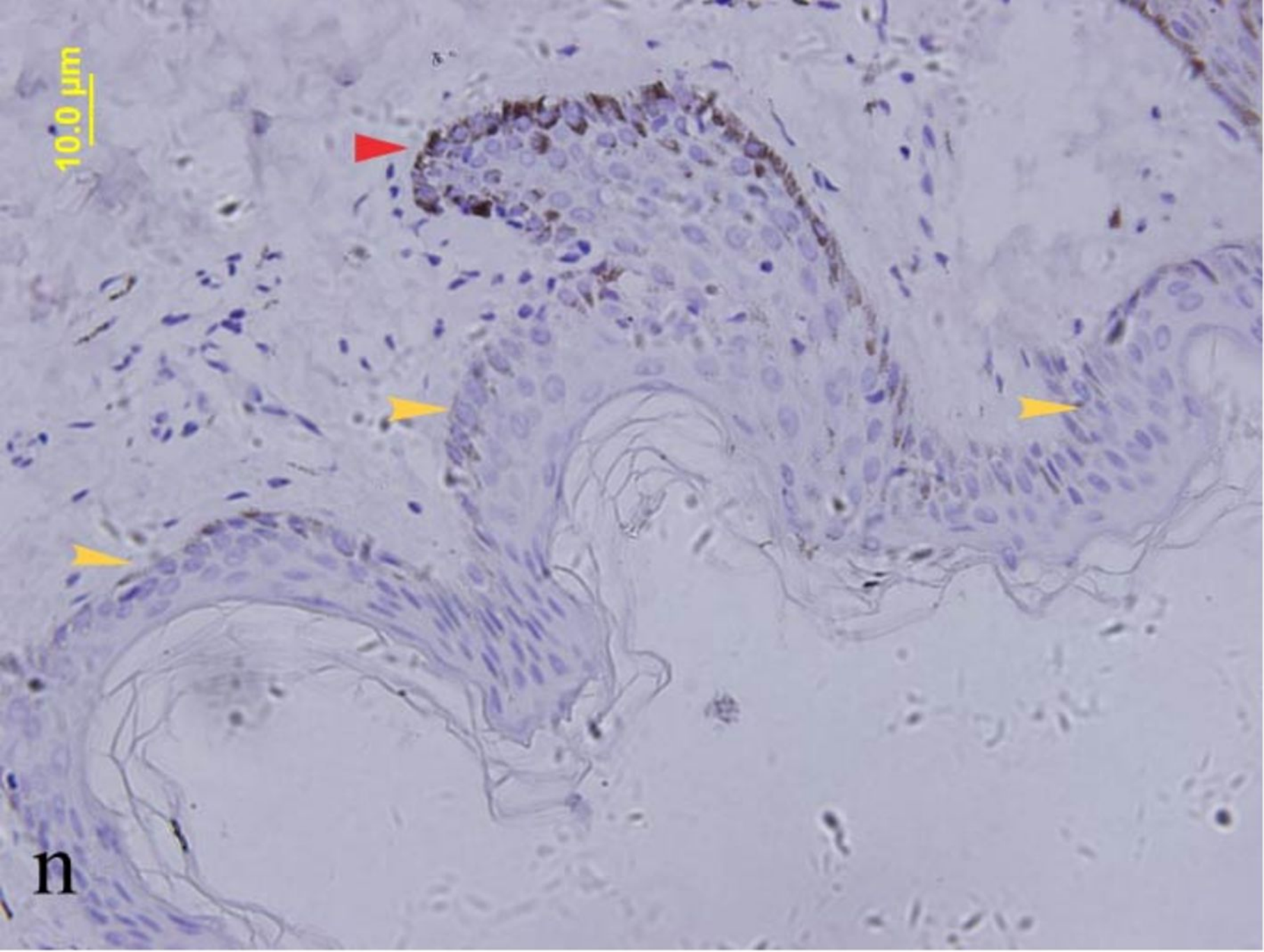
10.0 µm
n

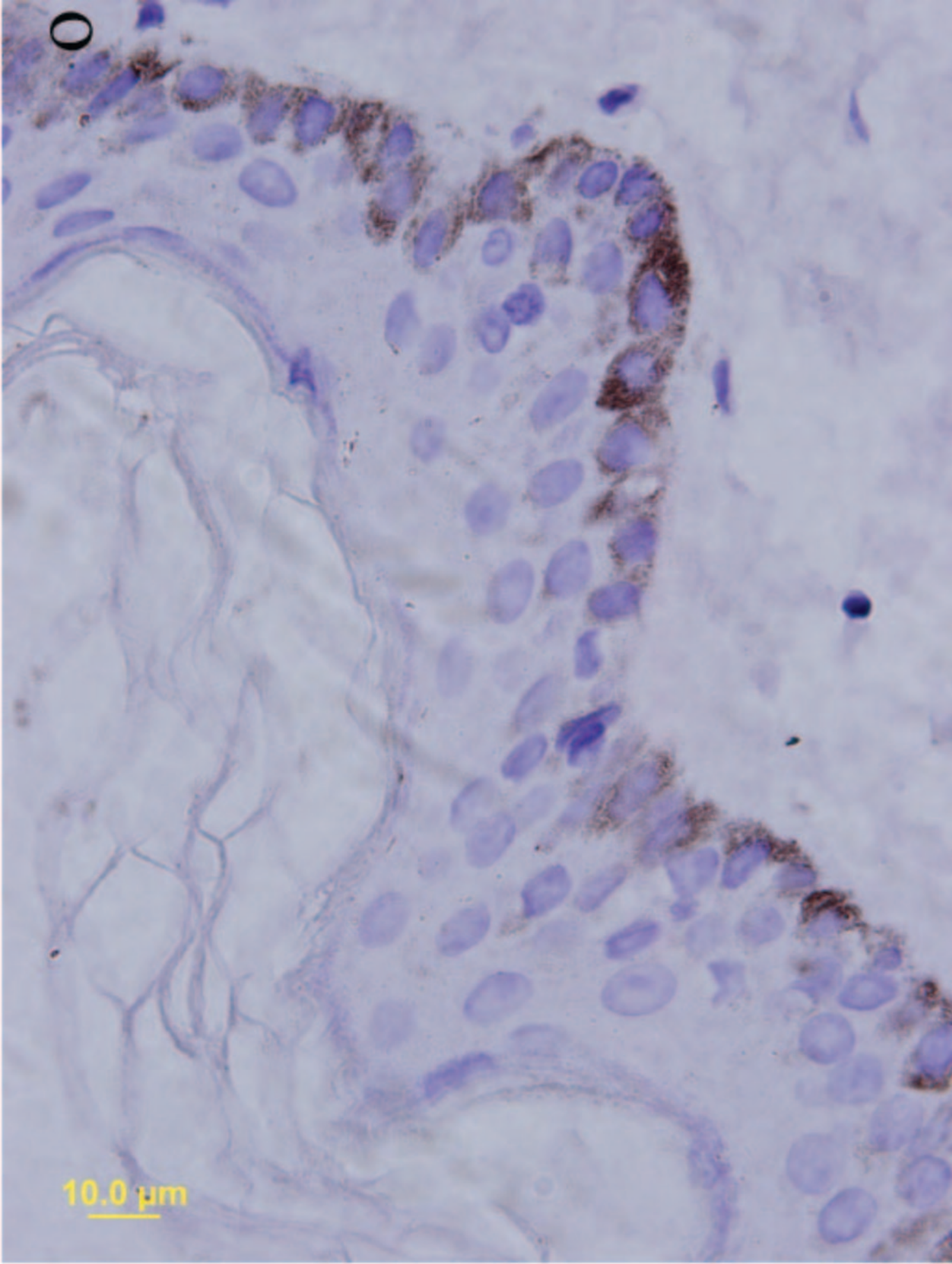
O
10.0 µm

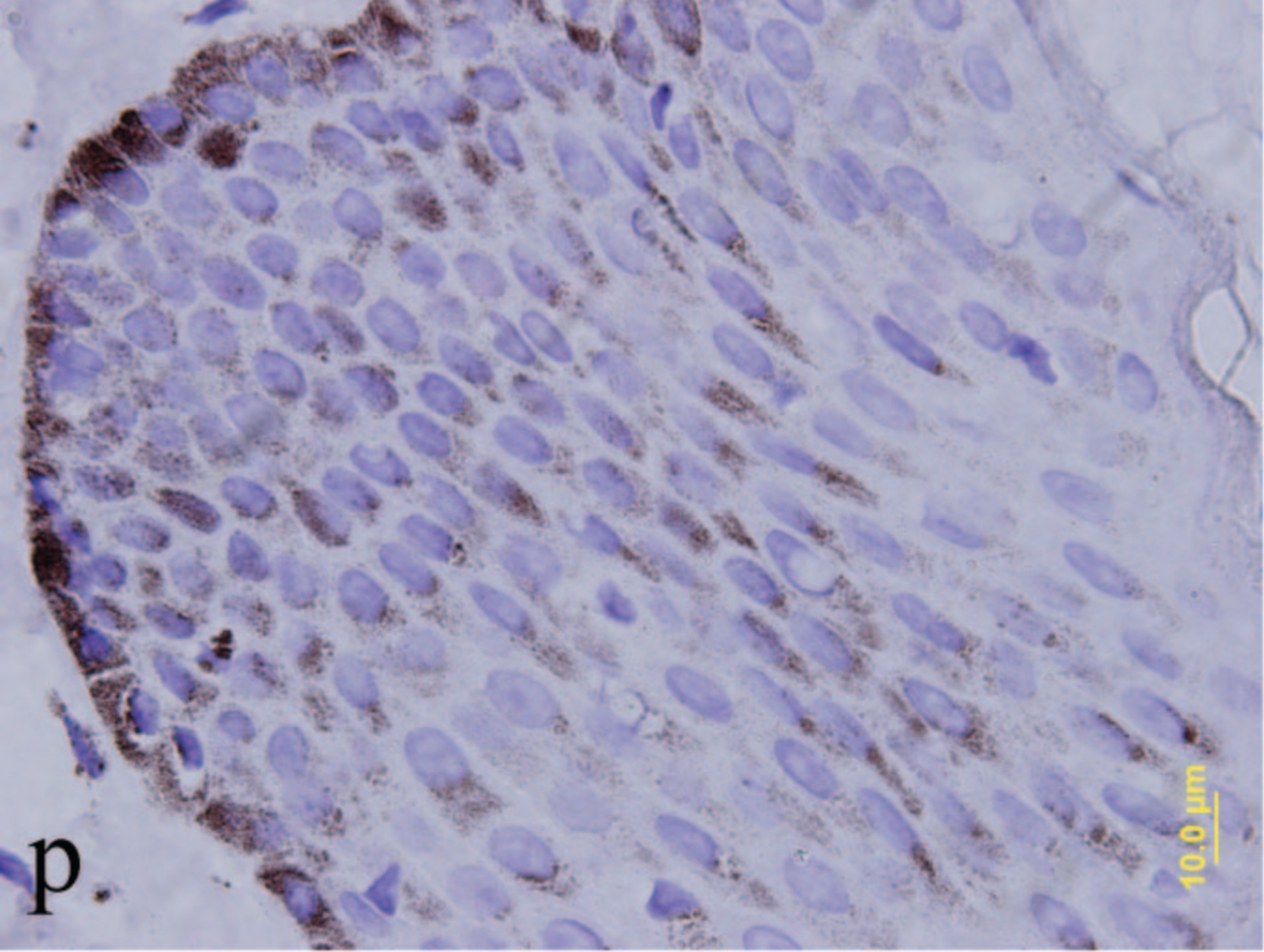
p
10.0 µm

q
10.0 µm

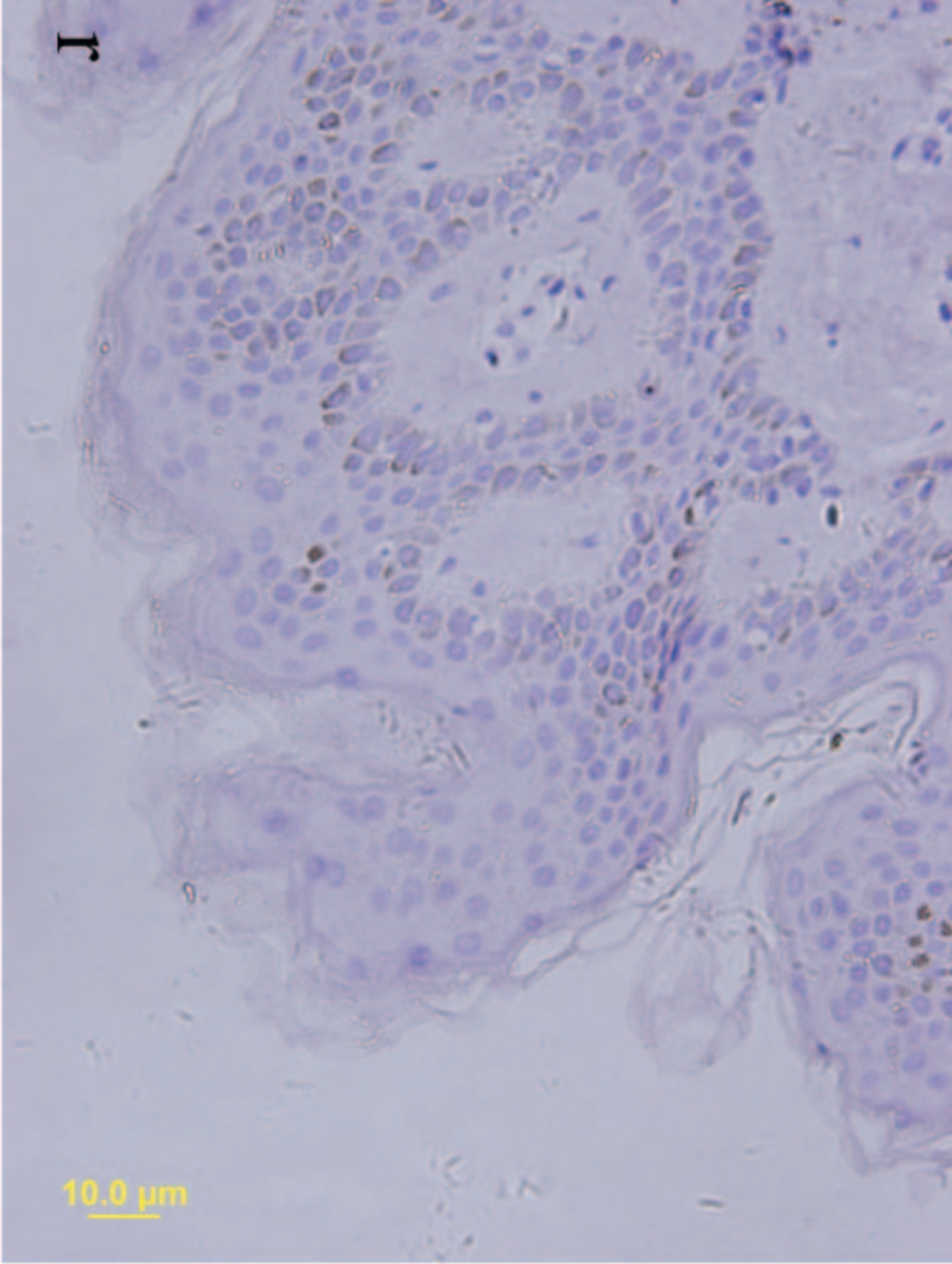
I
10.0 µm

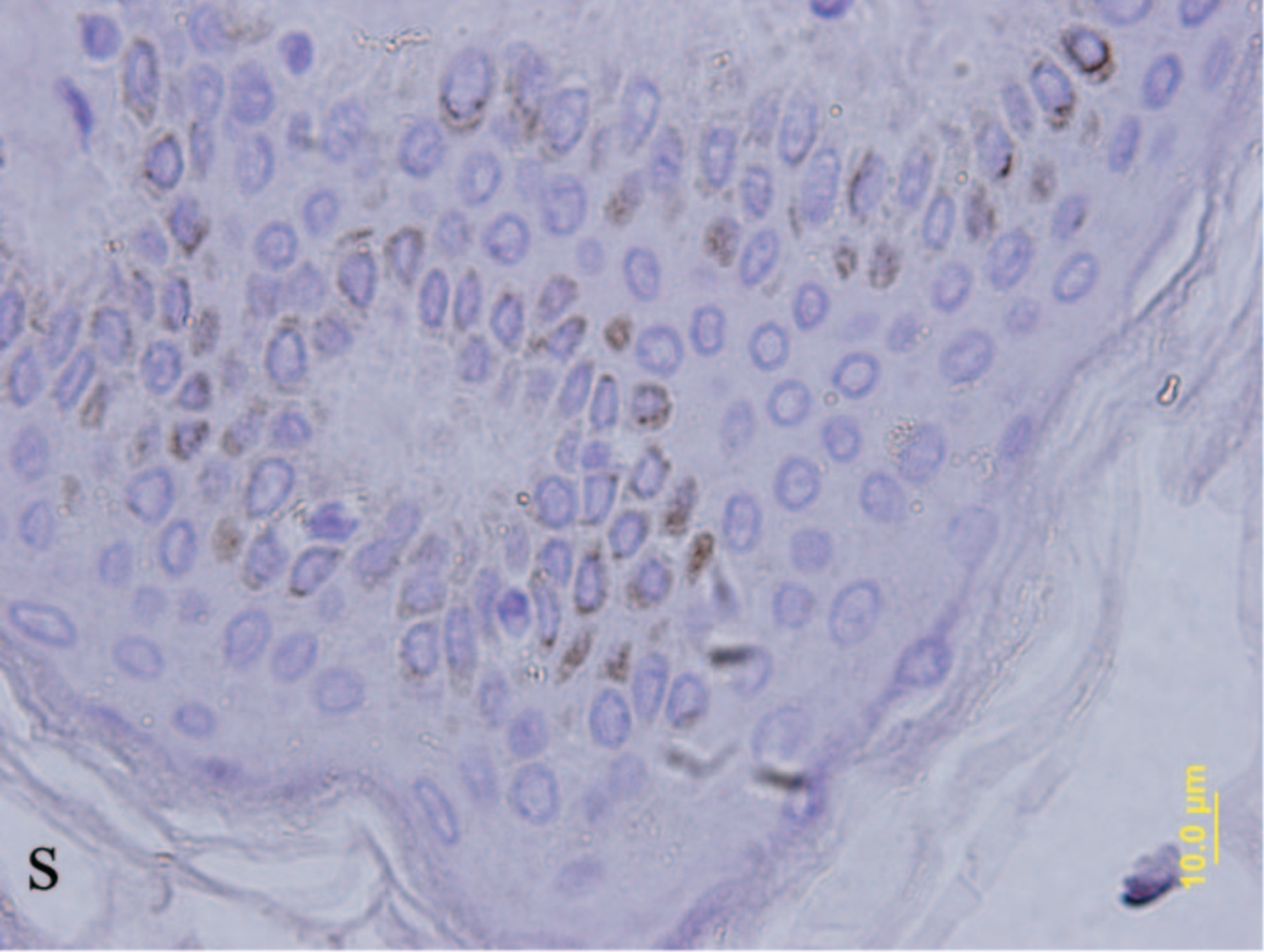
S
10.0 µm

a

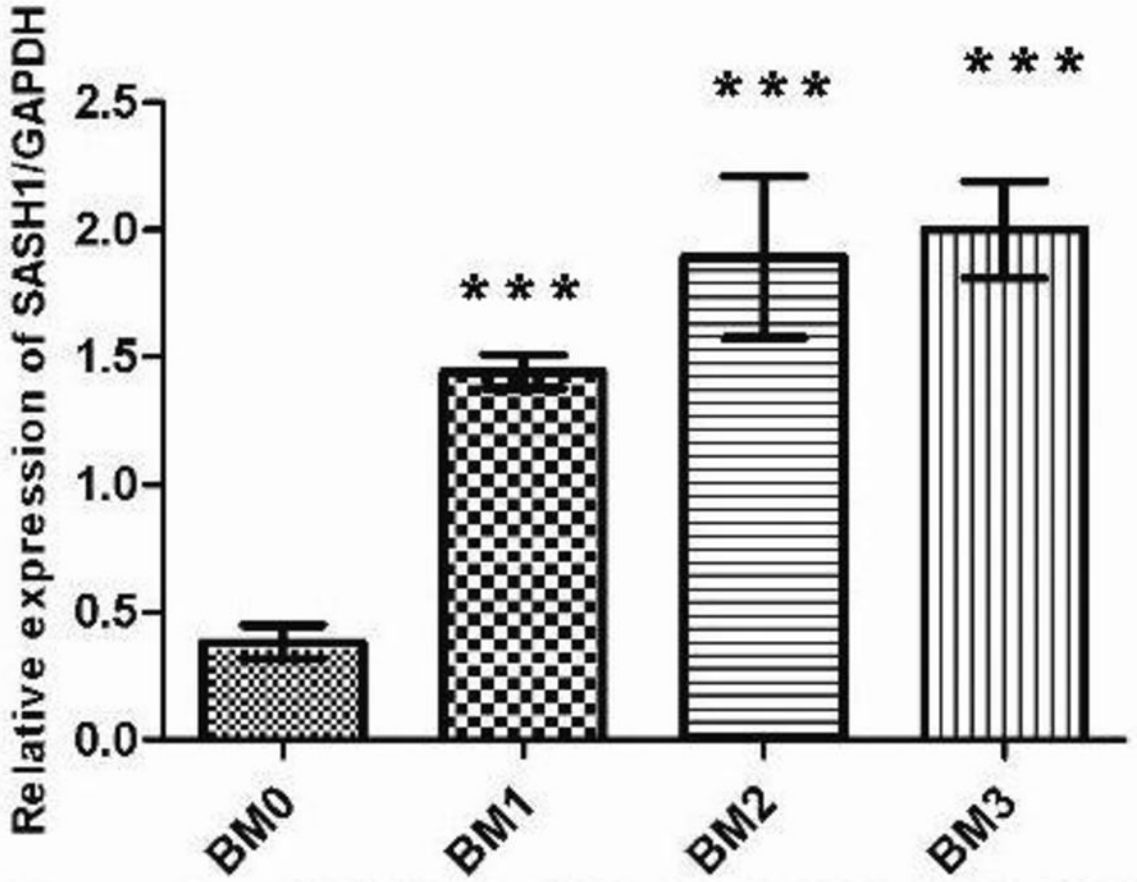

Expression of SASH1 in BM0- A375 ,BM1-A375 ,BM2 -A375 and BM3- A375 cells.

*** **indicates BM1, BM2 and BM3 vs BM0, respectively,p=0.001.**

a

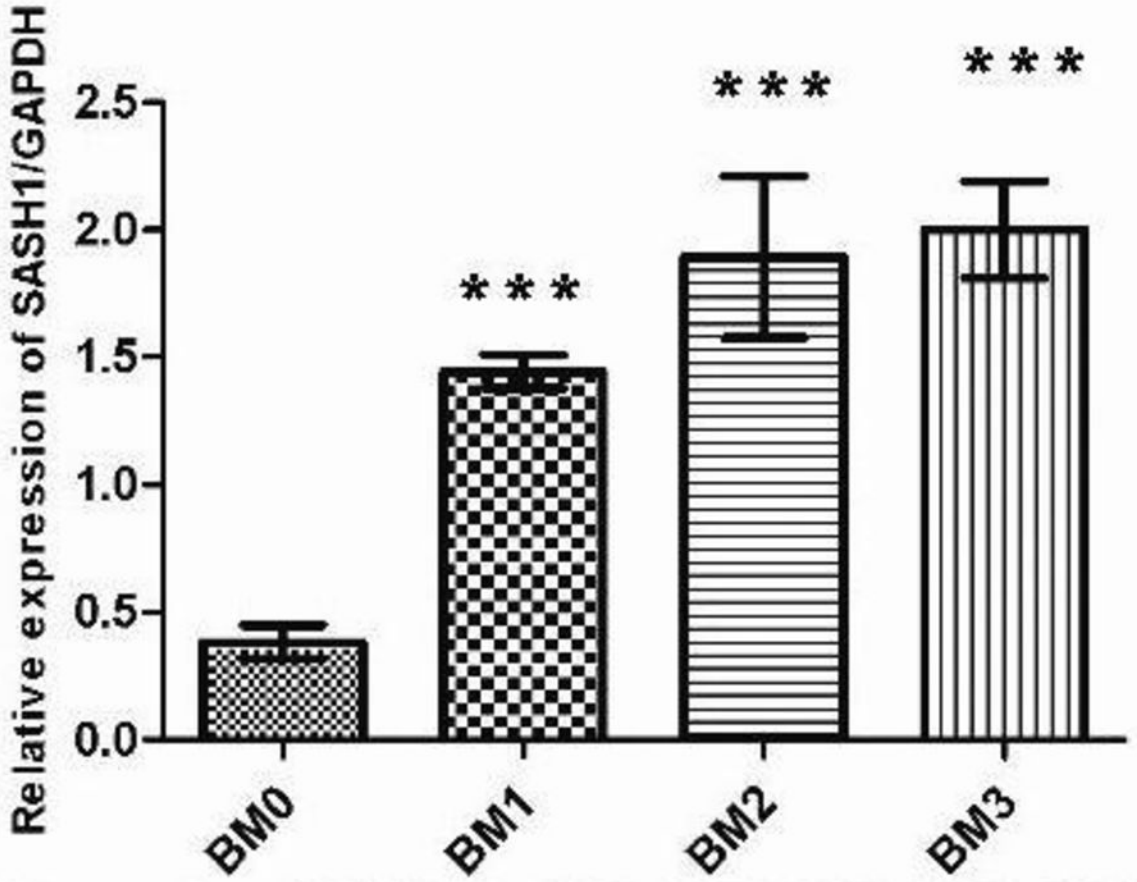

Expression of SASH1 in BM0- A375 ,BM1-A375 ,BM2 -A375 and BM3- A375 cells.

*** **indicates BM1, BM2 and BM3 vs BM0, respectively,p=0.001.**

b

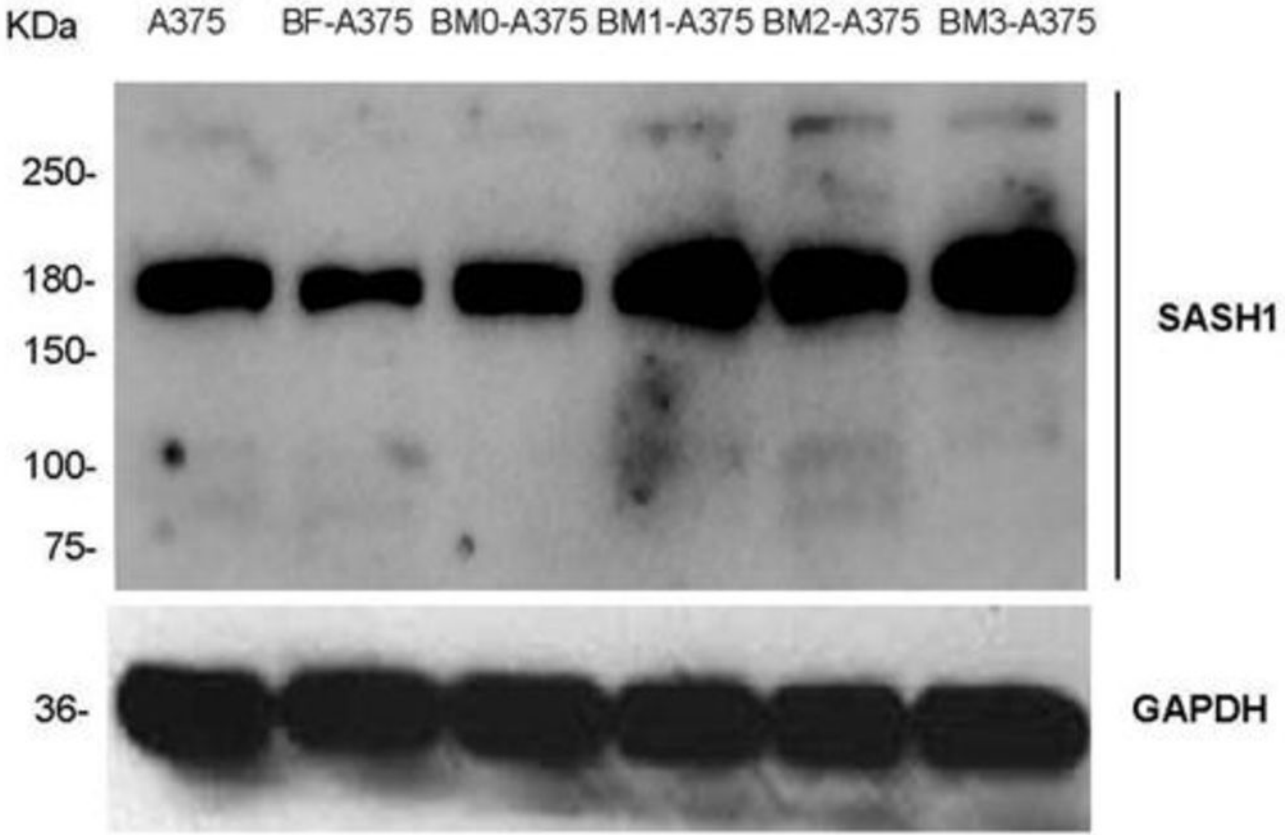
KDa
A375
BF-A375
BM0-A375
BM1-A375
BM2-A375
BM3-A375
250-
180-
150-
100-
75-
SASH1
36-
GAPDH

c

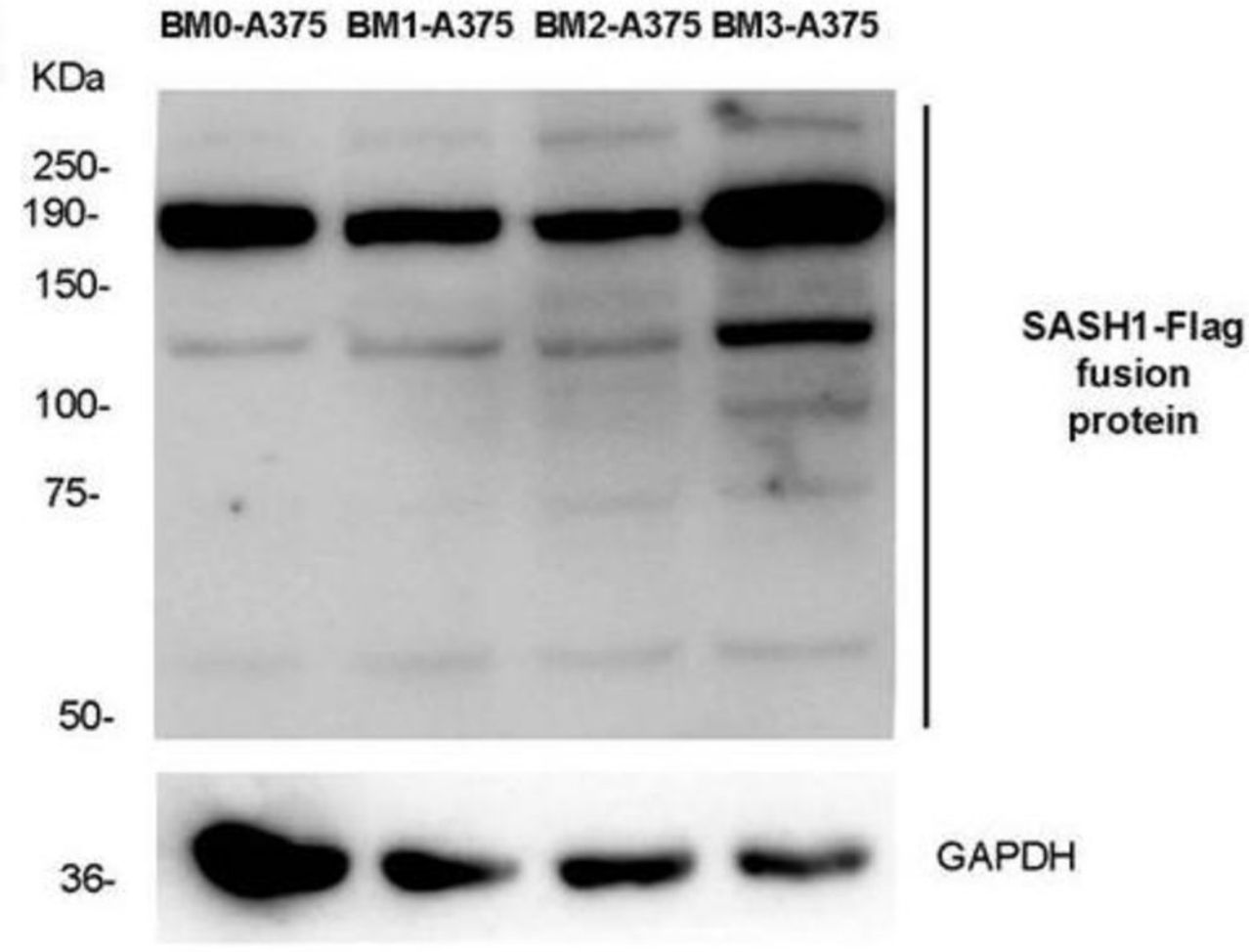
BM0-A375
BM1-A375
BM2-A375
BM3-A375
KDa
250-
190-
150-
100-
75-
50-
36-
SASH1-Flag fusion protein
GAPDH

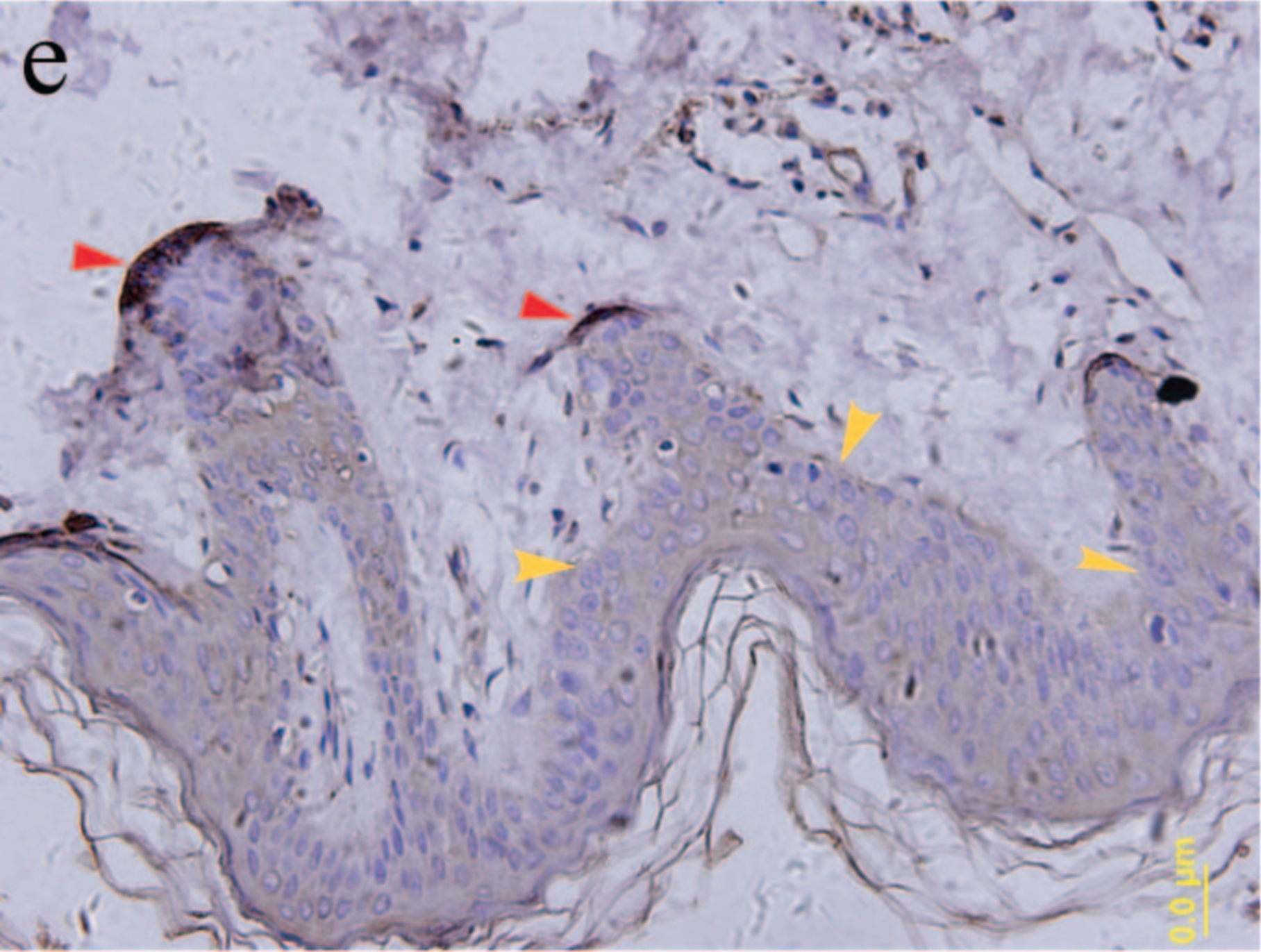
e
0.0 µm

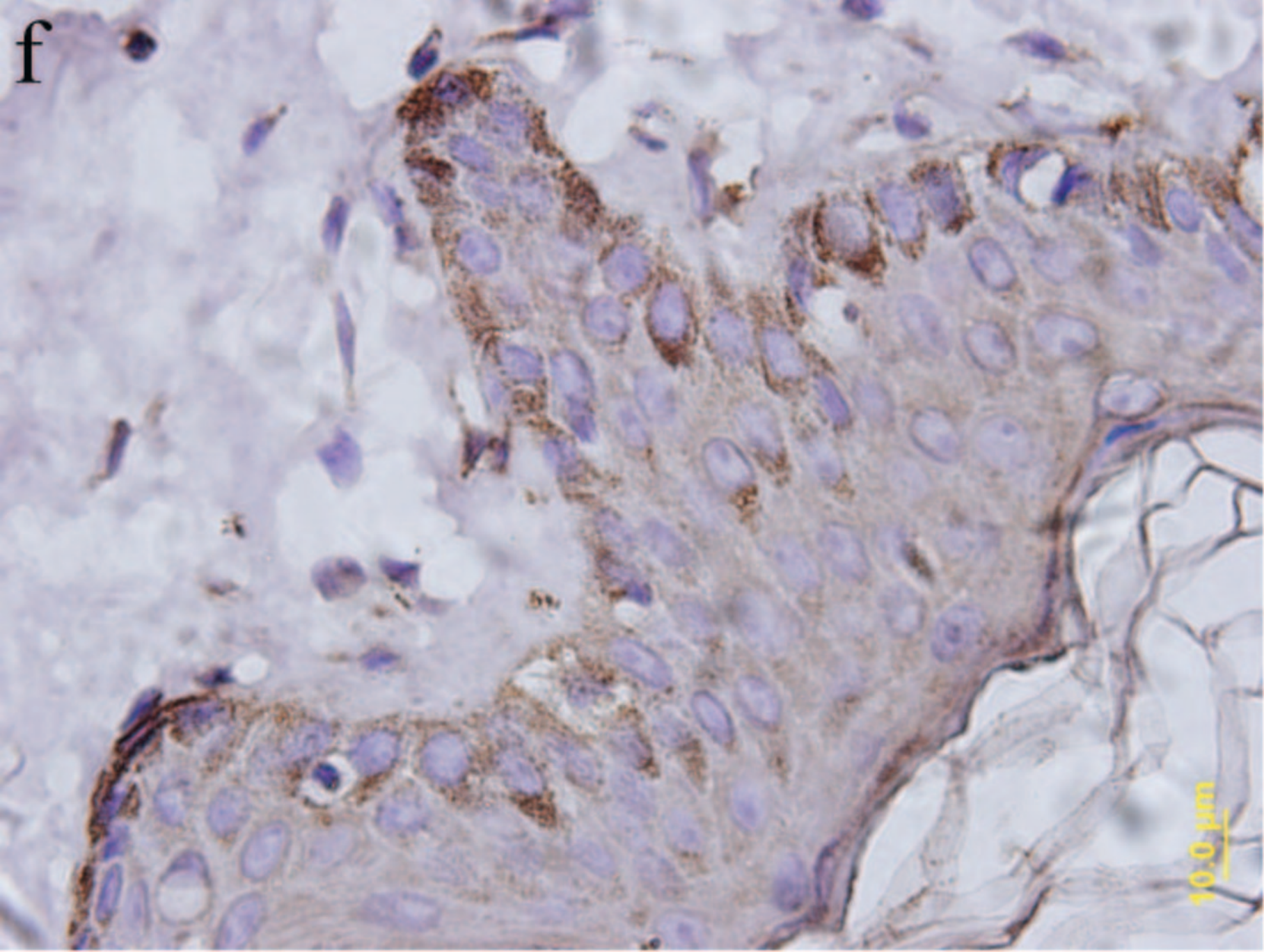
f
10.0 µm

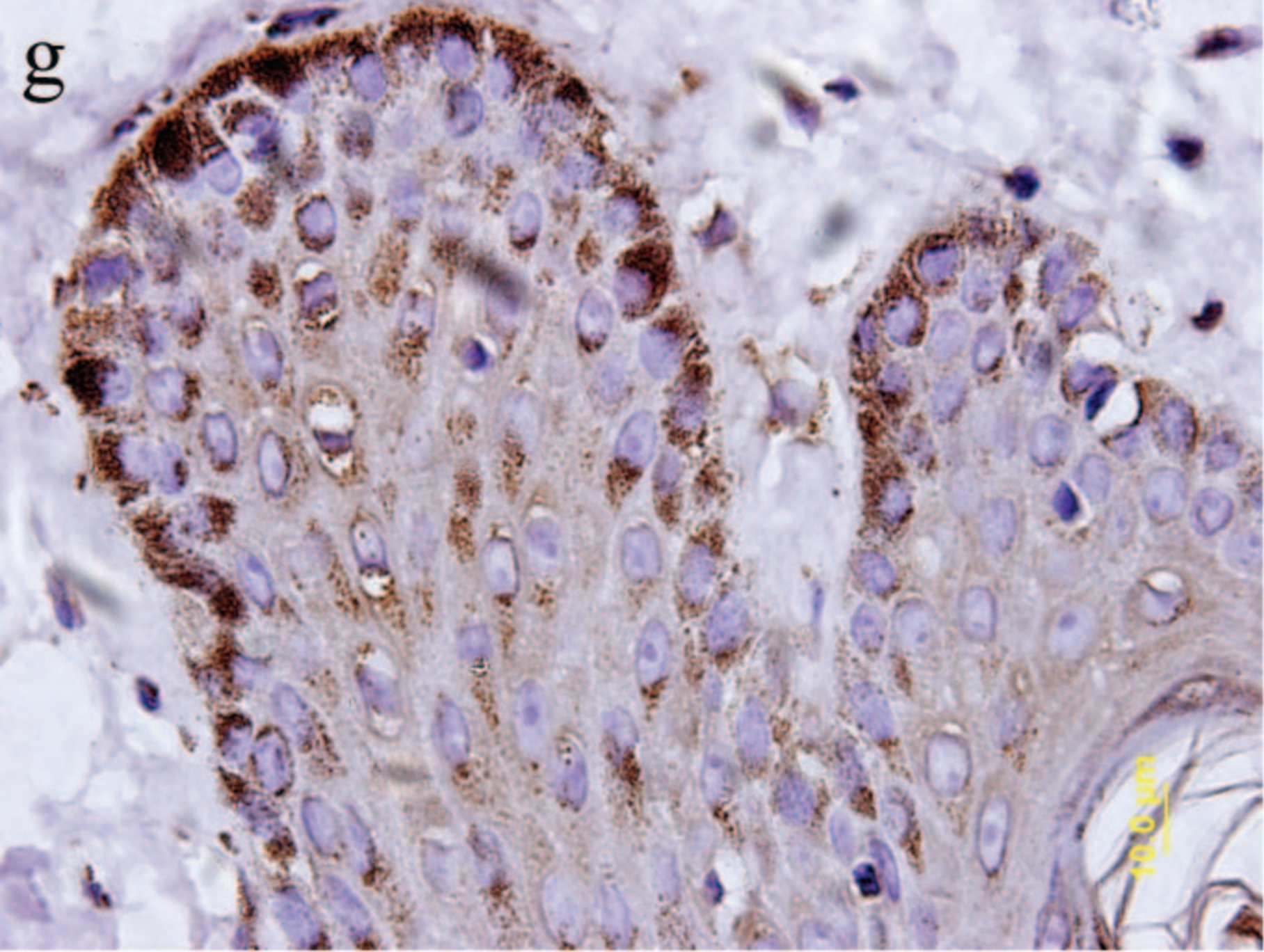
g
10.0 µm

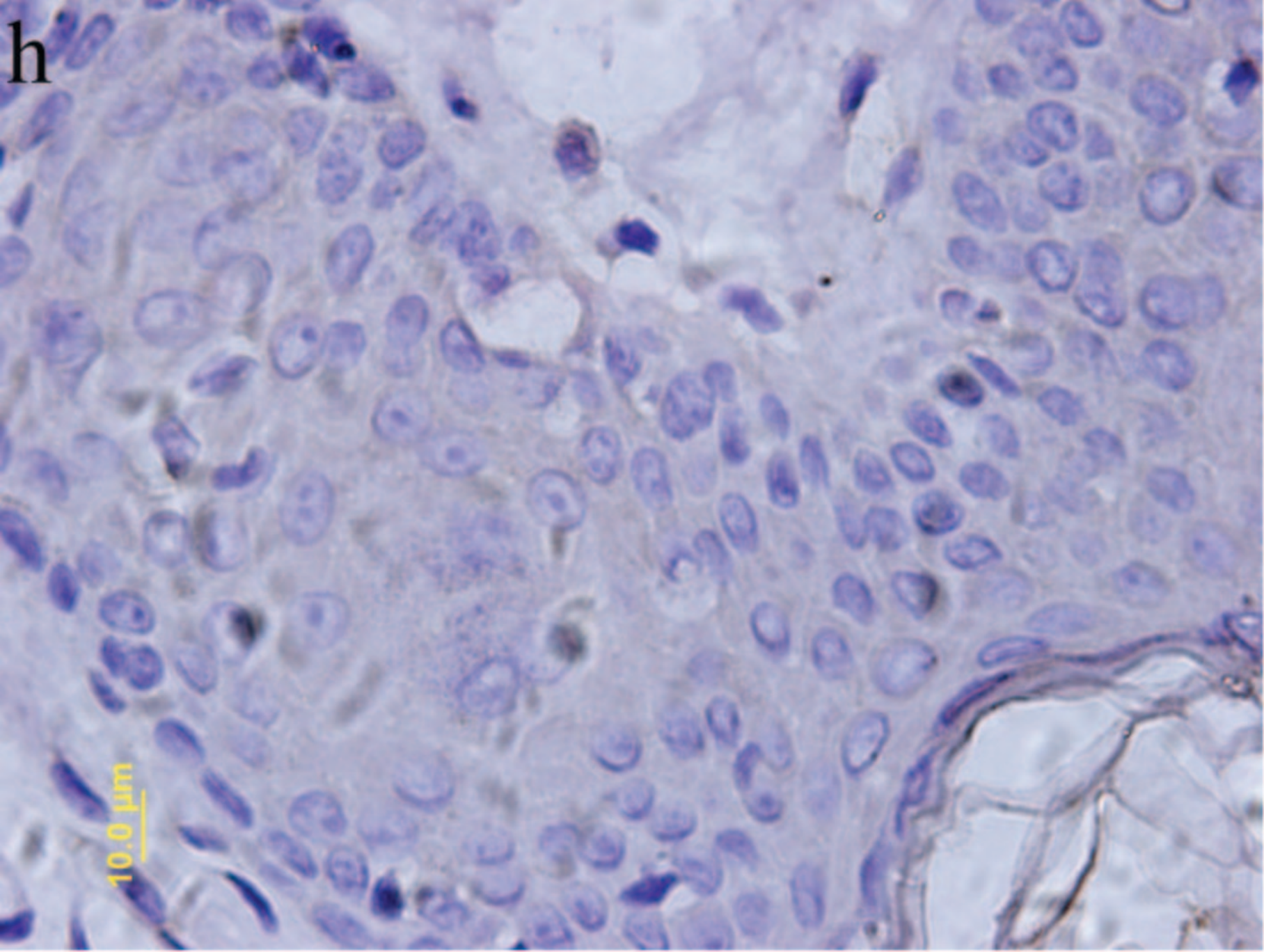
h
10.0 µm

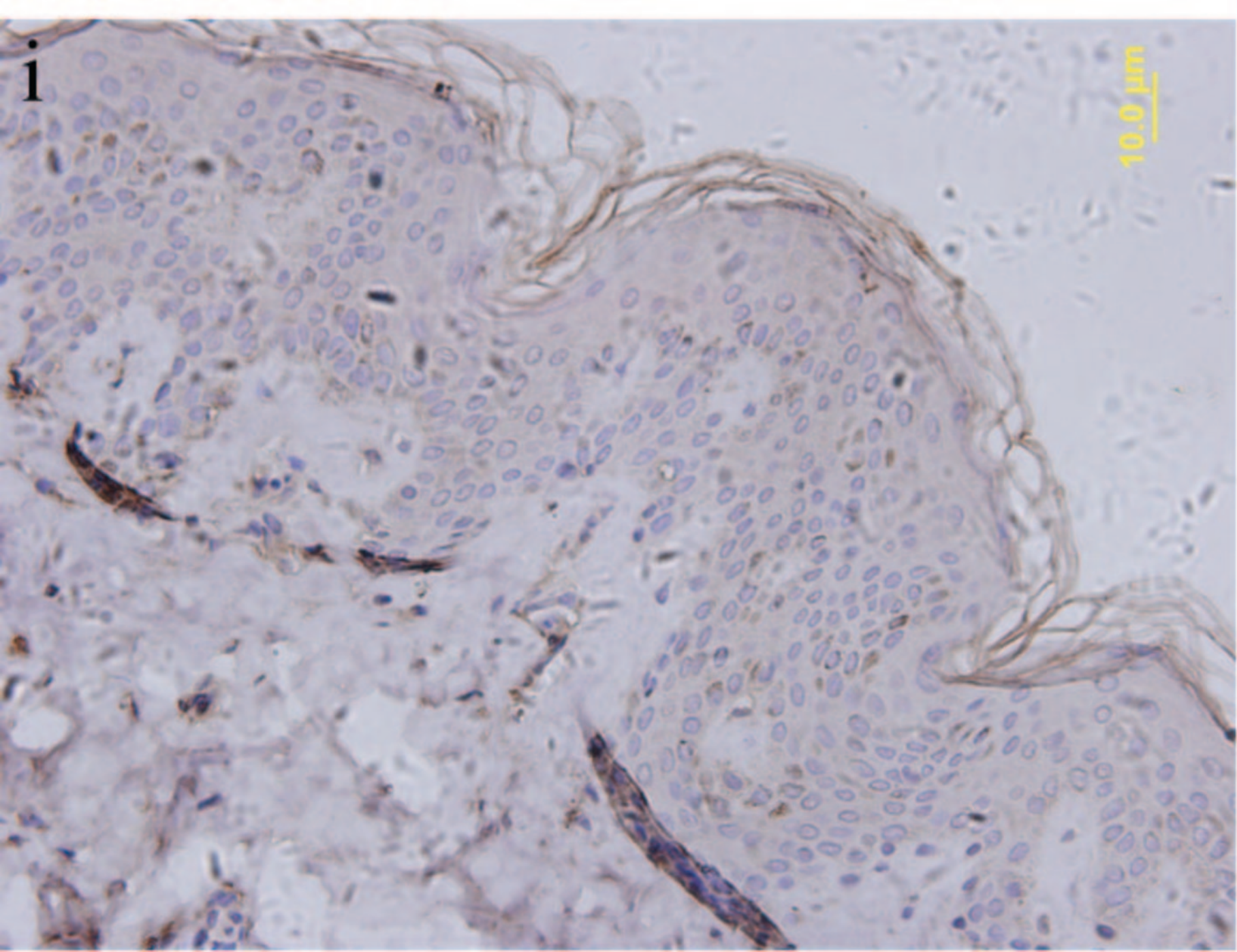
i
10.0 µm

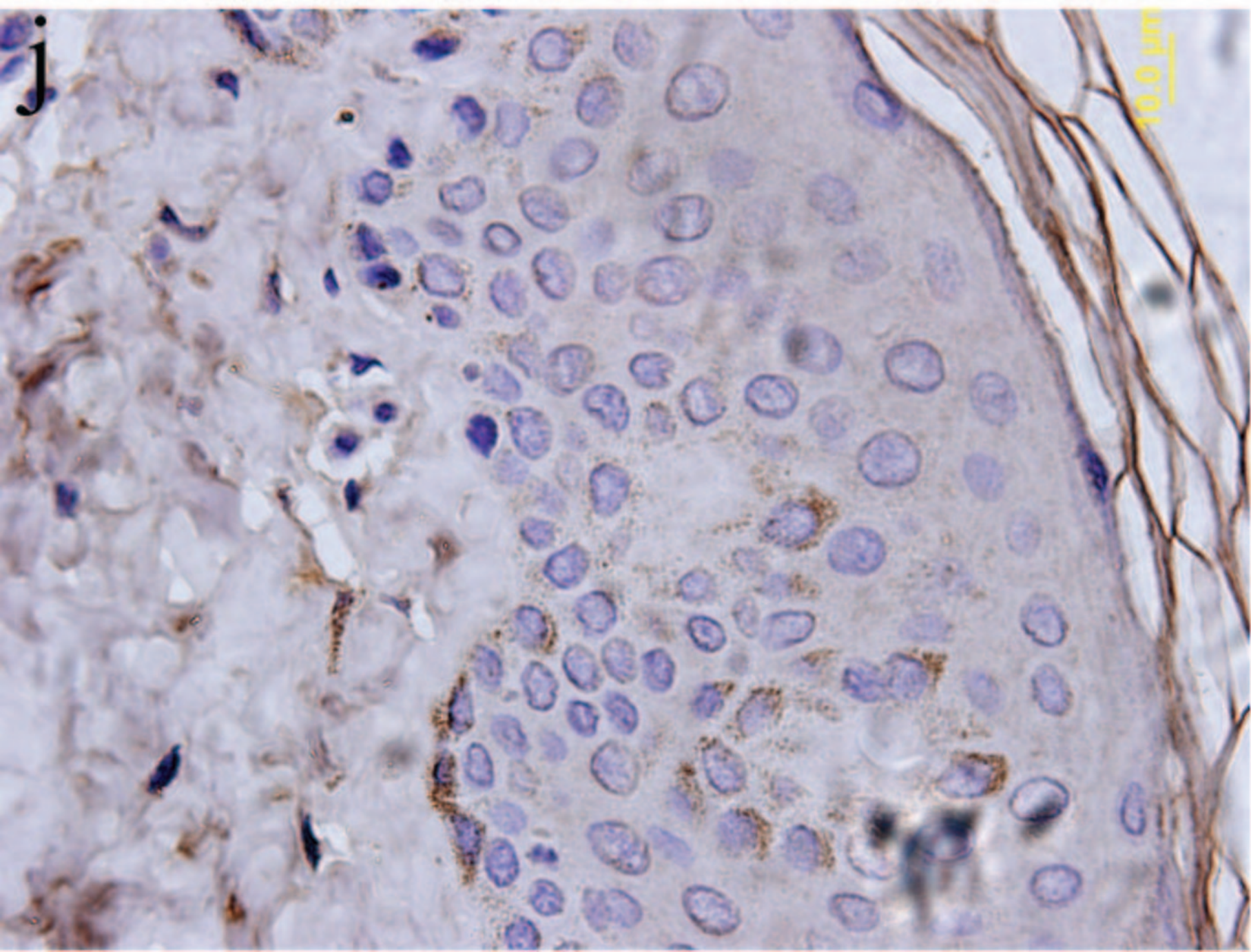
j
0.01 µm

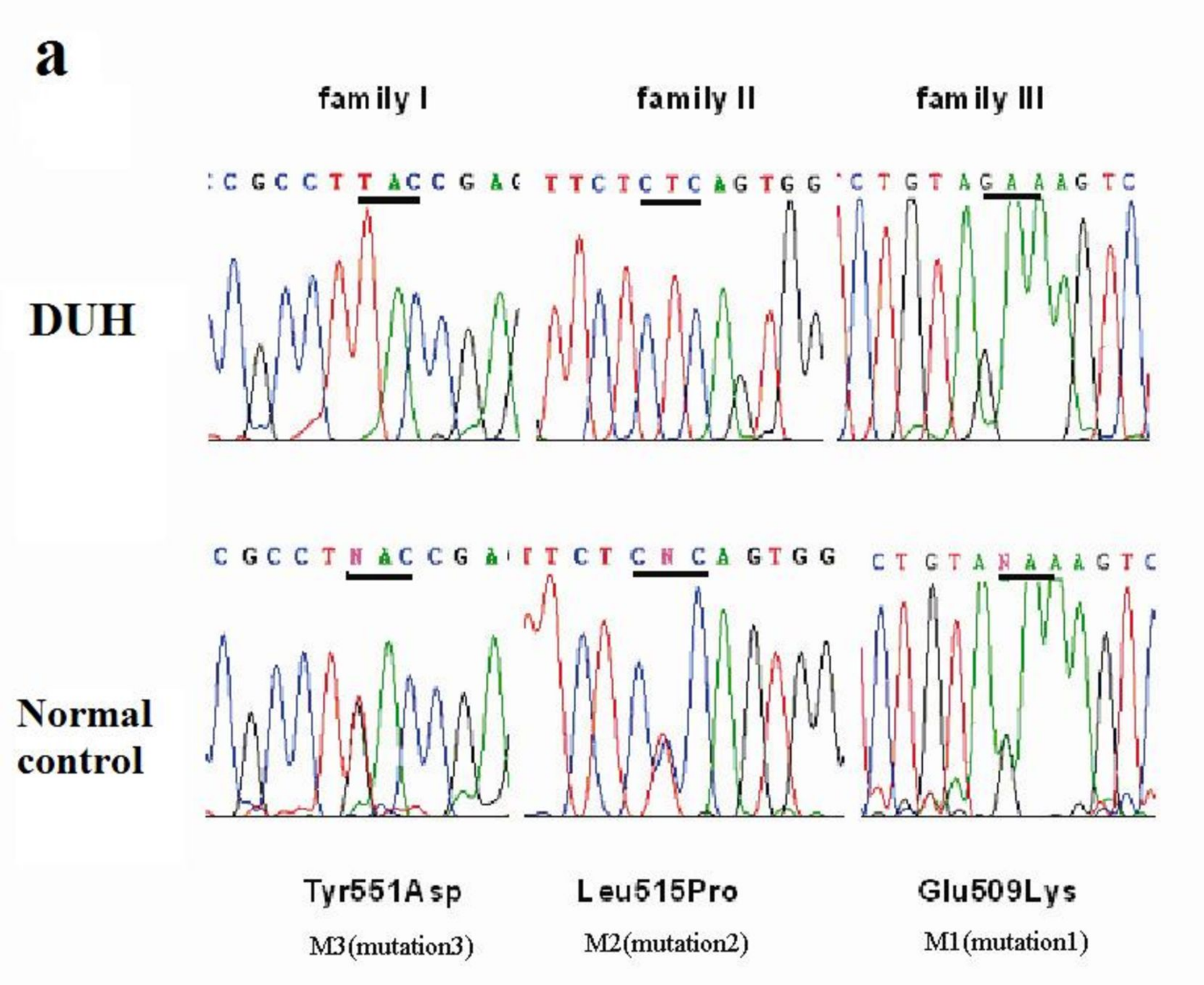
a
family I
family II
family III
DUH
Normal control
Tyr551Asp
Leu515Pro
Glu509Lys
M3(mutation3)
M2(mutation2)
M1(mutation1)

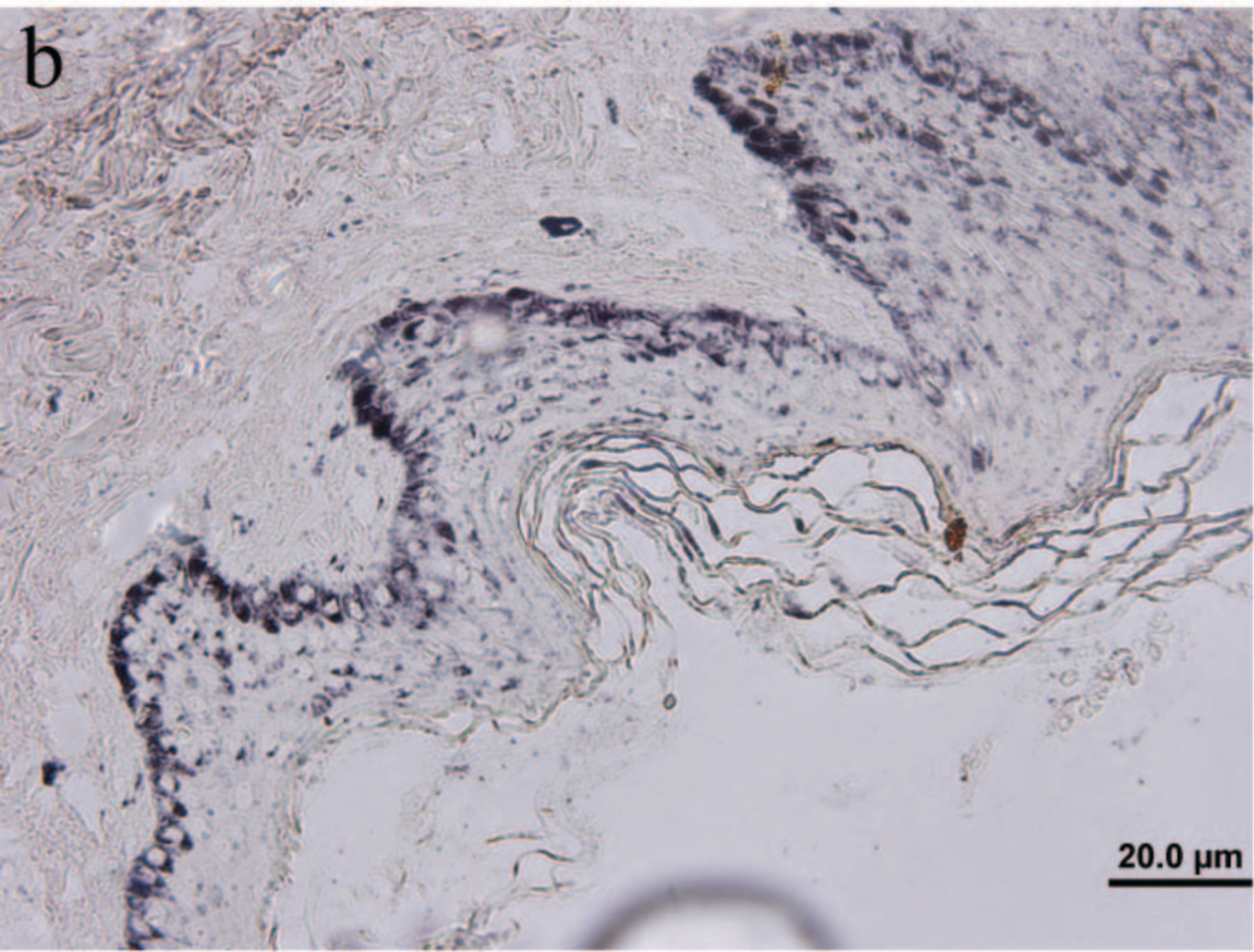
b
20.0 µm

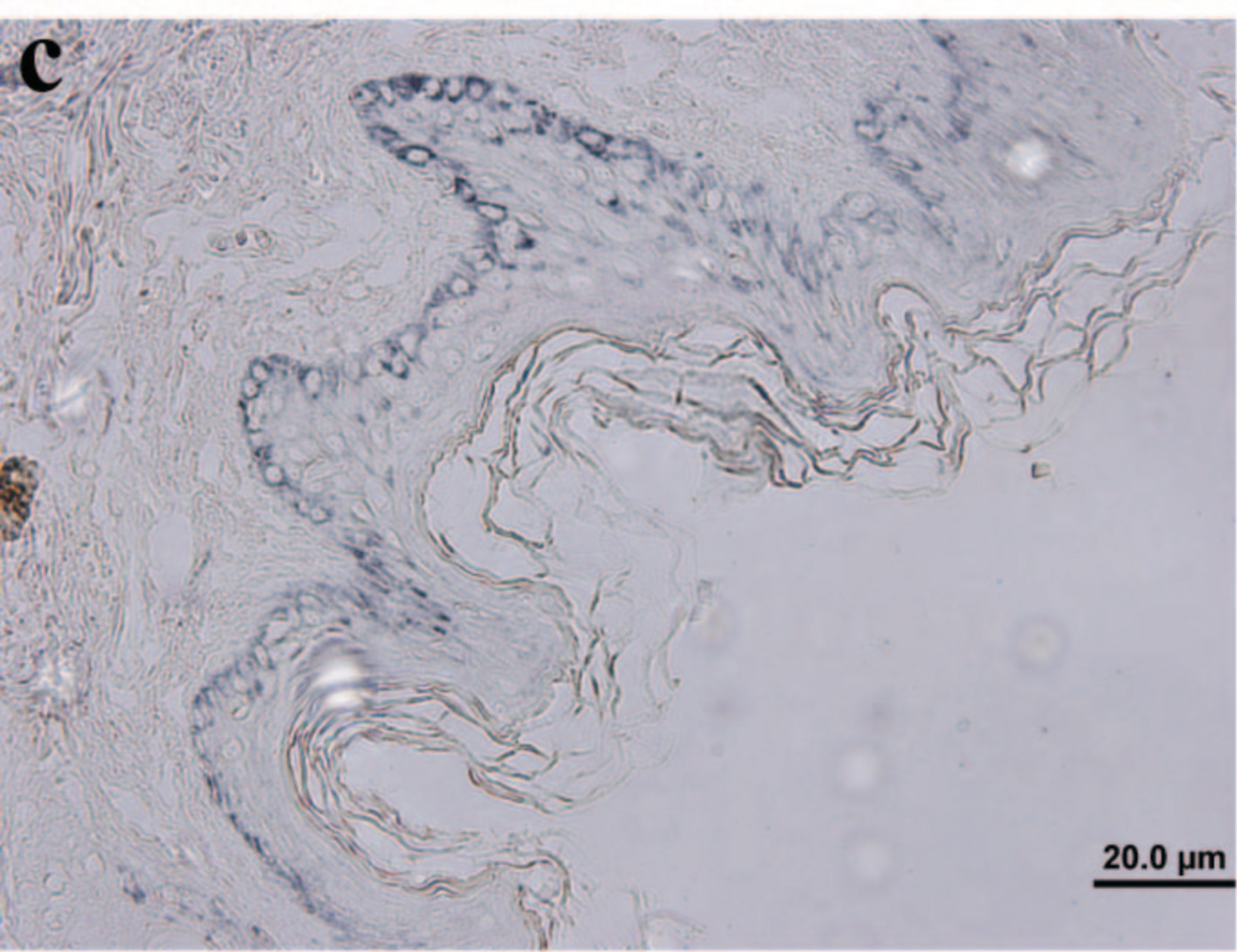
c
20.0 µm

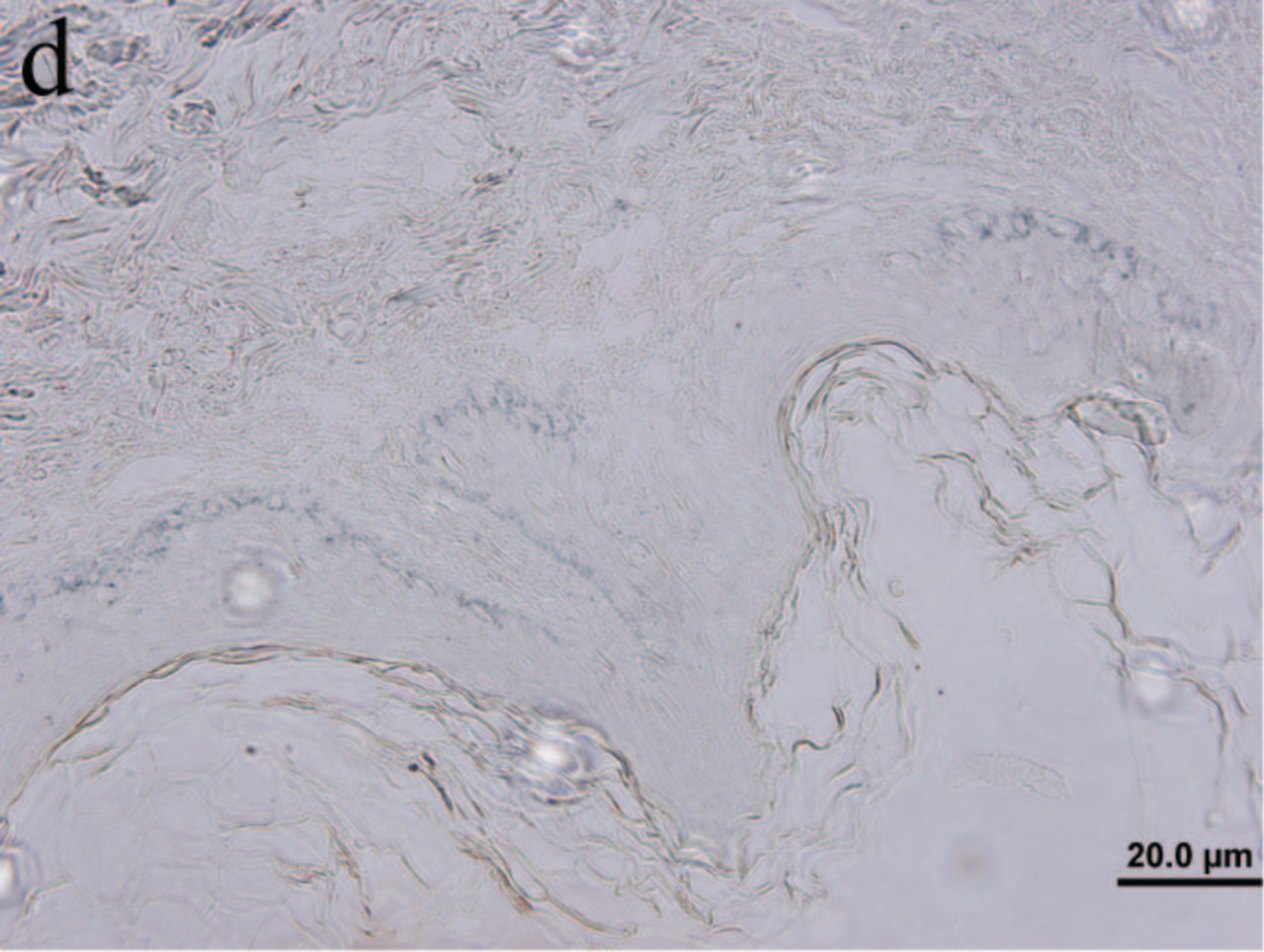
d
20.0 µm

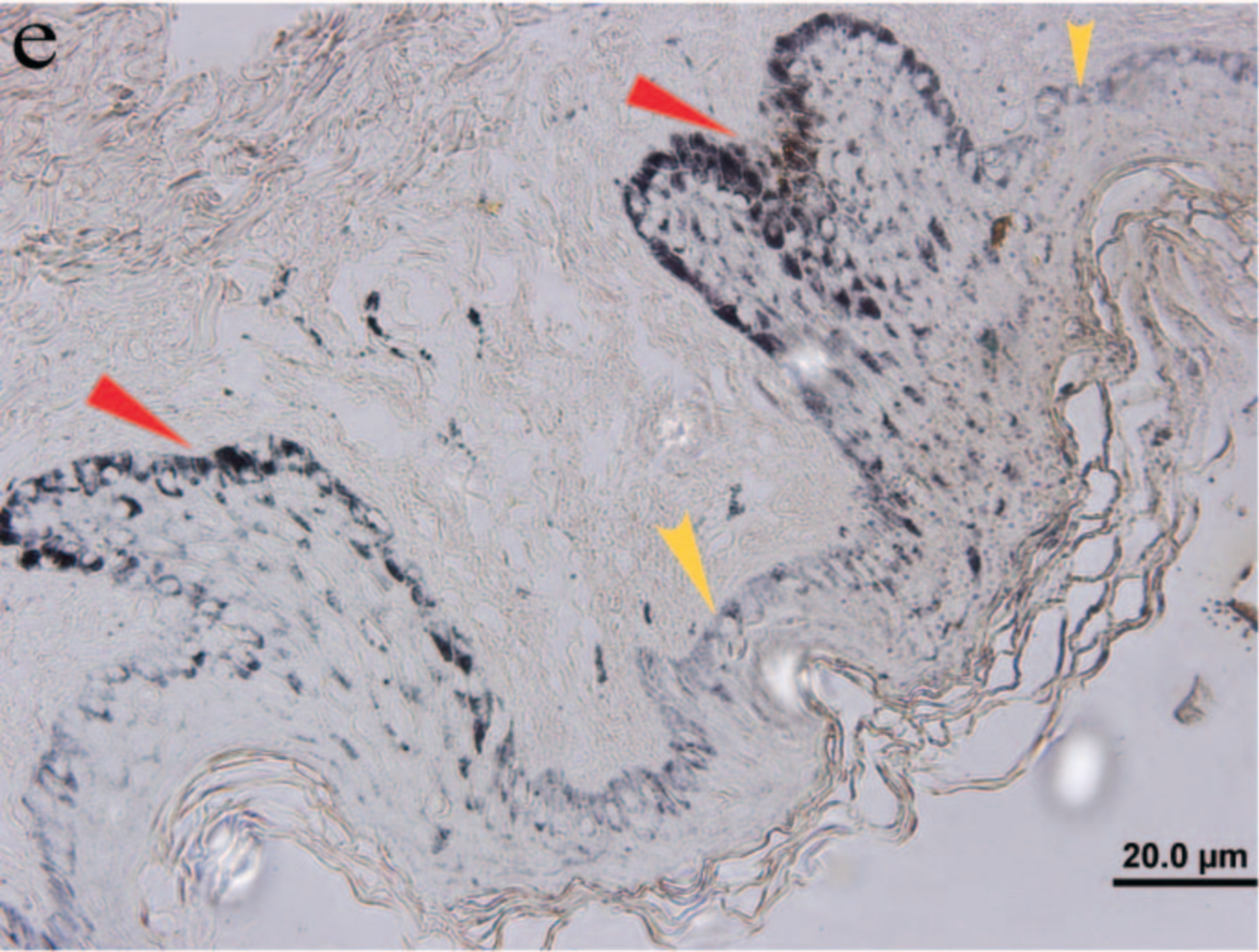
e
20.0 µm

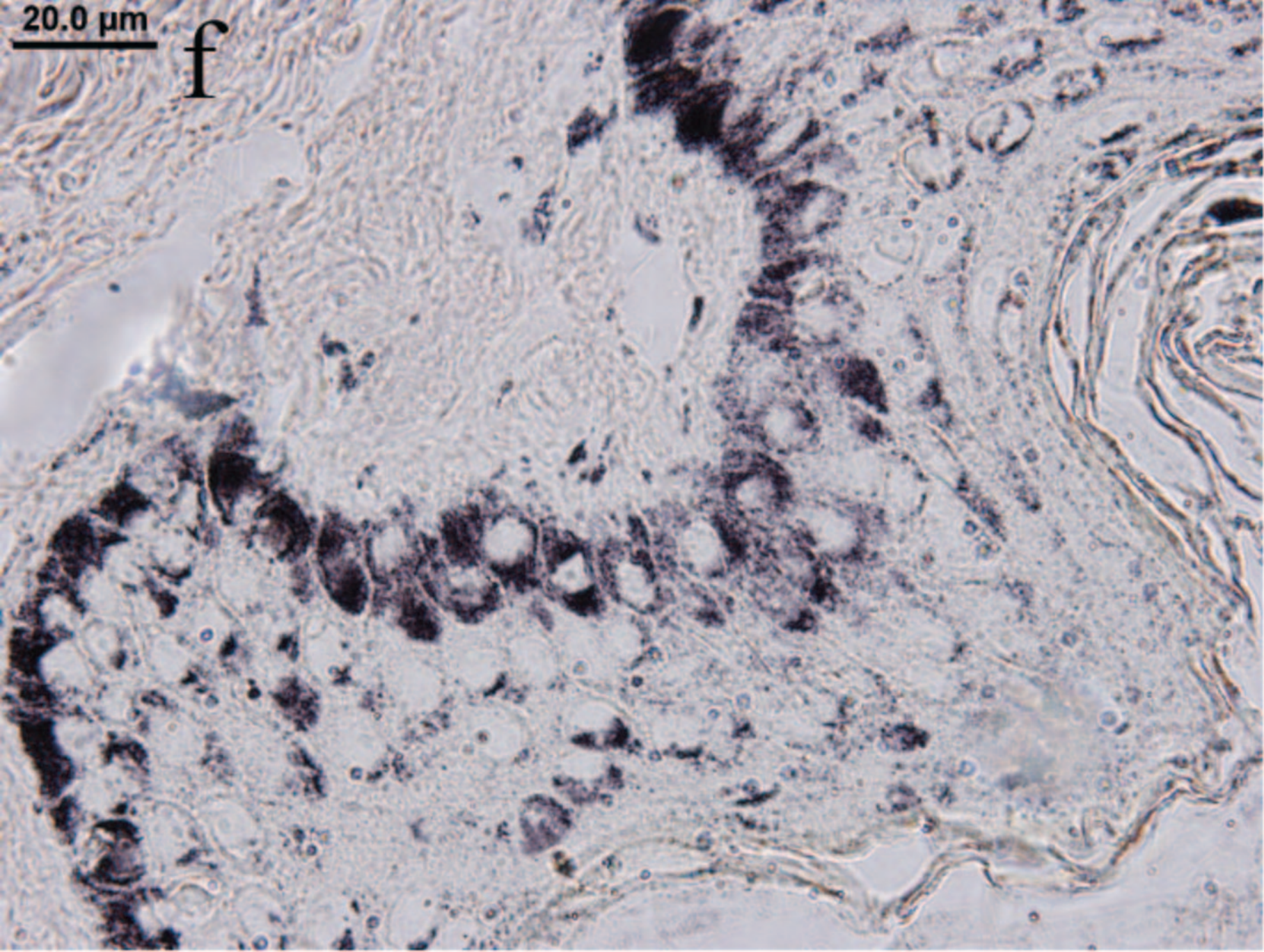
20.0 µm
f

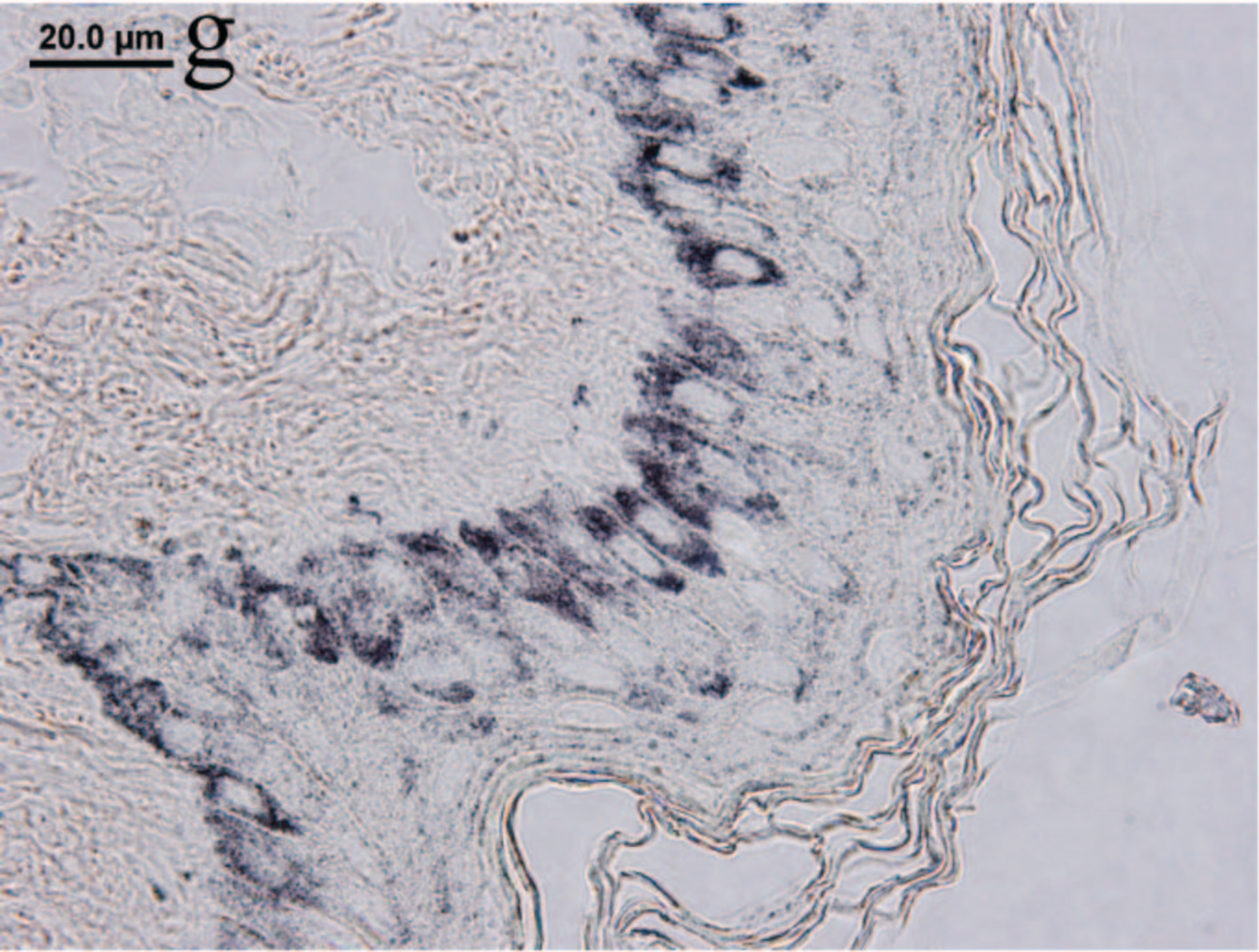
20.0 µm
g

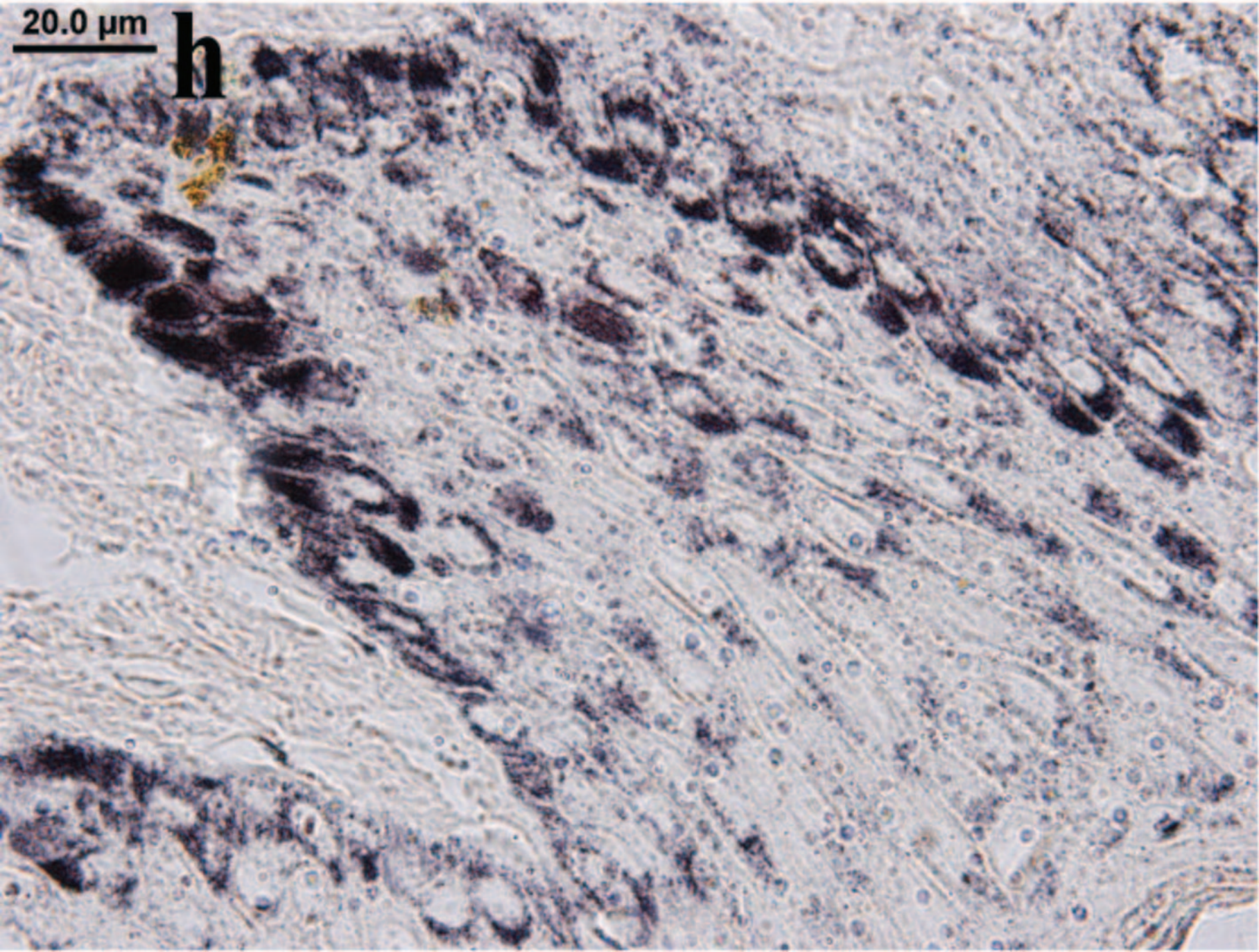
20.0 µm
h

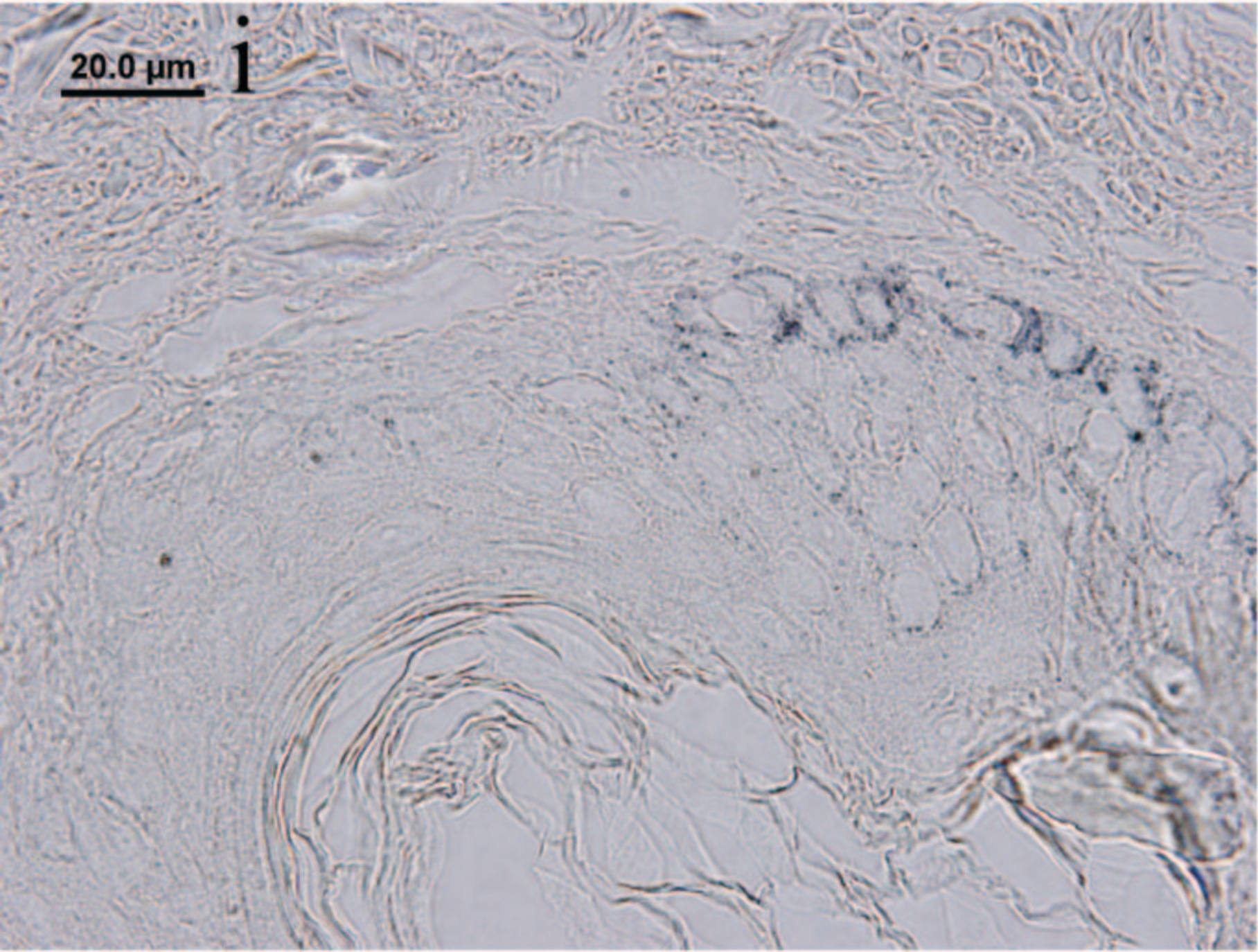
20.0 µm
i

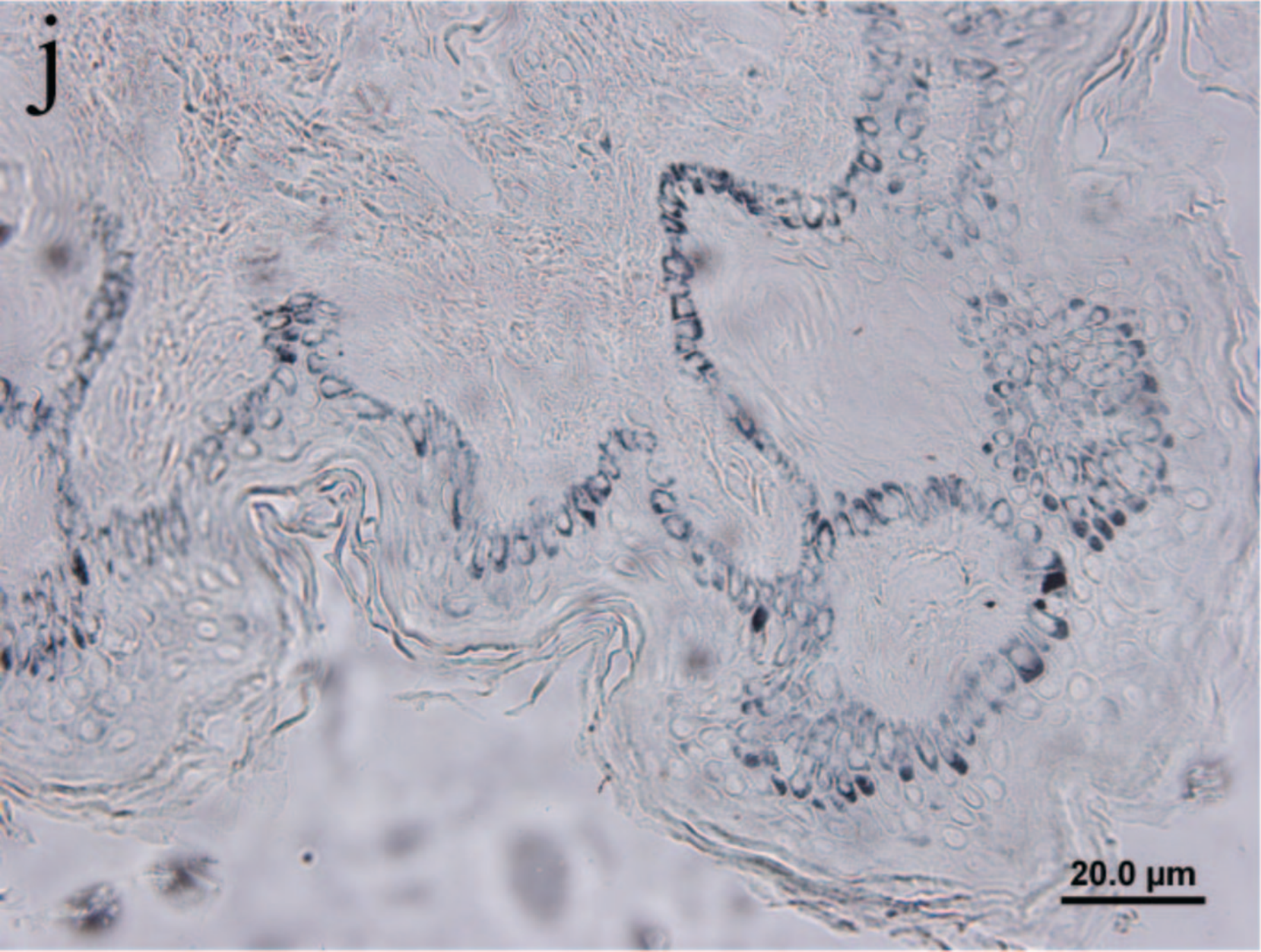
j
20.0 µm

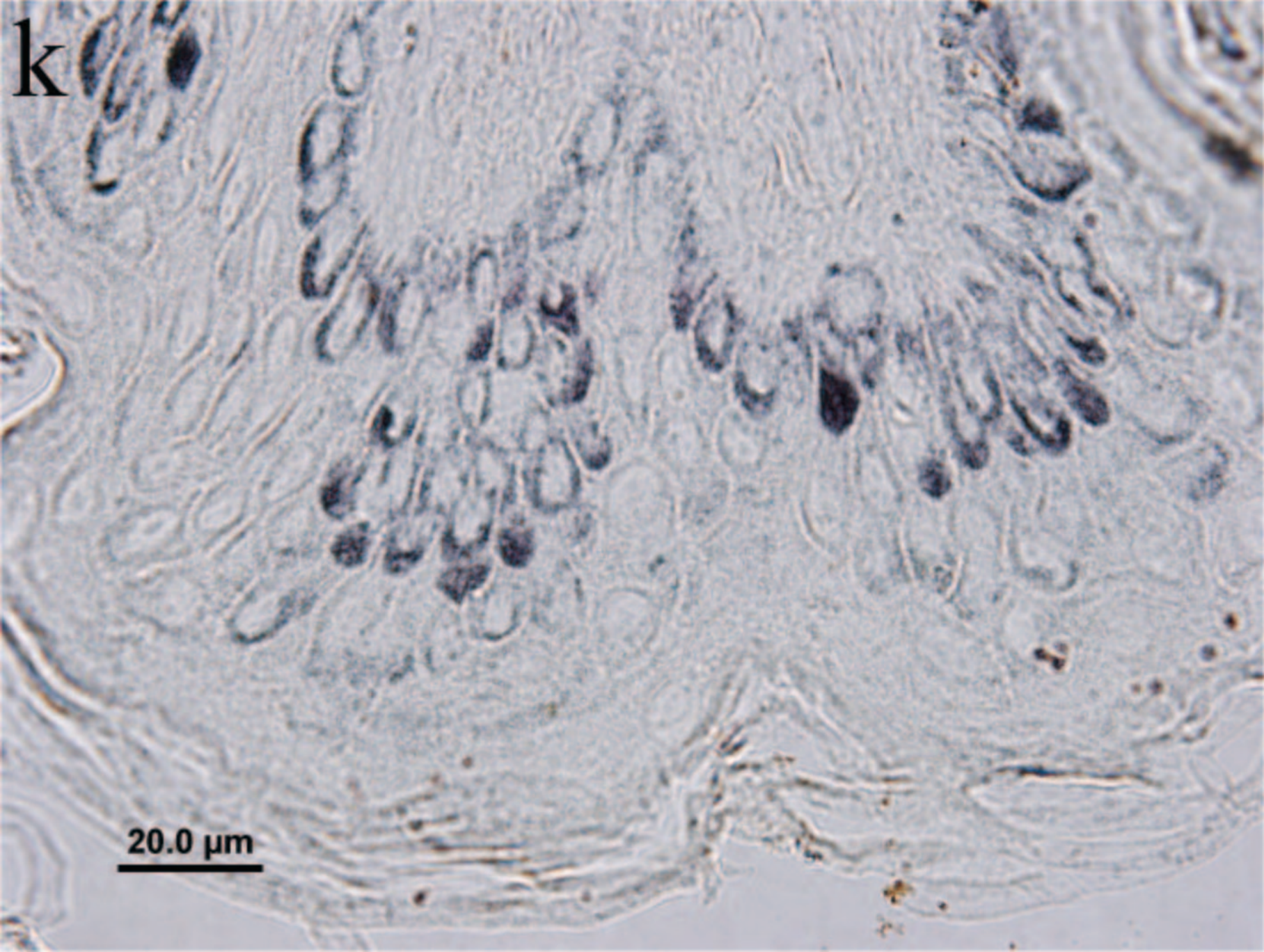
k
20.0 µm